$CR - /28948$

R-739

TRAVERSE GRAVIMETER EXPERIMENT

FINAL REPORT

by

Sheldon W. Buck, et al.

April 1973

CHARLES STARK DRAPER
LABORATORY

MASSACHUSETTS INSTITUTE OF TECHNOLOGY

CAMBRIDGE, MASSACHUSETTS, 02139

R-739

TRAVERSE GRAVIMETER EXPERIMENT
FINAL REPORT

by

Sheldon W. Buck, et al.

April 1973

THE CHARLES STARK DRAPER LABORATORY
A DIVISION OF MASSACHUSETTS INSTITUTE OF TECHNOLOGY
CAMBRIDGE, MASSACHUSETTS 02139

Approved:_____ Date:_26 Apr 73_
John B. Harper, Program Manager
Traverse Gravimeter Experiment

Approved:_____ Date:_26 Apr '73_
Philip N. Bowditch
Scientific Technology Director

Approved:_____ Date:_26 Apr 73_
David G. Hoag, Associate Director
Charles Stark Draper Laboratory

i

ACKNOWLEDGMENT

The authors wish to express their sincere gratitude to all personnel who took part in the Traverse Gravimeter Experiment. It was through their personal commitment to this program and a desire to be part of a once-in-a-lifetime opportunity that success was achieved in building the first instrument at the Charles Stark Draper Laboratory to reach the moon.

The authors also wish to express their appreciation to the following personnel for their relations with the Draper Laboratory and contributions to the program:

> Dr. Manik Talwani, Principal Investigator, of Lamont-Doherty Geological Observatory of Columbia University for his steadfast support and cooperation.

> Mr. Max Holley and Mr. Stanley Bachman of NASA/JSC for their technical direction and program management.

> Dr. Peter Mason of the Jet Propulsion Laboratory, assigned to NASA Headquarters, for his personal interest and technical insight.

> Mr. Stuart Law of Philco Corporation, assigned as our Flight Controller at JSC Mission Control, for taking the time to thoroughly understand the operation of this instrument.

Particular credit must be given to the engineering contributions of Arthur D. Little Company, Inc. for overall thermal-design assistance and the design and fabrication of the protective blanket for this instrument.

About one hundred persons from the Charles Stark Draper Laboratory contributed directly to this program. Engineers from Groups 20, 22B, 22F, 23, 35, 37, 38, and 50 helped analyze, design, build and test the gravimeter. The authors wish space permitted detailing each person's involvement, since credit for the success that this program received is deservedly theirs.

R-739

TRAVERSE GRAVIMETER EXPERIMENT
FINAL REPORT

ABSTRACT

A semiautomatic self-leveling lunar gravimeter has been designed for the Apollo 17 mission. This Traverse Gravimeter, which is completely self-contained and powered by an internal battery, was used to measure gravity at predetermined stops along the route of the Lunar Rover Vehicle. The gravity sensor is a vibrating string accelerometer (VSA) enclosed in a temperature-controlled oven and gimballed leveling assembly.

This instrument is capable of resolving gravity differences as small as 0.035 milligal (1 mgal = 0.001 cm/s) on the moon and yet also is able to measure the earth's gravity field of 980,000 milligals. Twenty-two measurements were taken on the moon during the Apollo 17 mission, during which the VSA temperature never varied more than $0.005^\circ C$. The flight results indicate an instrument accuracy of better than 2 mgal.

by   Sheldon W. Buck, et al.
April 1973

TABLE OF CONTENTS

TABLE OF CONTENTS (Continued)

TABLE OF CONTENTS (Continued)

TABLE OF CONTENTS (Continued)

LIST OF ILLUSTRATIONS

LIST OF TABLES

PART I

FINAL ENGINEERING REPORT

by

Sheldon W. Buck
John S. Eterno
Glenn Mamon
Richard T. Martorana
Robert G. Scott
William A. Vachon

1

SECTION 1

INTRODUCTION

In 2 years, a team of engineers, technicians, and others at the Charles Stark Draper Laboratory designed, built, tested, and supported the operation of the Traverse Gravimeter (TG) Experiment. The TG was proposed as a portable automated instrument to define the underground structure of lunar regions traversed by a Lunar Rover Vehicle (LRV). This was the first time a series of precise gravity measurements had been made on the surface of the moon.

It was hoped that the gravity readings would help solve the puzzle regarding the geological structure of the Sea of Serenity, which is near the landing site called "Taurus Littrow." The Sea of Serenity is represented by a large mascon on a gravity map and it is hypothesized that this huge positive gravity anomaly is caused by a dense material such as basalt (lava) flooding a large plain.

The TG was transported to the lunar surface on the Lunar Module (LM) descent stage of Apollo 17. After the LM landing, the TG was deployed on the lunar surface and initial measurements were made in the vicinity of the lunar module. Gravitational measurements were made at various stations where the LRV was stopped for geological examinations. Upon initiation, the TG automatically levelled, measured gravity, and conditioned the data to digitally display the measurement to the astronaut upon his command. The results of each measurement were transferred to earth by way of voice communication.

During the three traverses of Apollo 17, 22 gravity readings were taken at ten different locations. The direct gravity reading variations covered a range of 49 mgal.

SECTION 2

EXPERIMENT PURPOSE

Gravimetry is a major tool of geophysical exploration on earth where instrumental methods and interpretive techniques have evolved to an advanced state.

Commercial gravimeters are available for use on land, on the sea-surface and bottom, and in the air. None of these instruments is presently capable of measuring lunar gravity against an earth-based value. Therefore, this report describes the development of a gravimeter designed specifically for this task.

The first application of gravimetry to the moon was by means of a satellite. This provided a most important contribution to lunar tectonics - the discovery of positive gravity anomalies correlated with ringed maria, commonly called lunar mascons. Future satellite gravity studies will no doubt contribute to further understanding of large-scale structures (i.e., greater than 50 km). Only surface gravimetry, however, can yield the fine resolution required for exploring such lunar features as ridges surrounding the dark plains, edge effects of geological features, thickness variations in the mantle rock or lava flows, and density variations in the valley-highland borders, and for this purpose the traverse gravimeter experiment was designed. Without serious intervention in the astronaut's normal duties, a gravity map was obtained which yielded information on the "third dimension" of the geological features observed in the course of an Apollo mission. In this sense, the gravimeter was one of the most important geological tools in lunar exploration. In delineating the extent of lateral density variations on the moon with a scale of less than 50 km, the gravimeter provided essential clues to the question of the moon's origin and evolution.

4

SECTION 3

GENERAL INSTRUMENT DESCRIPTION

The traverse gravimeter (Fig. 3-1) consists of an instrument package including a battery-pack assembly, both enclosed in a multilayer insulating blanket which provides thermal protection. The instrument is lightweight, completely self-contained, and essentially automatic in operation, requiring no external power, recording devices, or telemetry. The gravimeter is rectangular in shape with a cylindrical surface at the front. It stands 20 inches high, 11 inches wide, and 9.75 inches deep, and weighs approximately 28 pounds. A folding handle at the top of the instrument is used for hand carrying and for securing the instrument to the LRV (Lunar Roving Vehicle) while three footpads at the base enable lunar-surface operations. A nine-digit display is found in the top of the case for visual readout of gravity data. A radiator at the top provides the primary means for heat expulsion. Both the display and radiator are protected from the dusty lunar environment by hinged plastic insulating covers.

The inner structure consists of a two-axis gimbal system which contains a vibrating-string accelerometer (VSA) housed in a thermally protected and evacuated two-stage oven assembly (precision and intermediate ovens). The oven assembly is enclosed in an electronic frame (E-frame) assembly of similar structural design which is pivoted about its axis and supported by a middle gimbal assembly. The middle gimbal controls the vertical positioning of the inner gimbal over a 30-degree range, and the middle gimbal assembly is attached through bearings to the base housing, with capacity to rotate through 210 degrees in order to invert the assembly for VSA calibration). Stepper motors and a gear train provide the drive and positioning of the gimbal assemblies, the motors reacting to signals from pendulums which work as level sensors. Heat for thermal protection of the inner (precision) oven is supplied by a temperature-control system while the intermediate oven is thermally protected by a preset on-off thermostat-heater combination.

The VSA employed as a gravity sensor was manufactured by the American Bosch Arma Company. Low power, small size, accuracy, and the excellent results obtained in an experimental sea gravimeter made the VSA the best candidate for use in a lunar gravimeter.

5

When the base of the TG is within ± 15 degrees of the horizontal, the control logic can level the system and permit measurement of the VSA difference frequency which is stored until the astronaut commands a visual readout. The display consists of nine digits, the first seven indicating the gravity reading and the last two showing the precision oven temperature and the status of temperature alarms.

A quantization in excess of 0.035 mgal per digit is obtained on a visual readout with an overall accuracy better than 2.0 mgal. This new, self contained instrument, powered by an internal 7.5 volt battery providing up to 375 watt hours of energy for all modes of operation over a 15-day period, was designed to be lightweight, reliable and simple to operate.

Fig. 3-1   Traverse gravimeter

SECTION 4

VIBRATING-STRING ACCELEROMETER

Gravity measurement with vibrating-string instruments was first accomplished about 1950 by R. Gilbert for use on a submarine and for measurements in a borehole. In the early sixties, other researchers made use of the vibrating-string accelerometer (VSA) in surface-ship gravimeters. In 1967 Dr. Charles Wing, formerly of the Department of Earth and Planetary Sciences at the Massachusetts Institute of Technology, perfected a gravimeter for surface ships and deep-sea-bottom experiments using military-surplus VSA's. Several surface-ship gravimeters based on Wing's initial design are in use today. These later gravimeters use VSA's built originally by American Bosch Arma for the Atlas program.

The traverse gravimeter makes use of 8-year-old surplus second-generation VSA's originally built by Arma for the Air Force for military applications. These units are smaller in size than the Atlas first-generation instrument and more suitable for a small experimental package. A critical review was made of existing accelerometers and gravimeters which could be modified for use on the moon. Fourteen individual devices representing the best from each of four categories (absolute, quartz, vibrating-string gravimeters, and accelerometers) were retained for consideration.* As a result of these tests, the VSA appeared the most suitable candidate for the program. The Arma units were built to withstand shock and vibration inputs consistent with use in aerospace systems. The VSA employed in the traverse gravimeter used less than a microwatt of power, and the drive amplifiers used only 30 milliwatts. The difference frequency between two strings in the VSA was amenable to ultraprecise determination of acceleration. The sum frequency output could be used as an independent check on the scale factor of the instrument.

There were, however, some disadvantages to the use of a VSA. To obtain the degree of stability required, the VSA required temperature stability of approximately 0.01°C. The instrument exhibited a drift in both bias and scale factor which

---

*Wing, Charles, and Sheldon Buck, Experimental Proposal for Manned Spaceflight Lunar Gravity Traverse Experiment, NASA, 10/17/69, pg 9.

Note: A complete bibliographical listing of all referenced documents is|included in the Bibliography at the end of Part II.

would need to be calibrated and verified to be repeatable across launch and translunar coast. The instrument also had a history of occasional tares (shifts) in bias and scale factor if subjected to shock and vibration.

4.1   Principle of Operation[*]

A schematic diagram showing the VSA cross-section and the instrument electronics is shown in Fig. 4-1. The VSA consists of two equal proof masses suspended from separate beryllium-copper strings and joined by a soft spring. Each string passes between the poles of a permanent magnet and both are rigidly attached to the support structure. Cross supports hold the masses rigidly in the transverse direction.

If an alternating current is applied to one of the strings, it will oscillate within the field of the permanent magnet at a frequency equal to that of the exciting current. As Fig. 4-1 indicates, the output of each drive amplifier is applied to a string and the back EMF developed by the moving string is used as positive feedback to the amplifier. Each string-amplifier loop will thus oscillate as its natural frequency.

Rayleigh derived the expression for the natural frequency of transverse vibration of a string or wire in tension rigidly clamped at both ends.

$$ f = \frac{1}{2} \left(\frac{T}{Lm}\right)^{1/2} \left(1 + \frac{2X}{L} \left(\frac{ES+T}{T}\right)^{1/2}\right) \tag{4-1} $$

where

f = resonant frequency
T = tension
L = string length
m = mass of the string
X = radius of gyration of the string cross-section about its midplane
S = cross-sectional area of the string
E = modulus of elasticity

The term in the brackets accounts for about a 1% correction. Thus Eq. (4-1) may be approximated by

$$ f = \frac{1}{2}\left(\frac{T}{Lm}\right)^{1/2}. \tag{4-2} $$

Next consider a wire fixed at one end, and a small proof mass with a prestress attached to the other end. Assume a fine cross-support for the mass and that the entire system is accelerated. The Eq. (4-2) becomes

---

[*]This derivation is based on previous work by George Bukow reported in Charles Stark Draper Laboratory Report E-2721.
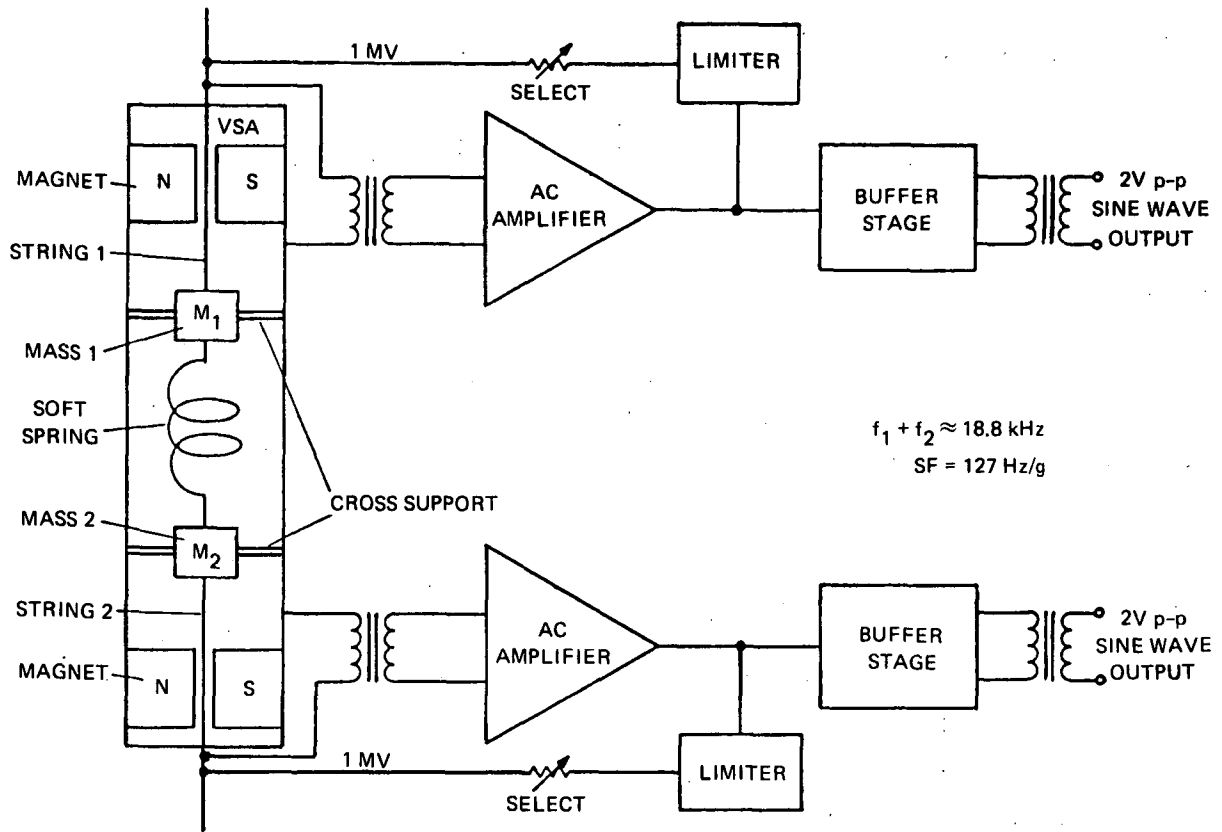
Fig. 4-1   Schematic diagram VSA and support electronics.

$$f_1 \approx \frac{1}{2}\left(\frac{T_0 + MA}{L_1\, m_1}\right)^{1/2} \tag{4-3}$$

where

T_0 = prestress
A = acceleration along the string
M = proof mass

Rewriting Eq. (4-3) in the form

$$f_1 = \frac{1}{2}\left(\frac{T_0}{L_1\, m_1}\right)^{1/2}\left(1 + \frac{MA}{T_0}\right)^{1/2} \tag{4-4}$$

9

and expanding in a MacLaurin series

$$f_1 = \frac{1}{2} \left(\frac{T_0}{L_1 m_1} \right)^{1/2} \left[1 + \frac{1}{2} \left(\frac{MA}{T_0} \right) - \frac{1}{8} \left(\frac{MA}{T_0} \right)^2 + \frac{1}{16} \left(\frac{MA}{T_0} \right)^3 \ldots \right].$$

(4-5)

The frequency can thus be represented by a power series of the acceleration

$$f = k_{01} + k_{11} A + k_{21} A^2 + k_{31} A^3 + \ldots$$

(4-6)

The usefulness of this device depends on the convergence of this series and its convergence rate.

A unique approach to improving linearity was taken by American Bosch Arma in designing the VSA for the Atlas ICBM. To the instrument already described is added a mirror image attached to the end of a coil spring as was shown in Fig. 4-1. Now instead of one frequency there are two, one for each wire.

If this second system is accelerated, the original string reads a positive acceleration while the second string reads a negative acceleration. Equation (4-5) becomes for the second frequency

$$f_2 = \frac{1}{2} \left(\frac{T_0}{L_2 m_2} \right)^{1/2} \left[1 - \frac{1}{2} \left(\frac{MA}{T_0} \right) - \frac{1}{8} \left(\frac{MA}{T_0} \right)^2 - \frac{1}{16} \left(\frac{MA}{T_0} \right)^3 \ldots \right].$$

(4-7)

and Eq.(4-6) becomes

$$f_2 = k_{02} - k_{12} A + k_{22} A^2 - k_{32} A^3 + \ldots$$

(4-8)

The output of the two-string VSA is defined as the difference between f_1 and f_2

$$f_1 - f_2 = (k_{01} - k_{02}) + (k_{11} + k_{12}) A + (k_{21} - k_{22}) A^2 + (k_{31} + k_{32}) A^3 + \ldots \quad (4-9)$$

Defining

$$K_0 = k_{01} - k_{02}; \quad K_1 = (k_{11} + k_{12}); \quad K_2 = (k_{21} - k_{22}); \quad K_3 = (k_{31} + k_{32}) \quad (4-10)$$

10

where

K_0 = bias (Hz)

K_1 = scale factor (Hz/g)

K_2 = second-order coefficient (Hz/g^2)

K_3 = third-order coefficient (Hz/g^3)

Eq.(4-9) becomes

$$f_1 - f_2 = K_0 + K_1 A + K_2 A^2 + K_3 A^3 + \ldots \qquad (4\text{-}11)$$

The even terms in Eq.(4-11) would disappear if the two wires were identically equal, but in general, no two wires can be made physically equal and kept equal by maintaining a perfectly controlled environment. In order to find the acceleration measured, the coefficients of the power series must be determined. (See Appendix B.)

The gravimeter display logic converts Eq.(4-11) to

$$f_1 - f_2 = \frac{1.92 \times 10^8}{D_N} = K_0 + K_1 g + K_2 g^2 + K_3 g^3 \qquad (4\text{-}12)$$

$$f_2 - f_1 = \frac{4.8 \times 10^7}{D_I} = -K_0 + K_1 g - K_2 g^2 + K_3 g^3 \qquad (4\text{-}13)$$

where

D_N 7-digit display value for normal (GRAV) measurement

D_I 7-digit display value for inverted (BIAS) measurement

g   VSA input-axis gravitational acceleration.

This quantization will be explained in the next section.

SECTION 5

ELECTRONICS

5.1   General Description

The electronics for the traverse gravimeter is designed with the goals of simplicity, minimum power consumption, and reliability as prime objectives. The number of types of components was held to a minimum in order to provide standardization and ease of testing. Integrated circuits were used for both analog and digital functions. Analog electronics consist of the VSA oscillator-amplifiers, mounted with the VSA in the precision oven; the temperature controller, multiplexer, and two pendulum-amplifier modules, which are located on the Electronics frame (E frame); the power-supply module mounted on the main housing; and the phase-locked loop mounted on the battery. Digital electronics are contained mainly in the logic and display module located directly behind the numerical display.

The two basic modes of operation of the TG are determined by the ON/STBY toggle switch on the display panel. In the standby mode (STBY position), used from launch until lunar traverse, power is supplied only to the oven temperature controls and VSA oscillator-amplifiers, maintaining a constant thermal environment for the VSA. At least 5 to 20 minutes before the gravity measurements are to be made, the system is placed in the operate mode (ON position of switch). Power is then supplied to a crystal oscillator and to a small part of the mode-control logic.

To initiate a gravity measurement, the GRAV pushbutton is depressed, supplying power to all system elements except the GRAVITY/BIAS and TEMP displays. The INDICATOR MODE light will then flash, indicating that the levelling loops are in operation. When the VSA assembly is within 7 arc minutes of the correct orientation with respect to gravity, the INDICATOR MODE light will illuminate steadily; and, after a delay of approximately 60 seconds, the gravity measurement cycle will begin. The instrument must remain level (within 7 arc minutes) for approximately 30 seconds or else the levelling and delay will be automatically recycled. Should a loss of phase lock occur during the measurement cycle, the three most significant digits of the GRAVITY/BIAS display will be zero when the operator activates the display. The levelling and measurement sequence must then be restarted as described above. If no level disturbance occurs, the gravity

12

measurement takes an additional minute. When the measurement is complete, the system automatically returns to the operate mode. Depressing the READ push-button activates the GRAVITY/BIAS and TEMP displays. To conserve power, the displays go off after 18 seconds, but may be reactivated by again depressing READ.

5.2   Circuit Description

A schematic of the gravimeter electronics is shown in Appendix B. The major circuits are discussed below.

The vibrating-string accelerometer (VSA) consists ideally of a pair of single vibrating strings back to back. Separate, but equal masses, joined by a soft isolating spring, are suspended by identical beryllium-copper strings. The difference frequency between the two strings is a nearly linear indication of gravity.

$$\Delta f = f_1 - f_2 = K_0 + K_1 g^2 + K_3 g^3 + \ldots \qquad (5-1)$$

The scale factor, K_1, is normally about 128 Hz/g. The bias K_0 will vary from one accelerometer to another and will usually lie in the range of 3 to 15 Hz. The stability of the scale factor is greater than that of the bias and is calibrated on earth. The bias is updated on the moon at the beginning of EVA-1 and at the end of EVA-3.

Each vibrating string passes through a magnetic field. The driving force of the string is furnished by an oscillator amplifier whose output is a current through the vibrating string and whose input is the back EMF created by the motion of the string in its magnetic field. The natural frequency of oscillation of each string is nominally about 9.5 kHz. The output voltage signal of each oscillator amplifier is voltage limited to provide a constant-current source to drive the string.

The VSA amplifiers have a closed-loop gain of about 500 at 9.5 kHz, (the natural frequency of oscillation of the VSA). The outputs of the VSA amplifiers are fed to the phase-locked-loop module where the two outputs are mixed. The output of the mixer is filtered to obtain the difference frequency and attenuate the sum frequency. The difference frequency is the signal to which the phase-locked filter is locked. The purpose of the phase-locked loop is to act as a narrow-band filter to attenuate the possible residual vibrations of the Lunar Roving Vehicle (LRV) which might occur when taking a measurement.

5.3   Gravity-Measurement Technique

The VSA difference frequency is approximately 20 Hz on the moon. It is desired to quantize this signal to approximately one part in 10^7. If zero crossings of the difference frequency were counted, it would take an extremely long time. It is much simpler to perform a period measurement. The method for doing this is explained in the following paragraphs.

13

There are really two timing clocks in the data readout. One is the 4-MHz crystal oscillator; the other is the VSA difference frequency. Binary countdowns from the 4-MHz oscillator provide the timing for the A/D encoder, the motor-drive electronics, power-supply synchronization, level-light flasher, and, above all, the gravity measurement itself. The 4-MHz oscillator is a temperature-compensated crystal oscillator (TCXO) with an accuracy of 2.5 parts in 10^7. Although frequencies as high as 4 MHz are not used in the gravimeter, 4 MHz was chosen based on the superior performance of crystals at that frequency. The VSA difference frequency acts as a clock to generate the gate during which time gravity is actually measured. The gate-generator logic selects a fixed number of cycles of the VSA difference at the appropriate time. The number of cycles selected is chosen to provide a gate width of approximately 1 minute. In order to keep the gravity measurement time approximately the same in all measurement modes, the number of cycles selected differs in the various modes. As shown in Table 5-1, the relationship between the gravity-measurement gate width, T_G, and the difference frequency, Δf, is 1536 in the Moon-Gravity mode, 384 in the Moon-Bias mode, and 9216 in both of the earth-measurement modes.

The logic that generates the gravity-measurement gate is prevented from doing so, however, until the system has levelled in both axes within ± 7 arc minutes. The gate-generator logic tests that the system is not only level but also has stayed level for at least 10 to 15 seconds. If the system is oscillating and a nonlevel signal is obtained, the gate-generator timing is recycled and a gravity measurement is not performed. Once this level settling time has passed, the gravimeter goes on to perform the gravity measurement. The gravity-measurement times will be constant for successive measurements. Table 5-1 also indicates that the quantization is not merely a function of the displayed number and the full-scaled value. The fact that the displayed number consists of a relatively large bias that is considered constant must be taken into consideration. If the bias were zero, then the quantization would be simply g/N where N is the displayed number and g is the full-scale value (980 gals on earth; 162 gals on the moon). Since the function being measured consists of a variable ($K_1 g$) and a constant (K_0), the actual quantization in milligals is:

$$\frac{g}{N}\left(\frac{K_0 + K_1 g}{K_1 g}\right) \quad \text{or} \quad \frac{1}{N}\left(\frac{K_0}{K_1} + g\right)$$

5.4   Automatic Levelling System

The seven-arc-minute level indication that permits a gravity measurement to be performed comes from the levelling section. There are two pendulums in the gravimeter. Each one is a two-axis device. One pendulum is used in the normal

14

TABLE 5-1

GRAVIMETER TIMING

Mode	Typical VSA Bias (Hz)	VSA Diff. Freq. (Hz)	Number of Counts	Quantization (mgal)	Gravity Measurement Time (s)	Total Time After Level (s)	PLL Hold Time (s)
Moon-Normal	7	28.1	6.81×10^6	0.0315	54.5	126.5	36.0
Moon-Bias	7	14.1	3.41×10^6	0.0317	27.2	63.0	N/A
Earth-Normal	7	134.0	8.62×10^6	0.122	69.0	160.0	46.0
Earth-Bias	7	120.1	9.55×10^6	0.099	76.5	177.0	N/A

Gravity Measurement Time (s) $= \dfrac{1536}{\Delta f}$ Moon-Normal

$= \dfrac{384}{\Delta f}$ Moon-Bias

$= \dfrac{9216}{\Delta f}$ Earth

Clock frequency = 125 kHz

Quantization $= \dfrac{1}{N}\left(\dfrac{K_0}{K_1} + g\right)$

N = Number of Counts

K_0 = Bias

K_1 = Scale Factor

orientation and the other in the bias mode. The pendulums are excited with an ac supply. The pendulum output signals are first normalized for scale factor, adjusted for phase shift, and trimmed for quadrature rejection before they are amplified, demodulated, buffered, and then multiplexed and sent to an A/D encoder. (In addition to the pendulum signals, the temperature monitor is also fed to the A/D encoder). The outputs of the A/D encoder are strobed into storage flip-flops, and then decoded to provide the information to the stepper-motor/gear-train assemblies to drive the gimbals. The A/D encoder provides four states of information about the X and Y axes of the pendulums: polarity, which determines the direction to slew the gimbals, and thresholds at ± 32 arc minutes, ± 7 arc minutes, and ± 3 arc minutes. The gimbal-gear-train ratio is 2700:1 so that each 90 degree step command to the stepper motor drives the gimbal 2 arc minutes. Above ± 32 arc minutes, the stepper motors are slewed at a fast clock rate of 122 arc minutes per second; below ± 32 arc minutes, a slow rate of 7.6 arc minutes per second is used. Below ± 3 arc minutes the motors are not slewed at all, and power is removed from the stepper motors. The ± 3-arc-minute deadband is well within the ± 7-minute threshold at which a gravity reading is enabled. On the moon, the gimbals respond to a 15-degree step in less than 20 seconds with only one overshoot. (The response to a 1.5 degree step is shown in Fig. 5-1).

5.5   Multiplexer and A/D Encoder

The A/D encoder is a 4-bit successive approximation encoder. The pendulum signals are scaled at 1-arc-minute-per-bit, so that full-scale output from the A/D is the ± 7 arc minute information. Polarity is obtained from the sign bit, and the ± 3-arc-minute deadband is determined by proper combinatorial logic. Thirty-two-arc-minute information for switching between the fast and slow levelling modes is obtained by using two level comparators, one at + 32 arc minutes and the other at − 32 arc minutes. The output of the multiplexer feeds both comparators as well as the A/D encoder, and the logic strobes the data out at the appropriate time to separate the information for the two gimbal axes.

The encoder sampling rate is 244 Hz/channel which is higher than the fastest slew rate of the gimbal (61 pulses per second). The stepper-motor driver consists of a two-bit shift register. The clock to this register is either the fast or slow clock. Below 3 arc minutes the clock is inhibited. The outputs of the two flip-flops in the shift register are gated to provide the four phases for driving the stepper-motor windings. The stepper motor is driven either clockwise or counterclockwise, depending on the polarity information from the pendulum. The temperature-monitor signal that also is fed to the A/D encoder is scaled to 0.005°C per bit. Therefore, temperature information up to ± 0.035°C is obtained. This temperature information is strobed at the time a gravity measurement is made and then transferred to the display along with the gravity information.

16
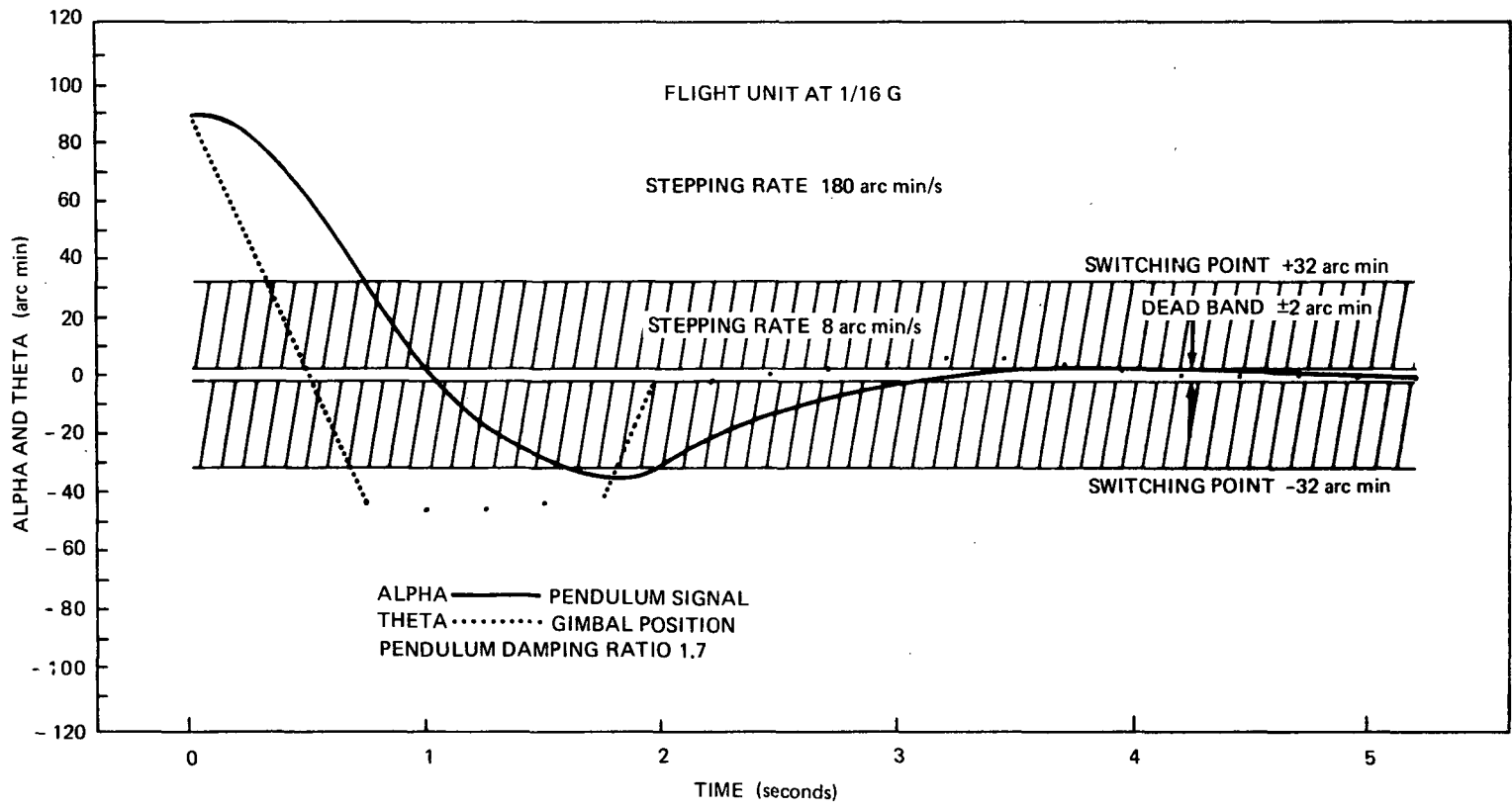
Fig. 5-1   Response to a 1.5-degree step.

5.6   The Phase-Locked-Loop Filter

Possible vibration resonances that might be experienced on the LRV are
believed to be at frequencies of one Hz and higher. The VSA difference frequency,
as was mentioned before, will be approximately 20 Hz on the moon and will vary
with gravity. To filter this signal by conventional methods, a very narrow band-
pass filter would have to be built and its center frequency would have to track the
VSA difference frequency. By using a phase-locked loop, the problems of a very-
narrow-bandpass tracking filter are eliminated and a low-pass filter in the loop
provides the required filtering. Vibrations applied to the VSA will appear as
frequency modulation on the string frequencies. Most phase-locked loops are
designed to track the frequency-modulation components on a fixed carrier signal.
In this case, it is desired that the loop attenuate the modulation and produce only
the carrier. In other words, the average value of the VSA difference frequency
over a period of time is sought. Gravity information is contained in only the very-
low-frequency bandwidth of the phase-locked loop.

Providing a narrow-band low-pass filter in the loop requires a very low
closed-loop gain in order for the loop to be stable. A low-gain loop provides a very
small lock-in bandwidth. In order to acquire the signal in a relatively short period
of time, the phase-locked loop was designed with two modes: a wide-band mode for
acquiring the signal and a narrow-band mode for filtering the VSA signal. The VSA
string frequencies are mixed and filtered in the phase-locked loop. A ring-diode
demodulator is used as the mixer, and a low-pass filter allows the difference frequency
to pass through, but attentuates the sum frequency (approximately 19 kHz) to below
1 mV. The filtered sine wave feeds a zero-crossover detector to provide a square
wave compatible with logic. (The divide-by-six circuit shown merely scales the
difference frequency for earth measurements to be approximately 20 Hz.)

The wideband filter feeds a sample and hold circuit. The narrow-band signal
is summed with the output of the sample and hold circuit into the voltage-controlled
oscillator (VCO). In the wide-band mode, the gain of the narrow-band loop is so
small that is has very little effect on the summation signal to the VCO. Some time
after the gravimeter has levelled, but about 30 seconds before the gravity measure-
ment begins, the phase-locked loop is switched from the wide-band mode to the
narrow-band mode. At this time, the sample and hold circuit holds the sampled
voltage into the VCO. The narrow-band loop now takes over. The purpose of the
sample and hold circuit is to determine the approximate bias voltage the VCO
requires at the time of a measurement. The narrow-band filter provides the remainder
of this voltage. The narrow-band loop provides in excess of 40-dB attenuation at one
Hz. This is achieved by using a two-pole Butterworth filter as the low-pass filter.
The closed-loop response of the narrowband loop is that of a third-order system:

$$\frac{0.68}{s^3 + 2.1s^2 + 1.1s + 0.68}$$

18

5.7 Temperature Control

A proportional plus derivative temperature controller maintains the precision oven to within $0.005^{\circ}C$. The precision inner oven contains the sensors and heaters as well as the VSA and its amplifiers. The sensors are two thermistors located in opposite arms of a four-arm bridge. The bridge is excited by a regulated low-voltage ac supply. The excitation is kept low and regulated to minimize the effects of self-heating. The bridge provides an output of about 18 mV/$^{\circ}$F to the temperature controller. The bridge signal is amplified in a high-gain preamplifier. By providing most of the gain ac, the problem of dc offset and drift is minimized.

After ac amplification, the bridge error signal is demodulated in a standard diode-ring phase-sensitive demodulator. The demodulated signal is buffered and scaled to a sensitivity of 50 mV/$0.005^{\circ}C$. The buffered signal is the temperature-monitor signal that is sent to the multiplexed A/D converter to provide information on the temperature controller. The demodulated output is also sent to the proportional plus derivative stage which provides the drive for the heaters. The time constant of this stage is adjusted to match the natural frequency of the whole system, which in turn is determined by the system gain and the time lag between heater and sensor.

The output stage consists of four transistors physically located on the precision oven structure. Thus, the heat of these transistors is utilized to heat the structure. Heater resistance, half in the collectors and half in the emitters of the four transistors, is distributed to make gains of the transistors less critical, and also to provide a uniform heat distribution to minimize temperature gradients.

5.8 Power Supply

In order to minimize power consumption, all analog circuits are operated from plus and minus five volts. Low-power TTL is used for the logic circuits operating at +5 volts. The only exceptions are the crystal oscillator which needs +12 volts, the stepper motor which requires +28 volts, and the LED display which requires +4 volts. The high power consumers which are the stepper motors, and the display are energized only when required. Thus, the average power is kept down by minimizing the duty cycle.

In the STBY mode, plus and minus 5-volt supplies are provided for the VSA oscillator amplifiers and the temperature controller. The heater is supplied with current from the battery. Therefore, the load on these supplies is essentially constant throughout the mission. The tight regulation of 0.2% is required to minimize the voltage sensitivity of the VSA amplifiers, as well as to provide a constant thermal load in the oven. Changes in supply voltage result in phase-shift changes in the VSA amplifiers. A change in phase-shift between input and output will result in an apparent frequency change and produce gravity-measurement errors.

To supply the temperature-controller excitation and demodulator reference, a low-power Colpitts oscillator is provided in the power supply. The oscillator drives a reference transformer that supplies the bridge excitation and demodulator reference, and also the pendulum excitation. Feedback is provided around the Colpitts oscillator to regulate the output to within ± 1% over temperature excursions and with battery variations. As with the 5-volt standby supplies, the ac loads are practically constant. The Colpitts oscillator also feeds a sine-wave amplifier which drives a flea-power chopper. The chopped signal is rectified and is fed to the -5-volt regulator. The plus and minus 5-volt regulators are similar and use an integrated-circuit regulator with low internal dissipation.

When switched to the ON mode, the flea-power chopper output is enabled to a low-level chopper. This chopper contains the circuitry to supply the unregulated input to the +12-volt regulator for the crystal oscillator and the -5-volt regulator for the analog circuitry used in the gravity-measurement modes. The -5-volt supply is not provided to these circuits in the ON mode. In addition, two other +5 volt regulators are energized in the ON mode. One regulator energizes the voltage-controlled oscillator (VCO) in the phase-locked loop. The other provides logic power for the mode-control logic and the BCD counter that stores the gravity measurement. The VCO supply is kept separate to provide isolation and to minimize the amount of load variation.

In the GRAV and BIAS measurement modes all the other power supplies are turned on except for the light-emitting diode (LED) display supply. The +5-volt logic supply is enabled to all the logic circuitry as well as the gimbal electronics and A/D converter. The -5-volt supply that is generated by the low-level chopper is supplied to the high-level chopper. This chopper produces 28 volts for the stepper motors.

The display (READ) mode enables the 4-volt regulator to be turned on. This in turn, drives the LED display. In addition, the +5 volts for the logic is provided to the LED display to energize the integrated-circuit decoders that are integral with the display units.

To minimize the possibility of asynchronous noise, the 4-kHz ac supply is synchronized with a 3.906-kHz clock from the binary countdown during the measurement modes of operation.

SECTION 6

MECHANICAL DESIGN

The mechanical design of the Traverse Gravimeter is illustrated in Figs. 6-1 and 6-2. The magnesium outer structure of the TG is rectangular in shape with a cylindrical front. A folding handle at the top of the instrument is used for hand carrying and for latching the instrument to the isoframe assembly on the pallet. Three feet at the base of the instrument provide a stable support for lunar-surface operations. Flight photographs indicate greater soil penetration by these inverted mushroom feet than was encountered during field-trip operation.

The outer surface of the TG is enclosed in a multilayered insulation blanket which provides thermal protection for the internal components. This blanket covers all outer surfaces with the exception of the display panel, radiator cover, the three feet, and carrying handle already mentioned. Details of the mechanical design related to thermal protection and temperature control are described in Section 7. The display and radiator covers are held closed by magnetic latches during lunar-surface operation and by Velcro strips during launch and translunar flight. The hinges sewn into the outer layer of the blanket were model-airplane-type pin hinges which have very low friction and no residual stiffness. Neither cover assembly was mechanically connected to the instrument housing and thereby did not compromise the thermal protection.

The isoframe assembly mounts to the rear of the TG and provides vibration isolation between the instrument and the pallet. To secure the TG to the isoframe assembly the two rear feet are placed in a cradle in the isoframe and the carrying handle is folded to a latched position. During the translunar phase of the mission, three shoulder pins secure the TG to the isoframe which is mounted to the geology tool pallet. Each shoulder pin is held in place by a PIP (spring-loaded ball lock) pin, and each of these shoulder-PIP pin combinations is removed by a steel-wire lanyard prior to deployment on the lunar surface. The shoulder pins require a reasonably close fit to avoid generating high-frequency vibrations which would negate the low-pass-filter benefits of the isoframe.

21

INDICATOR MODE LIGHT
  FLASH - Levelling
  ON - Measure
  OFF - Measurement Complete

PUSH BUTTONS

HANDLE ASS'Y
  CAM/SPRING ACTION
  ONE HAND OPERATION
  THERMALLY ISOLATED

RADIATOR COVER

DISPLAY COVER

ISOFRAME ASS'Y

VIBRATION ISOLATOR

HARD - MOUNT
PENETRATION

THERMAL BLANKET

AFT LEG ASS'Y

FWD LEG ASS'Y
  THERMALLY ISOLATED
  ISOFRAME RETAINED
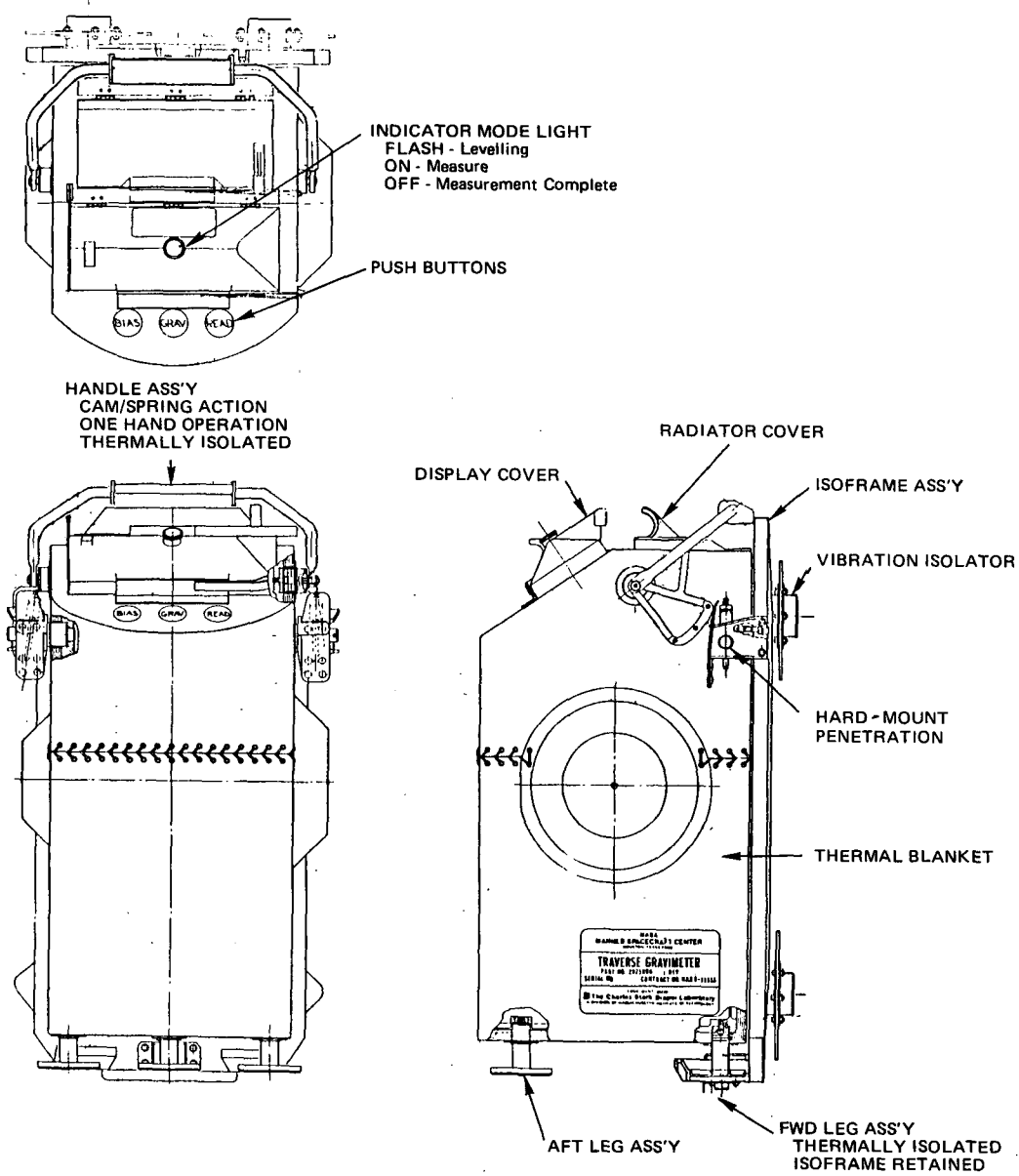
Fig. 6-1   Outline drawing of traverse gravimeter.

HANDLE ASS'Y

ON/STBY SWITCH

DISPLAY PANEL

DISPLAY HOUSING
MACHINING

PUSH BUTTONS

GIMBAL HOUSING

E FRAME/E-FRAME
MODULES

INTERMEDIATE OVEN

PRECISION OVEN

VSA

VSA
AMPLIFIER MODULES

MAIN COVER

PHASE-LOCK-LOOP
MODULE

BATTERY PACK ASS'Y

RADIATOR

COLLECTOR

THERMAL
ISOLATOR

RADIATION
SHIELD

SIDE MOUNT
HARD MOUNTED
FOR LAUNCH –
THERMALLY
ISOLATED ON
LUNAR SURFACE

BASE HOUSE
MACHINING

SIDE COVER

GEAR BOX

THERMAL
ISOLATOR/
SUPPORT

LOWER SHELF
BATTERY SUPPORT
MACHINING

Fig. 6-2 Cutaway view of traverse gravimeter.

The isolators were selected and supplied by Barry Division of Barry Wright Corporation, who also analyzed the performance of the isoframe system for all probable input combinations including three-axis vibration, shock, and accelerations.

Space and interface limitation prevented the use of the isolator case supplied by Barry so special ones were fabricated. The resilient element was a moulded elastomer called Barry "Hi-Damp."* Figure 6-3 shows the effect of the isoframe on the VSA response to the LM α-axis flight random vibration levels.
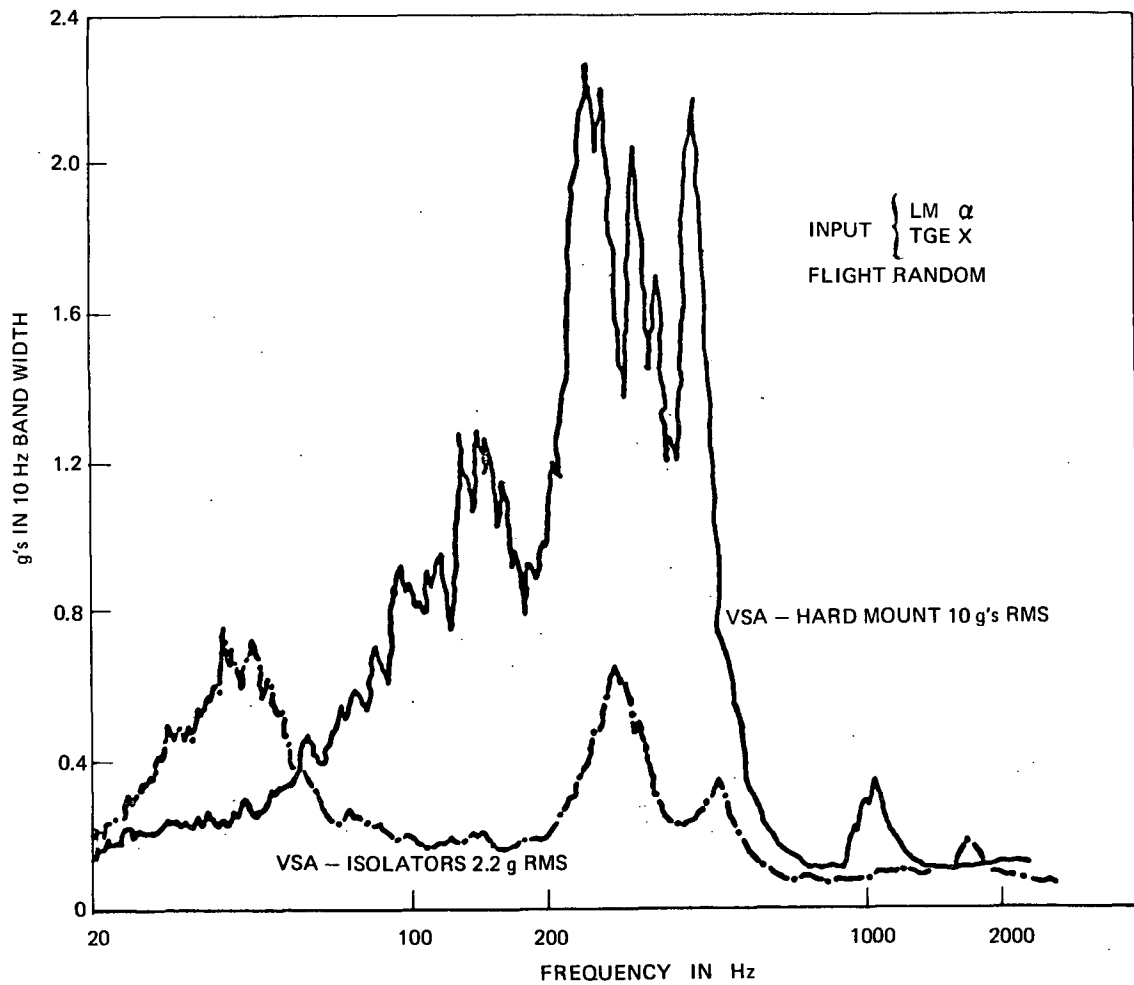
Fig. 6-3   Effect of rubber isolators.

---

*A comparison of some of the predicted and measured responses can be found in memo GRV-T-196.

As described in Section 3, the inner structure of the TG consists of a two-axis gimbal system which contains a vibrating string accelerometer (VSA) housed in and thermally protected by a two-stage oven assembly designed to operate in a vacuum environment. The oven assembly is enclosed in an electronics frame (E frame) assembly of similar structural design. The E-frame assembly is pivoted about its axis and supported by a middle gimbal assembly. The middle gimbal controls the vertical positioning of the inner gimbal over a ± 15 degree range. The middle gimbal assembly is coupled through bearings to the base housing and can rotate from -15 to +195 degrees. Stepper motors and a gear train provide the drive and positioning of the gimbal assemblies. The stepper motors react to signals from pendulums which act as level sensors.

The dip-brazed aluminum gimbal was designed to act dynamically as a compliant spring between the instrument housing and the E-frame assembly. The thin-shell gimbal structure has a natural frequency of 80 Hz in the LM α direction when loaded by the mass of the E-frame/oven assembly. The oven assemblies were previously shown to have a lowest natural frequency near 180 Hz. Thus the gimbal acts as a low-pass filter for isolating the VSA input axis from vibration.

The gear box assemblies (Fig. 6-4) reduce the stepper motor output by 2700 to 1 in four stages. Thus, one pulse to the stepper motor produces a gimbal shaft rotation of 2 arc minutes. An antibacklash sector gear was attached to the gimbal shafts in order to reduce angular position uncertainty while allowing for reasonable manufacturing and assembly tolerances. Beryllium was selected for the gear-box housing to more closely match the thermal expansion of the stainless-steel gears, bearings, and shafts. Silicone oil was used for lubrication. These gear-box assemblies operated under high-vacuum conditions for periods up to 2 weeks and with temperature excursions of 100°F without difficulty. A teardown inspection of FS-2, the qualification model rebuilt as a spare flight unit revealed the Y-axis gear box had lost its antibacklash due to improper operation and running beyond the sector-gear limits during a BIAS measurement. However, the gear box assemblies showed no degradation from thermal-vacuum or vibration testing. Limit switches and a cam on the sector gear protect the gimbal assembly from overtravel while making normal gravity measurements in case the TG was initially more than 15 degrees from vertical or accidentally knocked over. However, the lack of a cam in the inverted position of the Y-axis gear box made the gravimeter vulnerable; when after being initially level during a BIAS measurement, the case was tipped beyond 15 degrees during the measurement portion of this mode. The flight crews were cautioned about this operational problem and an emergency procedure was developed to reengage the gear train without anti-backlash in the event this problem occurred on the moon, which thankfully it did not.

25

90° STEPPER MOTOR

MOTOR DRIVE ELECTRONICS

MICRO SWITCHES

SECTOR GEAR CAM
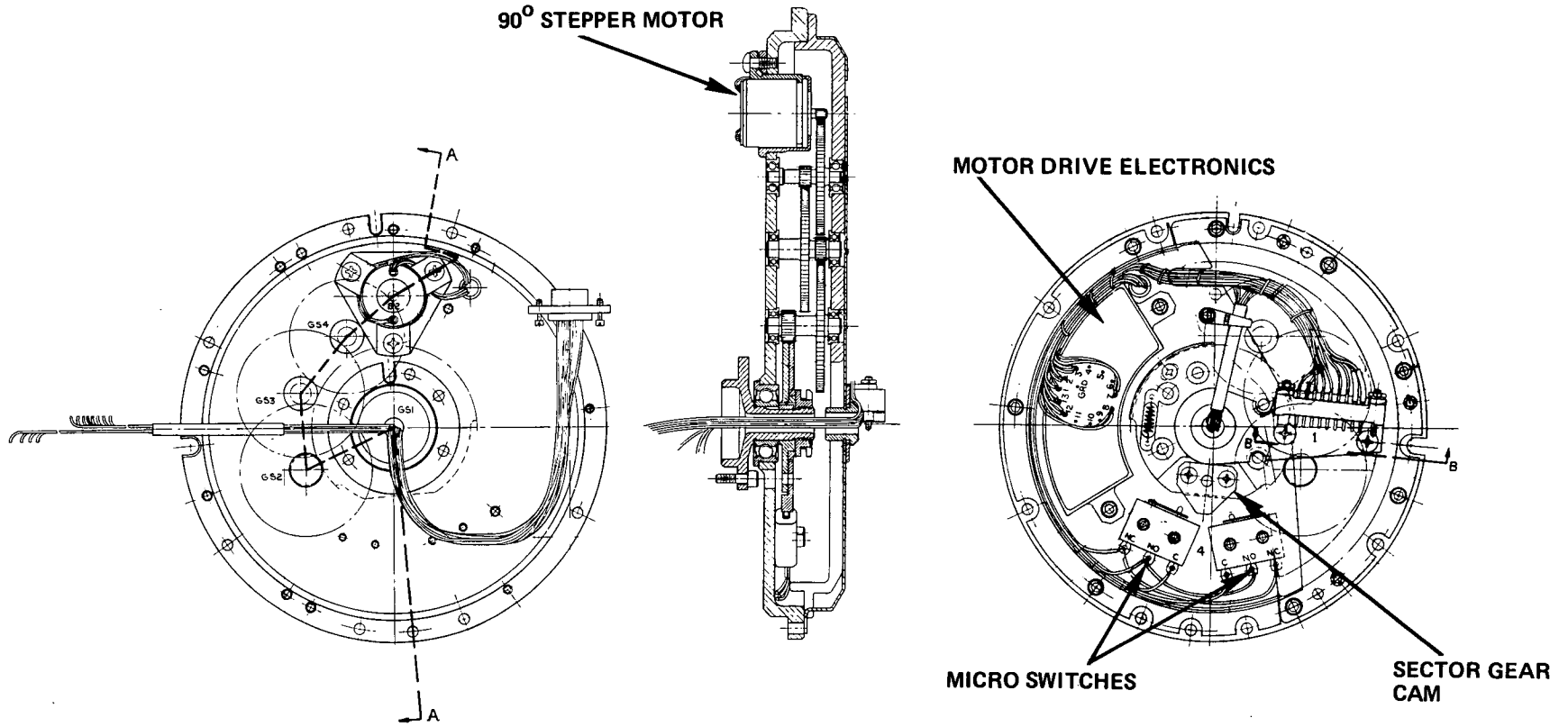
Fig. 6-4   Gear-box assembly, Y axis.

The limited-travel gear box design permitted the use of a flexible wire harness to be run through the gimbal assembly, thereby eliminating the need for slip rings and allowing the use of coaxial shielded cables for the two VSA string outputs in addition to the multiplexer output. Ball bearings lubricated with silicone oil were used throughout the gimbal design. These bearings were preloaded to 100 pounds during assembly because of the anticipated 13-g peak combined launch loads.

Ninety percent by weight of the mechanical parts were fabricated of magnesium because stiffness rather than stress was the limiting design parameter. All mechanical parts were machined from bar or tooling stock to reduce total manufacturing time and tooling costs. As an example, one completed isoframe could be fabricated in a week.

A detailed stress analysis of the instrument and isoframe was performed by Littleton Research and Engineering Corporation. The analysis included static, dynamic, and acoustic inputs. Summaries of this work may be found in reports C-207-1 through C-207-5 from this company. Teledyne Materials Research supported the design and analysis effort with mechanical testing of materials and components. The results were transmitted in their biweekly letter reports.

SECTION 7

THERMAL DESIGN

The concept for thermal control of the Lunar Traverse Gravimeter Experiment package is that the gravity sensing and other control elements are thermally isolated from the outer environment while a discrete path is provided for rejection of absorbed as well as internally generated heat. Inherent in the thermal design are mechanical constraints of low weight and volume. This section summarizes only the key points in the thermal design; many details associated with the thermal design and its modeling will be found in Appendices C, D, and E.

7.1   Thermal Requirements

The basic requirements of the TG thermal design were the following:

(1)   Control the temperature of the Vibrating String Accelerometer (VSA) and critical measurement circuitry which is temperature sensitive to a prescribed temperature with sufficient stability that temperature-induced gravity errors are a small part of the total error budget of the instrument. It was determined that the VSA should operate at approximately 122°F and remain within $\pm 0.01^\circ$C throughout a lunar extra-vehicular activity (EVA) while the external environment can vary from -100 to $+250^\circ$F.

(2)   Choose a battery size such that it is adequate for the worst possible mission in terms of electrical power consumption.

(3)   Provide an adequate thermal environment in which electronic components and modules as well as mechanical equipment can function reliably.

The thermal environments for which the TG was designed were specified by two parameters:

(1)   The predicted thermal response of the Lunar Module (LM) Quad III geology pallet during translunar stowage in the hottest and coldest missions. This information was supplied by Grumman Aerospace Corporation, the Lunar Module contractor, based on computer model

28

predictions. Figure 7-1 is a plot of the worst-case hot, nominal, and cold pallet temperature histories during translunar stowage and the post-touchdown thermal soak-back period prior to instrument removal.

(2) Sun elevation angle with respect to the lunar horizon during the lunar stay. These angles were specified for each type of mission at the time of landing as follows:

Hottest Mission:	20.3 degrees
Nominal Mission:	13.3 degrees
Coldest Mission:	6.8 degrees

During the lunar stay, it was required that the TG ride on the rear of the LRV pallet during periods of extravehicular activity (EVA). An additional degree of experiment flexibility, however, dictated that the TG be easily removed from and replaced on the pallet in case it was deemed necessary to make all gravity measurements on the ground due to excess LRV motion. Therefore, two distinct mounting configurations were required of the TG; the hard-mounted translunar stowage ride which must withstand launch and lunar landing, and a less restrictive removable mounting for the lunar phase.

Once the LM had landed, initiating the lunar phase of the mission, it was required that the TG be able to survive the hottest or coldest Quad III soakback temperature history (Fig. 7-1) for a maximum period of 17 hours and function during the remaining lunar phase. The 17 hours was predicated on a maximum of 16 hours from landing to astronaut egress followed by an estimated 1-hour period before the TG was removed from Quad III. The subsequent lunar time line was defined as a 6-hour EVA followed by two 7-hour EVA's with 14-hour rest periods after the first and second EVA.

At no time during the lunar stay could the TG thermal-control requirements impact the parking attitude of the LRV. Furthermore, it was of utmost importance that the thermal control of the TG require a minimum of participation on the part of the astronauts. Such an emphasis ruled heavily against a deployable sun shield or open Optical Surface Reflectors (OSR's) which must be constantly dusted.

7.2 Thermal Design - General Description

The thermal design finally chosen for the TG employed two key uniquenesses of the experiment to full advantage. First, the fact that the TG was easily removable from the LRV pallet for gravity measurements on the lunar surface enabled the instrument to be placed in the shade of the LM for cooling during rest periods. Second, the gravity data which was read in real time from the TG display by the astronaut could also contain thermal information. With such information, the
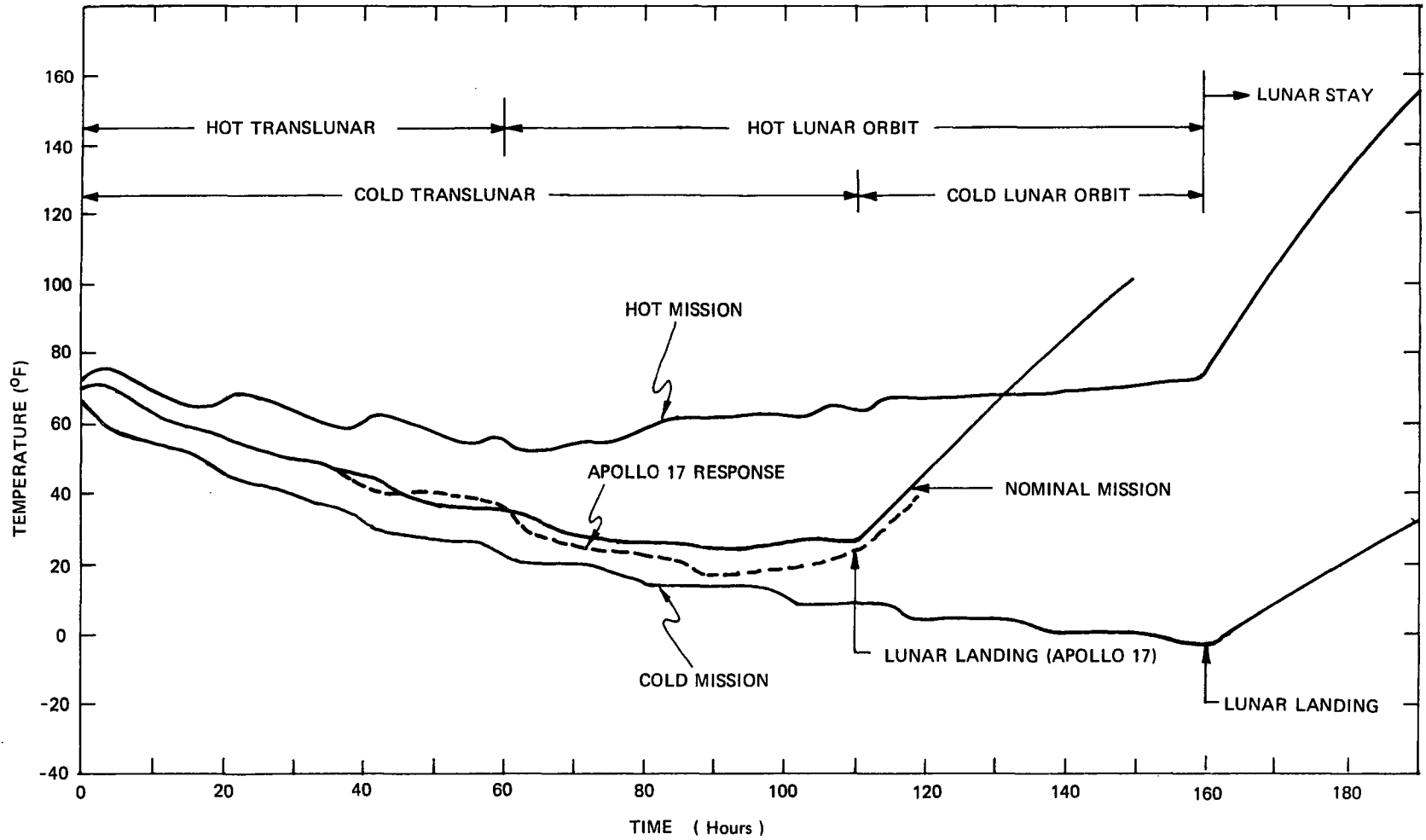
Fig. 7-1   Quad III stowage pallet temperatures.

acquisition of which caused immeasureably small impact to the astronaut's time line, real-time recommendations could be made by ground personnel should the instrument's function become in danger for thermal reasons.

Thermal control was obtained from the time of launch to the completion of the lunar mission. During stowage in the LM Quad III, hard-mount pins penetrated the protective outer blanket and yet did not compromise the control capability. During the lunar phase the TG was designed such that thermal control was completely automatic during even the hottest or coldest EVA. At that time the unit was completely enclosed by the thermal blanket, isolating it from the heat and dust of the lunar environment. During rest periods, it was placed in the shade of the LM and its radiator exposed to outer space for cooling. With the high radiative cooling capabilities afforded by the LM shade during the relatively long (14-hour) rest periods, the overall instrument thermal design centered on building sufficient thermal isolation into the TG that it could survive the hottest EVA with no cooling required for up to 7 hours while in the sun on the LRV pallet. Samples of the TG thermal response are found in Appendix D.

Figure 7-2 will help to describe the thermal design and will be referred to often in the following sections. Basically, the desired thermal isolation from the external environment was derived by a double oven on the inner structure surrounding the VSA, both of which contain temperature-control capabilities. In addition, the complete outer surface of the TG was enveloped by a high-performance multi-layer thermal insulation system. The details of the whole design will be found in the following sections.

7.3   Inner Structure Design

The TG inner structure refers to the Vibrating-String Accelerometer (VSA), Precision Oven (P), and Intermediate Oven (I).

The precision oven is a thin-walled body of revolution which houses the VSA and the VSA amplifier. Machined from magnesium stock, displaying fairly good thermal conductance (5.75 Btu/h-in.-$^\circ$F), this unit displays negligible circumferential temperature gradients with the low heat-flow rates involved. Because the VSA dissipates a very low level of constant power (approximately 10^{-5} watts) it is possible to use the P oven as the primary means for temperature control rather than the VSA itself.

A 0.65-watt electrical heater is bonded to each end of the P oven for thermal control at 122°F ± 1°F with an accuracy of better than ± 0.009°F. A temperature of 122°F (50°C) was selected as the minimum sensor temperature which would permit a heat-rejection temperature-control mode in the hottest environment. The VSA is mounted with the P oven using an aluminum flange for good coupling. It is estimated that with a vacuum of less than 10 ^{3} torr, the thermal resistance between the VSA and P oven is approximately 2°F/watt.
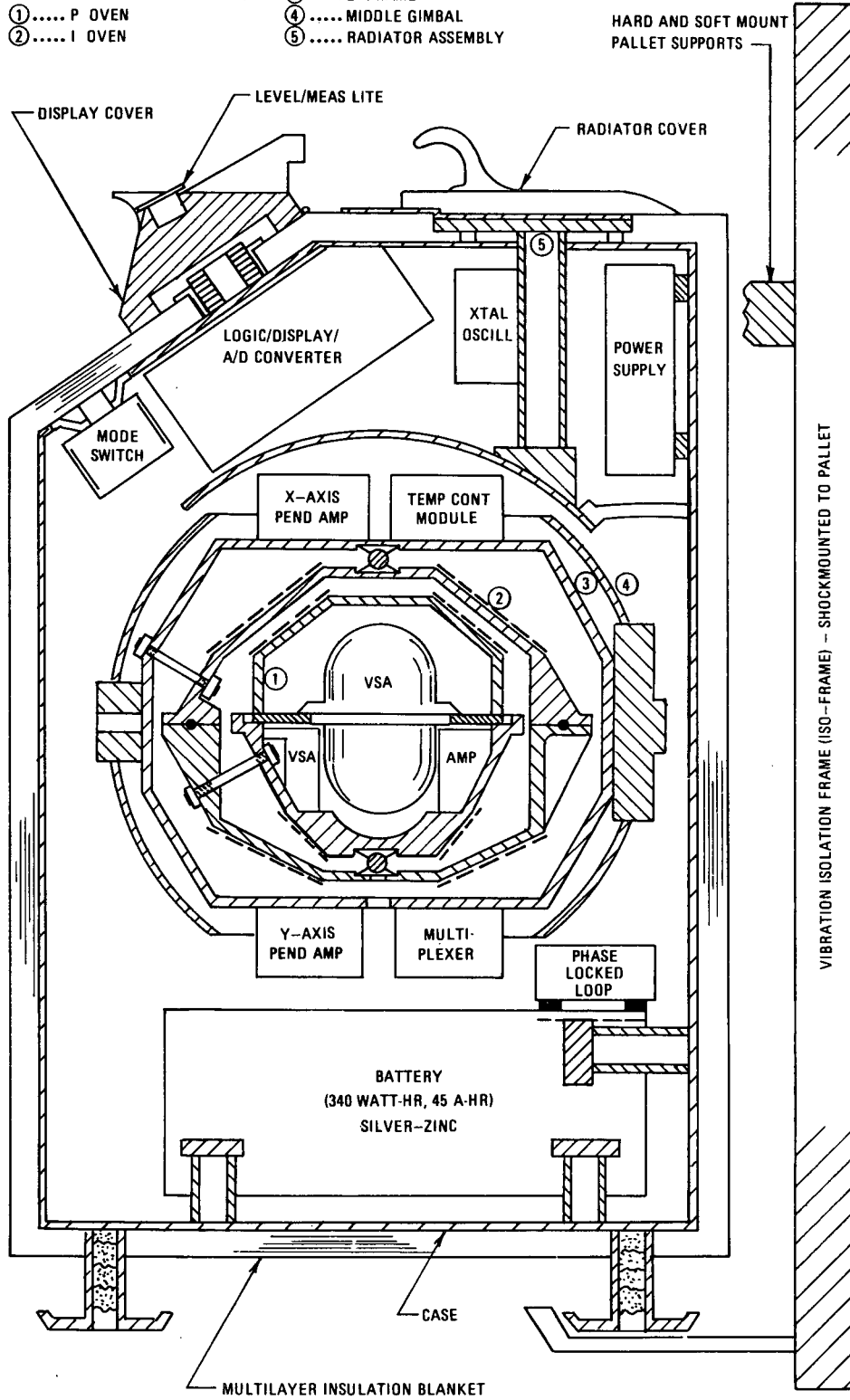
Fig. 7-2   TG   thermal design cutaway.

Within the P oven, and thermally attached to the P-oven structure, is the amplifier for the VSA signal. The heat-dissipating transistors (power transistors) of the P-oven temperature controller are also mounted directly to the P-oven structure. The VSA amplifier is housed herein for temperature stability. The driver transistors are installed here in order to minimize the electrical power required for temperature control and also to make the temperature-control circuitry behave in a linear manner.

The sensor for the P-oven temperature control is a four-arm ac bridge employing two thermistors in opposite legs and Vishay reference resistors in the other legs. The thermistors are imbedded in drilled holes in the lower half of the P oven. The Vishay resistors are bonded to the outer surface of the lower half of the oven. The resistance of the thermistors is a nominal 810 ohms at 122°F. The bridge is powered by only 1.6 volts (rms) in order to minimize self-heating effects. The resultant bridge output sensitivity is approximately 18.7 millivolts/$^{\circ}$F. Additional details are found in the electronic design section of this report (Section 5).

The surfaces of all ovens are gold plated prior to the installation of heaters and components. The thermal radiative emissivity of the plating was measured at 0.041. Gold was chosen for its low emissivity and resistance to tarnishing and degradation by handling.

Immediately outside the precision oven is the cylindrically symmetric I oven. The P and I ovens are thermally isolated from each other by three conically oriented strings like three legs of a tetrahedron. These strings are tensioned titanium rods (0.040 inch diameter). Centered below the strings is a high-thermal-resistance spring-loaded hollow titanium ball mount used to tension the titanium strings. Calculations and test data both indicate that with a pressure of less than 10^{-3} torr, the thermal resistance between P and I ovens is approximately 85°F/watt.

Under certain conditions during laboratory tests it was desirable in order to simulate outer-space thermal control to have a vacuum within the I oven. Therefore, the covers for the supporting strings and the I-oven flange are vacuum sealed with O-rings. In addition, all wires fed into or out of the I oven passed through hermetic feed-throughs. In this manner, a vacuum pump may be put on an opening in the bottom of the oven and a good vacuum achieved. More will be said on this point at the end of this section.

A 1.5-watt heater is bonded to each end of the outer surface of the I oven. The heaters are activated in an on-off manner by a thermostatic switch when the I-oven temperature goes below 60°F.

Because the primary thermal isolation of the VSA from the outer world is between the P and I ovens, this area is extremely sensitive to many effects. A few will be mentioned.

Residual gas pressure within the I oven can lead to molecular conduction and a degraded thermal impedance. Detailed mathematical analogs of the thermal paths between the ovens showed that, at a gas pressure of 1 micron within the ovens, the thermal resistance is reduced by approximately 17% over the value at zero pressure. The gas may arise from adsorbed and absorbed molecules as well as evaporation of volatiles such as adhesives. To minimize this problem, the ovens and all components except the VSA are initially vacuum baked at elevated temperatures for extended periods. In addition, after the VSA is installed the unit is kept under vacuum as much as possible in order to avoid contamination and continue the evaporative cleaning process.

A second effect, which caused major control problems, was that of the electrical wires between the VSA and the I oven and between the P oven and the I oven. The wires caused the three following problems:

(1) Wires between the P and I ovens seriously degraded the overall thermal impedance.

(2) The presence of jacketed wires on the outer surface of the P oven contributed to radiative coupling to the I oven.

(3) Wires between the VSA and the I oven were heat paths which made the VSA temperature respond to shifts in the I-oven temperature, independent of the P-oven controller.

The first problem was solved by employing long-length low-conductance manganin wires between the ovens. The second and third problems were solved by heat stationing to the outer surface of the P oven all wires passing from or through the P oven. A low-emittance aluminum tape (3M Scotch No. 425) was used wherever possible to cover and fasten all exposed wires.

A steady-state 36-node thermal mathematical computer model of the inner structure was created in order to explain and enhance the performance of P-oven temperature control. The model accurately predicted temperature gradients within the P oven as a function of the I-oven temperature as measured on a well-instrumented lab mockup.

Historically, early in the design phase, an important thermal-design requirement for the TG was that following its last earth-based calibration, the VSA should never cool down from its operating temperature until the lunar mission was complete. It was feared that large VSA scale-factor changes would result from thermal cycling if the unit were to cool down and reheat. It was originally planned that the unit would be kept under laboratory thermal control until 2 days prior to launch, at which time it would be placed in the rocket. For the 2-day period on earth and the remainder

of the mission, the TG would control its temperature by internal battery power. In order to achieve this goal while employing the same battery and heater sizes, it was necessary to maintain a high P-to-I-oven thermal impedance by keeping a vacuum within the I oven while on earth. After launch, a puncture device would break a membrane on the I oven in order to use the vacuum of space as a pump. The vacuum within the I oven was also necessary for earth-based laboratory tests in which it was necessary for test purposes to replicate the environment seen by the VSA in a lunar mission.

A major problem was the achievement and maintenance of a good vacuum within the I oven during the 2-day prelaunch period during which no I-oven pumping was available. In order to achieve a good I-oven vacuum, the covers for the supporting strings and the I-oven mating flange were vacuum sealed with O rings. All wires fed into or out of the I oven were sent through hermetically sealed feedthroughs. A pumping port and removable vacuum valve were designed for the I oven. As mentioned earlier, all components within the I oven, except the VSA, were vacuum baked in order to drive off molecules which could later evaporate and degrade the vacuum. An Indium and rubber O-ring seal in parallel were planned for all I-oven O rings in order to combat the gas permeability of rubber. Periodic titanium flash gettering was also contemplated as a means of enhancing the vacuum.

Due to an extension of the mandatory period on the launch pad to 7 days and the unavailability of external power to Quad III of the rocket during that period, the TG battery had to be either enlarged or the thermal mission requirements altered. In parallel, however, with the TG thermal design, precise laboratory tests were being conducted in order to determine the amount of the VSA scale-factor shift due to a cooldown from $122^{O}F$ to $65^{O}F$ and back again a week later. These tests showed that the scale-factor shift was less than 5 parts per million; well within the instrument error budget. In light of changing requirements and the above test results, a decision was made to launch the instrument cold and have a pressure-actuated switch turn the instrument on to the standby mode when the pressure within the TG case dropped below approximately 0.2 atmosphere during the rocket ascent. The P oven would then come under thermal control at $122^{O}F$ within 3 hours. The long translunar stowage period (110 hours minimum) would enable the VSA to stabilize at its normal operating temperature prior to lunar operations. Laboratory tests had further shown that a 2- or 3-day period was required for the VSA to stabilize after a thermal transient in order to minimize VSA bias drift.

7.4 Gimballed Structures

Enclosing the I oven is the E frame, another cylindrical magnesium structure of similar design to the P and I ovens. The E frame is thermally isolated from the I oven in exactly the same manner as that of the I oven and the P oven. A thermal resistance of approximately 47°F/watt was achieved with a pressure of less than 10^{-3} torr.

Between the I oven and E frame a thin thermal radiation barrier is placed in order to enhance the thermal impedance (not shown in Fig. 7-2). The barrier is vacuum formed from Lexan and subsequently coated with metallic aluminum by vacuum deposition. The barrier helps to reduce the radiative coupling between jacketed wires and high-emittance portions of both the I oven and the E frame. The barrier contained numerous holes owing to the presence of the pendulums on the E frame and other protuberances on both structures.

As shown in Fig. 7-2, two electronic modules are placed on each end of the E frame. While in the standby mode of operation, only the temperature-control module dissipates electrical heat. While the operate and measure modes, all other E-frame modules are electrical heat sources. Even though the E frame is not as well isolated as the I oven, it will undergo temperature changes much attenuated from those of the outer housing. It is for this reason that the E frame was chosen for some of the analog electronics; which includes the amplifiers for the two, two degree-of-freedom pendulums and the P-oven temperature-control circuitry. After the analog signals are amplified in order to minimize errors, they are also multiplexed at the E frame. They are then sent to the analog-to-digital converter on the housing.

External to the E frame is the Middle (M) gimbal, which houses the axis drive for the E-frame trunnion. The M gimbal is a gold-plated thin-walled aluminum sphere with cutouts for the E-frame modules. It is a trunnion which is bearing-pivoted to the side walls of the external housing. The thermal impedance between the E frame and the M gimbal and between M gimbal and case were both measured to be approximately 9°F/watt. This value takes into account the parallel heat paths of radiation and conductance across the bearings.

7.5 Radiator

A major mode of heat expulsion from the instrument is via an external surface radiator. The external radiator has a surface area of 12 square inches to radiate to space. The surface is formed by contigously bonding segments of second-surface mirror material (fused silica) to a substrate of aluminum. The surfaces, when newly manufactured, display an absorption coefficient to solar energy, α_s, of 0.083 and a normal thermal emittance of 0.842. When covered with lunar dust and

subsequently cleaned with a soft bristle brush, tests indicate that the resultant solar absorptance, α_s, is less than 0.2.

If the radiator were not covered during times of LRV motion and local astronaut activity, it was felt that lunar dust would soon coat its surface and drastically increase its solar absorptance. Constant radiator dusting by the astronaut was deemed too time consuming. Secondly, if it were a cold mission, in which excessive internal battery energy was being consumed for heat, an uncovered radiator would drastically increase this consumption. Therefore, for dust protection and mission flexibility a dust cover was designed for the radiator. Because the TG could accept all heat inputs both radiative and electrical during an EVA with no required cooling, the only time the radiator dust cover would be opened was for cooling during rest periods in the LM shadow. In the LM shadow, however, the low α_s of an OSR is not necessary because there is no solar radiation. For this type of mission the radiator could be a painted black surface with high values for both α_s and ϵ_H. It was, however, decided that for contingency purposes only a backup means of deriving a level of cooling in the open sunlight should be incorporated. Thus, the inclusion of the OSR's on the radiator surface.

The 12-square-inch size was selected such that the astronaut could employ one standard operating procedure for both hot or cold thermal missions. In a cold mission, though, a larger radiating surface with the instrument in the shade of the LM could lead to overcooling and excess battery energy consumption.

A study was made to observe the effects of the presence of the LM on TG radiative cooling during rest periods. It was found that for the worst possible TG location in the LM shadow, the I-oven temperature was 5°F hotter at the end of the lunar mission than if the LM presence were neglected. This effect was deemed of small order.

Part of the design of the radiator involves the transfer of energy from within the unit to the radiating surface. The design requires that the heat being liberated by the E frame be radiatively absorbed by the spherical shell which envelopes the upper surface of the E frame. In order to maximize this coupling, the inner surface of the hemisphere was painted flat black and the end surface of the E-frame modules was of a black electronic conformal coating. The heat received by the hemisphere is conveyed to the external radiating surface via a hollow rod of aluminum with a cross-sectional area of approximately 0.1 square inch. At the top surface, this rod attached to the 12-square-inch rectangular radiating area to which the second surface mirrors are bonded (see Fig. 7-2).

Considerable design effort was expended in mechanically mounting and yet thermally isolating the radiator assembly from the case structure such that as the

radiator expels heat it draws a minimum from the outer housing. High-strength epoxy fiberglass laminate (NEMA G-10) material was used for three hemisphere mounts and two upper radiator mounts. A net thermal resistance of approximately $39^\circ F$/watt was achieved between the radiator assembly and the case.

7.6 Case and Case-Mounted Electronics

The outer case structure is composed of basically two distinct parts: the base housing on which all mechanical components are mounted, and the case covers. All such parts, fabricated of magnesium, are buffed and gold plated on the inner surfaces and nonbuffed gold plated on the outer surfaces.

The base housing itself is machined from a solid piece of magnesium and has an average wall thickness of approximately 0.060 inch. For the heat-flow rates involved in the TGE, the case was found to be approximately an isothermal boundary.

In order to provide a smooth surface on which the multilayer insulation thermal protection system or blanket could readily mount, the recessed areas on the outer surface of the base housing were filled with a semirigid light-weight foam, and all screws were flush flat-head screws. All mounting holes for external members such as feet and handles contained flanges that were flush with the outer-housing dimensions. In general, the inner portions of these penetrations were raised bosses on the inner-case surface.

The case itself acts as a heat sink for three heat-dissipating electronic modules; the power supply, crystal oscillator, and logic-display analog-to-digital (A/D) converter. Table 7-1 lists all module powers in different operating modes. A portion of the power supply contributes heat throughout the mission in the standby mode in order to provide power for P-oven bridge excitation. In the operate and measure mode, considerable power-supply heat is dissipated. Negligible heat is dissipated at the crystal oscillator during only operate and measures modes of operation. The logic-display A/D converter dissipates no power in the standby mode, low power while in operate mode, but considerable power during measure and display modes.

The nine-digit display employs light-emitting diodes (LED's) which exhibit a decreasing light output intensity with increased temperatures. At temperatures of $175^\circ F$ the output intensity of most LED's is approximately half the value emitted at $75^\circ F$. Because of the high level of ambient light on the moon in sunlight, combined with the visually degrading effects of the astronaut's helmet sun filters, it is of utmost importance to maintain a high value of LED light output. The large mass of the display module was used as the immediate LED heat sink. Special LED mounting surfaces were machined on a thickened portion of the aluminum display-module housing. The module was itself well coupled to the TG case as a heat sink. By such action,

TABLE 7-1

ELECTRICAL POWER DISSIPATIONS (IN WATTS)

Module \ Operation Mode	Standby (Stowage, Soakback, and Rests)	Operate	Measure (Incremental Amount)	Display (15-second Duration) (Incremental)	TRAVERSE Ave. of Operate and Measure plus Display for 10 Meas/Trav
VSA Amp and Sensors	0.030	0.030	-	-	0.030
E Frame					
Temp Controller	0.0175	0.0175	-	-	0.0175
2 Pend Amps	0.002	0.002	0.018 (195 s)	-	0.0036
Multiplexer	0.023	0.023	-	-	0.023
2 Pendulums	0.0028	0.0028	-	-	0.0028
1/2 Stepper Motor			2.7 (15 s)	-	0.0187
Total (E Frame)	0.0453	0.0453	-	-	0.0682
Middle Gimbal					
1 Stepper Motor	-	-	5.4 (15 s)	-	0.0374
Case Mounted:					
Logic-A/D Display	-	0.258	1.9 (195 s)	11.158	0.5075
Xtal Osc.	-	0.025	0.025 (195 s)	-	0.02725
Power Supply	0.127	0.776	2.776 (195 s)	8.538	1.087
1/2 Stepper Mode	-	-	2.7 (15 s)	-	0.0187
Total (Case)	0.127	1.059	-	19.696	1.64045
Phase-Lock Loop (on Battery)	-	0.495	0.04 (195 s)	-	0.499
Indicator Light (In Display Cover)	-	-	0.33 (15 s) + 1.325 (180 s)	-	0.1133
TOTALS	0.2023	1.6293	-	-	2.3558

39

the modules were kept well within acceptable limits for all types of thermal missions. More details on the mechanical design of the display are included in Section 8 where human-factors design considerations are discussed.

A thermal constraint was, however, imposed on the use of the display. Each time the data was displayed for approximately 15 to 18 seconds the LED's would dissipate in excess of 11 watts of power very locally. In development tests, it was found that near the LED location the temperature would rise approximately $5^{\circ}F$ per display reading. Right at the LED's the temperature change was not known but was felt to be considerably higher. Therefore, for reliability and maximum LED performance, it was recommended that no more than two successive displays be initiated. If a third display was required, a wait of at least 2 minutes is necessary.

7.7   Battery and Phase-Locked Loop

The TG power source is a 45 ampere-hour (nominal 7.5 volts) silver-zinc secondary (rechargeable) battery. It is placed in the bottom portion of the TG for mechanical stability. The battery size is dictated by the power requirements for thermal control in the worst-case cold mission.

Because the battery exhibits a sensitivity to temperature, efforts were made to control its thermal environment. At high temperatures, self discharge within the battery posed a problem on overall life expectancy. An easily achievable design goal of keeping the temperature below $125^{\circ}F$ was specified. At low temperatures, the cell voltage decreases, again limiting the amount of energy that can be derived. More important, however, is the fact that in the TG certain voltage regulators require a minimum driving voltage in order to function. As a result, a minimum battery temperature of $40^{\circ}F$ was specified. To ensure this, a 1-watt heater, controlled in an on-off mode by a thermostat, was installed in the battery. The maximum duty cycle on the heater, under the coldest conditions, was estimated to be approximately 2/3rds, leaving a 50% heater power margin. An overly large heater was not selected for fear of causing large voltage changes at the battery when turned on. Such changes could potentially influence the sensitive electronic control and measurement circuitry on the inner structure. This same fear existed on the heater selection for the I oven. In selecting the battery heater it was estimated that battery self-heating due to internal resistance was negligible. Because the battery contained a heater it became a factor in the system power budget, necessitating good thermal isolation from the surrounding case structure.

The temperature-sensitive phase-locked loop filter was mounted to the upper surface of the battery in order to achieve thermal stability. The phase-locked loop is sensitive to rates of temperature change during a measurement and not to the value of temperature itself. It was located on the battery for three reasons:

40

(1) It is too large to put on an inner structure member or E frame.

(2) It could take advantage of the large thermal mass of the battery in order to minimize its time rate of temperature change.

(3) It's own electrical power dissipation can augment the battery control power required in a cold mission, minimizing the total energy consumed.

A maximum rate of temperature change of $0.02°F/minute$ was obtained. The presence of the phase-locked loop further emphasized the desire for the thermal isolation of the battery from the case. The battery itself was mounted to the case with hollow plastic (NEMA G-10) standoffs which exhibited a total thermal conductance of 0.092 Btu/h. $°F$. The outer surface of the battery was buffed and gold plated. The phase-locked loop module was potted within its housing and covered with low emittance aluminum tape in order to minimize radiation interchange with the case. The total radiative view area from battery/phase-locked loop and the case was approximately 0.0587 square feet; which, when combined with the thermal mass resulted in a first-order thermal time constant of 75 hours relative to the TGE case.

7.8   Multilayer Thermal Blanket

All external surfaces of the TG are covered with a multilayer thermal protection system or blanket designed jointly with, and fabricated by, the Arthur D. Little Company of Cambridge, Massachusetts. The blanket is a critical component in the thermal performance of the TG because it minimizes the thermal response of the case to external thermal changes and therefore enhances the performance of not only the critical inner structure, but also the case-mounted modules. In an instrumented test, the thermal blanket displayed an overall effective emittance (including covers) of less than 0.01. This effective emittance can be seen in the following radiative equation for heat flow rate as a function of temperature difference:

$$q = \sigma A_s \epsilon_{eff} (T_s^4 - T_{case}^4) \qquad (7-1)$$

where

ϵ_{eff} = blanket effective emittance

A_s = blanket surface area

T_s = blanket surface temperature

T_{case} = TG case temperature

σ = Stefan-Boltzmann constant

The above emittance produced an equivalent linear conductance through the blanket of approximately 0.07 Btu/h -°F at a 100°F case temperature.

The body of the blanket is 3/8-inch thick and contains 10 layers of double aluminized mylar, each layer of which is spaced apart by 2 layers of dacron bridal-veil material. The outer surface of the blanket is an enclosure of 3.2-ounce-weight blue dacron cloth for abrasion resistance and as a container for the blanket itself.

The blanket assembly is basically two separate pieces which mate at a parting line around the lateral surfaces of the TG. In order to assemble the blanket to the TG, first the top portion of the blanket is installed as a unit. Subsequently the TG is inverted and the lower portion is interwoven at the parting line layer-by-layer. The parting line itself is distributed in the form of five staggered steps of 2 aluminized layers per step over a distance of approximately 1.5 inches. This means of assembly is simple and yet minimizes radiative leakages at the parting line. The parting line of the outer dacron cover is sealed by a hand lacing with nylon cord. Lacing is employed in favor of a zipper because it is less bulky.

An important feature of the blanket is the fact that the three push-buttons in the display area are activated by pushing on the outer surface of the blanket in 1-inch circular spots labelled BIAS, GRAV, and READ. The force for button depression is transmitted through the blanket itself. This design feature minimizes blanket penetrations and therefore heat leaks.

In order to provide the force for button activation with minimum compression and damage to the blanket, the button areas contain discs of rigid foam stitched into the blanket. Good blanket fatigue life with such a design was observed.

The main body of the blanket has four large and eight small penetrations. The large penetrations are for the display and radiator, over which hinged covers are sewn; and the two ends of the outer gimbal mounts, over which removeable cups are fastened. The display and radiator covers are fabricated of five layers of vacuum-formed vacuum-coated polysulfone plastic spaced apart by a low conductance rigid foam. The covers overlap the main body of the blanket by approximately one-half inch in order to minimize thermal short circuits by the blanket surface. The covers are pivoted on plastic hinges stitched into the blanket itself and fastened to the covers. The launch-load hold-down for the covers is by a removeable orange velcro piece which is discarded at the lunar surface. The cover fastening for lunar operations is by a soft magnetic latch which provides a latching force of approximately twice the earth weight of the cover. This latch is not strong enough to overturn the TG when the covers are opened while the TG is resting on the lunar surface. The display cover is held open by an arm which bears a magnet that contacts a pole piece on the top surface of the blanket when the cover is pivoted 90 degrees.

A light is mounted in the top surface of the display cover which indicates when the instrument is levelling itself (flashing light) and when a measurement is being made (solid light). The light is mounted to an aluminum heat sink which distributes the electrical heat throughout the top of the display cover.

The other large penetrations to the main blanket body are the outer gimbal mounts. These cup-shaped covers also consist of five layers of vacuum-formed vacuum-coated polysulfone plastic with each layer separated by two layers of bridal veil and a layer of double aluminized mylar. The gimbal-mounted covers are separate portions of the blanket which are installed as the layers of the lower portion of the blanket are installed.

The eight small blanket penetrations comprise three hard-mount penetrations, two of which are used for soft mounting during lunar operations; two handle penetrations, and three bottom penetrations for the feet. The following is a tabular breakdown of the heat leaks through the blanket due to the small penetrations:

Penetrations	Quantity	Conductance (Btu/h-$^{\circ}$F)
Hardmount/Softmount	3	0.0066
Handle	2	0.00372
Feet	3	0.0046
Total	8	0.0149

It can be seen that the penetration conductance is small compared to the equivalent blanket conductance of 0.07 Btu/h-$^{\circ}$F.

Polysulfone plastic was chosen for all vacuum-formed portions of the blanket because it exhibits good strength properties up to a temperature of approximately 325°F. Lexan plastic was ruled out because its softening temperature is approximately 280°F. It can be seen by an analysis in Appendix C that thermally black adiabatic vertical surfaces looking at a flat hot moon can attain temperatures of close to 280°F when receiving simultaneous solar input and radiation from the moon. The sun elevation angle at which one would obtain a maximum temperature on a vertical adiabatic surface much like that of the blanket is 26.6 degrees. All TG missions, whether cold or hot, could have been exposed to this sun elevation angle. It was feared that either the side cones or the front of the display cover could soften and distort under such conditions. As a result polysulfone plastic was adopted for all plastic parts of the blanket.

43

7.9 Visual Thermal Performance Indications

Based on the interface information provided by the Grumman Aerospace Corporation specifying temperature bounds on the Quad III LRV pallet (Fig. 7-1) the thermal design as described was very adequate to achieve the mission requirements. It was, however, desirable to receive positive confirmation of thermal performance during a real mission. In addition, if the interface temperatures were altered late in the program or in error, the thermal mission could be marginal or in jeopardy. Furthermore, the real-time ability to implement lunar-surface contingency procedures pointed out the need for knowledge of the TGE thermal conditions and safety margins.

As described earlier, the fact that the astronaut would manually read gravity data and voice it to earth in real time provided a simple means of simultaneously receiving thermal information. The last two digits of the nine-digit data display were chosen as coded thermal information. The coding is given in Table 7-2. The eighth digit codes both the sign of the ninth digit and four gross thermal conditions on the instrument; nominal, cold, warm, and very warm. None of the eight-digit indications can alone specify a failure or even a time of failure. They can, however, give an excellent indication of the general thermal health of the instrument. If the time is known when the indication changes from one condition to another, as will be seen later, thermal-math models enable the prediction of the safety margin or the expected time before a thermal failure occurs.

A cold indication is registered by a thermostat on the battery which activates for temperatures below $47^{O}F$. This thermostat is the second one found on the battery. Using one for control during a cold mission and one for cold-mission indication eliminates electronic logic which would be associated with the $40^{O}F$ control thermostat. The battery was selected for the cold-alarm switch because in a cold mission the battery energy output and the control of its own temperature is of major importance.

The warm indication is derived from a thermostat mounted on the I oven which closes for temperatures in excess of $95^{O}F$. If such an indication is seen, it is felt to be a good sign in that the unit is not in danger of overheating and yet minimizes battery energy required for heating.

If the battery temperature is above $47^{O}F$ and the I oven is below $95^{O}F$, a nominal thermal mission is indicated. This is the most desirable type of mission from a battery-power and thermal-control point of view and is indicated by either a zero or one in the eighth display digit. A zero was observed throughout the Apollo 17 lunar mission.

44

TABLE 7-2

TEMPERATURE ALARMS AND CODES

Digit	EIGHTH DIGIT		NINTH DIGIT
	I Oven (T_I)	Battery (T_B)	Shift of P-Oven Temperature From Original Set Point
0	$60 < T_I < 95^O F$	$47^O F < T_B$	$+ 0.009^O F$ per unit of ninth digit
1	$60 < T_I < 95^O F$	$47^O F < T_B$	$- 0.009^O F$ per unit of ninth digit
2	$60 < T_I < 95^O F$	$40 < T_B < 47^O F$	$+ 0.009^O F$ per unit of ninth digit
3	$60 < T_I < 95^O F$	$40 < T_B < 47^O F$	$- 0.009^O F$ per unit of ninth digit
4	$95 < T_I < 110^O F$	$47^O F < T_B$	$+ 0.009^O F$ per unit of ninth digit
5	$95 < T_I < 110^O F$	$47^O F < T_B$	$- 0.009^O F$ per unit of ninth digit
6	$110^O F < T_I$	$47^O F < T_B$	$+ 0.009^O F$ per unit of ninth digit
7	$110^O F < T_I$	$47^O F < T_B$	$- 0.009^O F$ per unit of ninth digit

The very warm indication (6 or 7) is again derived from a thermostat on the I oven which activates when the temperature is nominally above $110^{O}F$. This alarm is included primarily to indicate the status of the I oven immediately upon removal of the TGE from Quad III. If the I-oven temperature is above $110^{O}F$ at the beginning of the first EVA it was a mission rule that the astronaut place the TG in the shade of the LM and not take it on the first traverse. At the completion of the first EVA and rest (20 hours total),the TG I oven should have cooled below $110^{O}F$ such that it should be able to complete the remainder of the mission normally.

As seen in Table 7-2, the 9th digit of the display represents how many increments the precision oven temperature has deviated from its nominal set point. Each digit represents an increment of $0.009^{O}F$. The sign of this increment is coded into the eighth digit.

During the flight of Apollo 17, personnel from both NASA and MIT, who were cognizant of every phase and function of the TG, were present in Mission Control in Houston. Any anomalous temperature behavior, as shown by the 8th and 9th digits, could have been interpreted by these personnel and recommendations made.

7.10   Apollo 17 Mission - Thermal Results

The Apollo 17 mission finally launched at 0:33 hours (EST) on 7 December 1972 after a 2-hour-40-minute hold. The translunar stowage thermal prediction, shown in Fig. 7-1 was supplied by Grumman personnel in real time. The timeline is completely nominal in that time lost during the launch pad hold was made up during the translunar phase. It can be seen that at the time of landing (14:55 hours, EST, 11 December 1972) the LRV pallet temperature was estimated to be $24^{O}F$. Premission thermal predictions for a nominal mission (see Fig. 7-1) estimated that the pallet temperature at landing should be approximately $27^{O}F$.

Figure 7-3 is a computerized estimate of the lunar mission thermal response from the time of landing based on the initial conditions established by the full trans-lunar stowage history. It can be seen that approximately 5 hours after landing, the TGE was removed from Quad III, the hardmount pins removed, and the unit placed in the operate mode for EVA 1. At no time during the lunar mission did the I-oven temperature reach $95^{O}F$ to indicate a warm mission, nor did the battery temperature drop to $47^{O}F$ to indicate a cold mission. The mission was completely nominal. This fact was borne out by every lunar surface data reading for which a zero appeared in the eighth display digit every time. The ninth digit was similarly constant during the lunar mission, always reading a digit one. Thus, it is concluded that Apollo 17 experienced a slightly colder than nominal mission and the P oven controlled within $0.005^{O}C$ throughout the lunar mission.
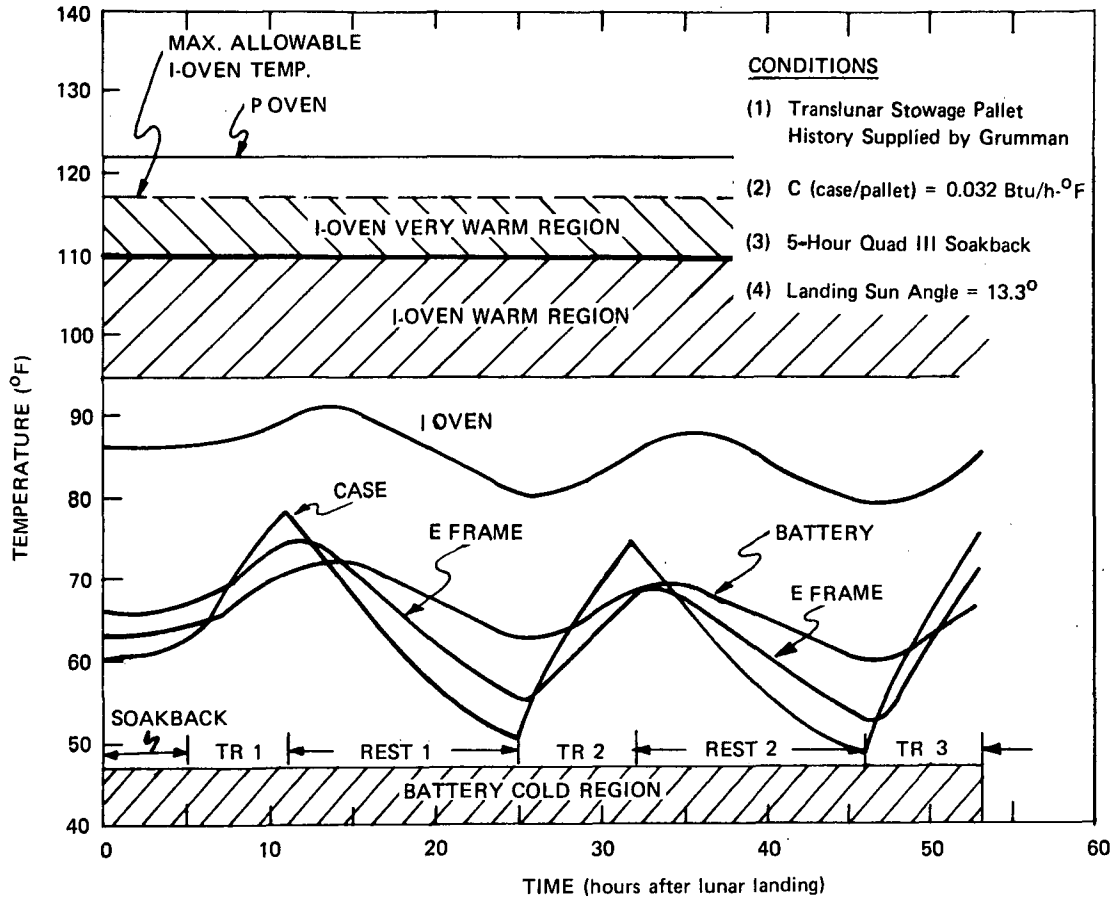
Fig. 7-3   Apollo 17 lunar mission computerized thermal response.

SECTION 8

HUMAN FACTORS

Flight-crew-operation considerations impacted the gravimeter design in several areas besides the obvious size and weight constraints. The two prime human-factor-engineering problems were the development of the instrument display panel and the latch for securing the gravimeter to the isoframe on the geology pallet.

A red light-emitting diode (LED) display was selected early in the program for low-electrical-power requirements for light-emitting efficiency and for direct-drive compatibility with the digital logic. A display breadboard was built and tested in a brightly sunlighted ambient. This breadboard demonstrated several serious problems in visibility (readability). These problems consisted of several different characteristics but could be grouped together as exhibiting poor display "contrast" under the test conditions. The objectionable characteristics observed were: 1) bright first-surface reflections from the faceplate, 2) objectionable secondary (internal) reflections, 3) poor background color (white/grey) of the LED background, and 4) internal light scattering.

Readability of a display can be expressed by measuring the brightness of a display and the brightness of the background and comparing them as a ratio. This ratio is called "contrast." More specifically, contrast (C) is

$$C = \frac{B_1 - B_2}{B_2} \qquad (8\text{-}1)$$

where

B_1 = the brightness of the LED character
B_2 = apparent brightness of the background

From this equation, contrast can be improved by increasing the brightness of the display or by decreasing the apparent brightness of the background.

A red or grey filter is normally used for this type of display to suppress the undesirable characteristics noted above. However, a filter of this type absorbs 75 to 90% of the light emitted by the LED. The traverse gravimeter display could not

tolerate a loss of this magnitude under the brightly sunlighted ambient of the lunar surface. A display system was utilized which uses no light absorbing filters. Figure 8-1 illustrates the design features of the gravimeter display panel.

In order to enhance contrast, B_1 was increased by selecting LED's for maximum light output (efficiency). This increased the brightness by 50%. The apparent background brightness, B_2, was improved by using a dark substrate and coloring the adjacent microcircuitry black. The first-surface external reflections were minimized by tilting the display faceplate 20 degrees to the Line of Sight (LOS). The reflection of the observer's LOS was thereby directed to a black surface (the underside of the display cover). The LED display was recessed into the traverse gravimeter so that the observer was looking into a shallow dark well. This limited the observer to a 20 degrees viewing angle but greatly enhanced the readability. The stray light in the system was trapped in a seven-layer baffle (see Fig. 8-1). Finally, the scattered light from the LED was minimized by painting the LED package exterior black except for a small viewing window.

Field test results indicated the gravimeter display was difficult to read when not shaded from direct sunlight or under bright diffuse lighting conditions. No trouble was anticipated during lunar operations because there would be no atmosphere and shadows would appear black. During the mission debriefings, the crew was asked for their comments which confirmed our design assumptions. Indeed, the crew said they would recommend this type of display for future spaceflight applications. By careful attention to preserving light transmission and enhancing contrast, a light-emitting diode can be designed for a high ambient-light background.

The mounting system which attaches the traverse gravimeter to the isoframe has two modes of operation. The first is the launch/boost phase or "hard mount" and the other is the Lunar Rover phase.

In the first, the traverse gravimeter is rigidly attached to the isoframe by means of stainless-steel mounting pins secured into stainless steel bushings in the TG base housing by means of ball-lock (PIP) pins. (The ball-lock pins and mounting pins are connected by a lanyard which is pulled by the astronaut.)

There are three bushings in the base housing; one in each side, and one in the bottom. No effort was made to thermally isolate the traverse gravimeter from the pallet in the launch/boost mode, but provisions had to be made in the mounts to provide this isolation on the moon.

Fastened to each bushing is a thin walled (0.030-inch) tube made of laminated epoxy glass (NEMA G-10). When the "hard" support pins (concentric with the G-10 tube) are removed by the astronaut, the two side mounts "drop" a small distance (0.020 inch) and come to rest on small lips of the support fitting mounted on the

49

20° VIEWING CONE
(FIELD OF VIEW)

LINE OF SIGHT

PRIMARY REFLECTIONS
OF SUNLIGHT & HELMET
VISOR IMPINGE UPON
BLACK SUNSHADE

SOLAR ELEVATION ANGLE
15° NOMINAL

DISPLAY
FACE
PLATE

LIGHT TRAP
BAFFLING

LED PACKAGE

PUSH
BUTTON

LED DISPLAY

SECONDARY
REFLECTIONS
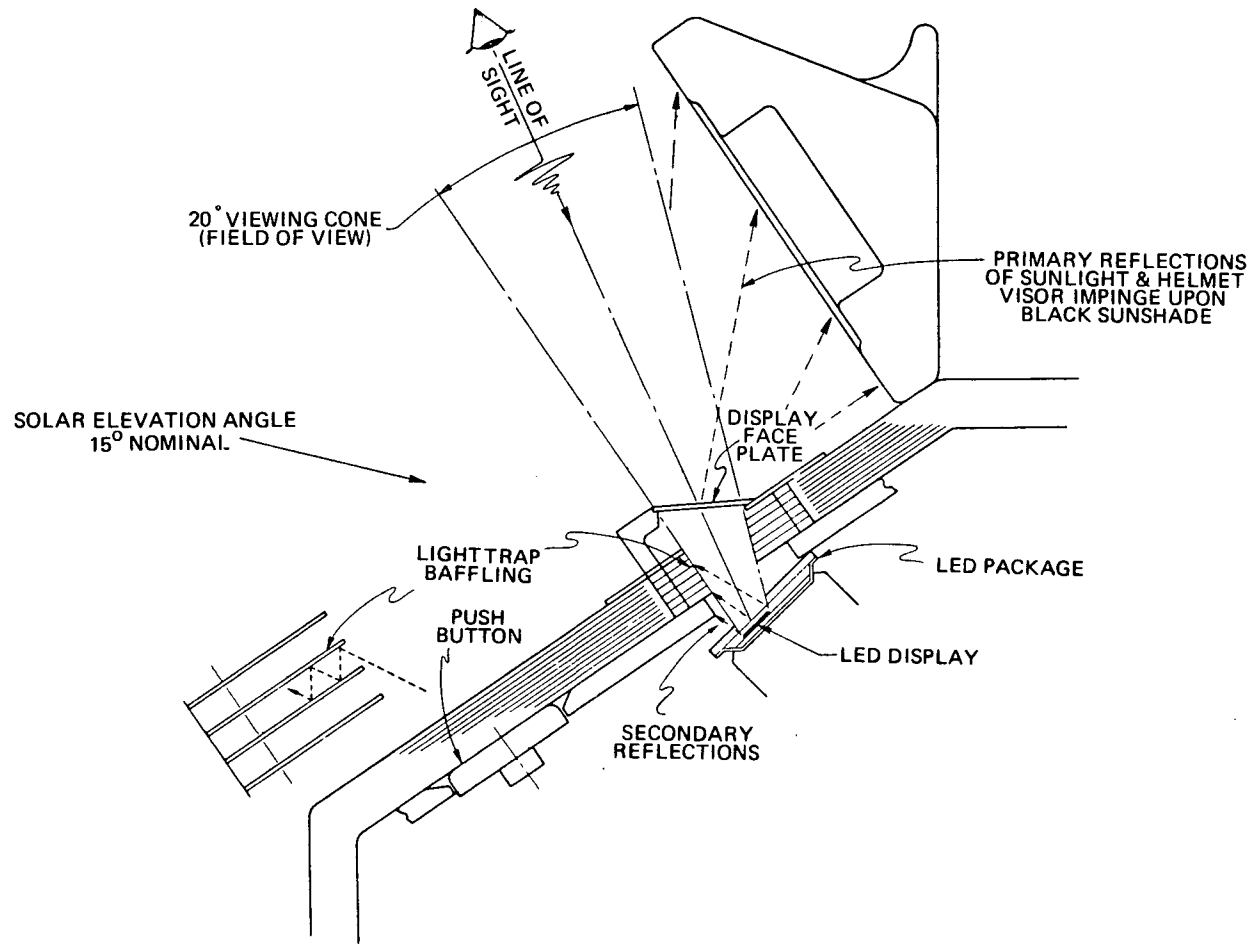
Fig. 8-1   LED numeric display technique.

isoframe. These side mounts provide thermal isolation between the traverse gravimeter and the isoframe, and at the same time provide structural support for the Lunar Rover environment.

The carrying handle is used to secure the traverse gravimeter in place on the Rover (see Fig. 8-2). A cam is fastened to the pivot portion of the handle which is free when the handle is vertical. When the handle is rotated (about 45 degrees forward) the cam comes in contact with a spring (on the isoframe fitting). When the handle is in contact with the isoframe, the spring is "over center" on the cam, and a lug on the spring comes in contact with the NEMA G-10 side mount. Thus, upward motion of the traverse gravimeter is prevented by this attachment. To release this lock, and remove the TG from the Rover, the astronaut must rotate the handle to the vertical position.
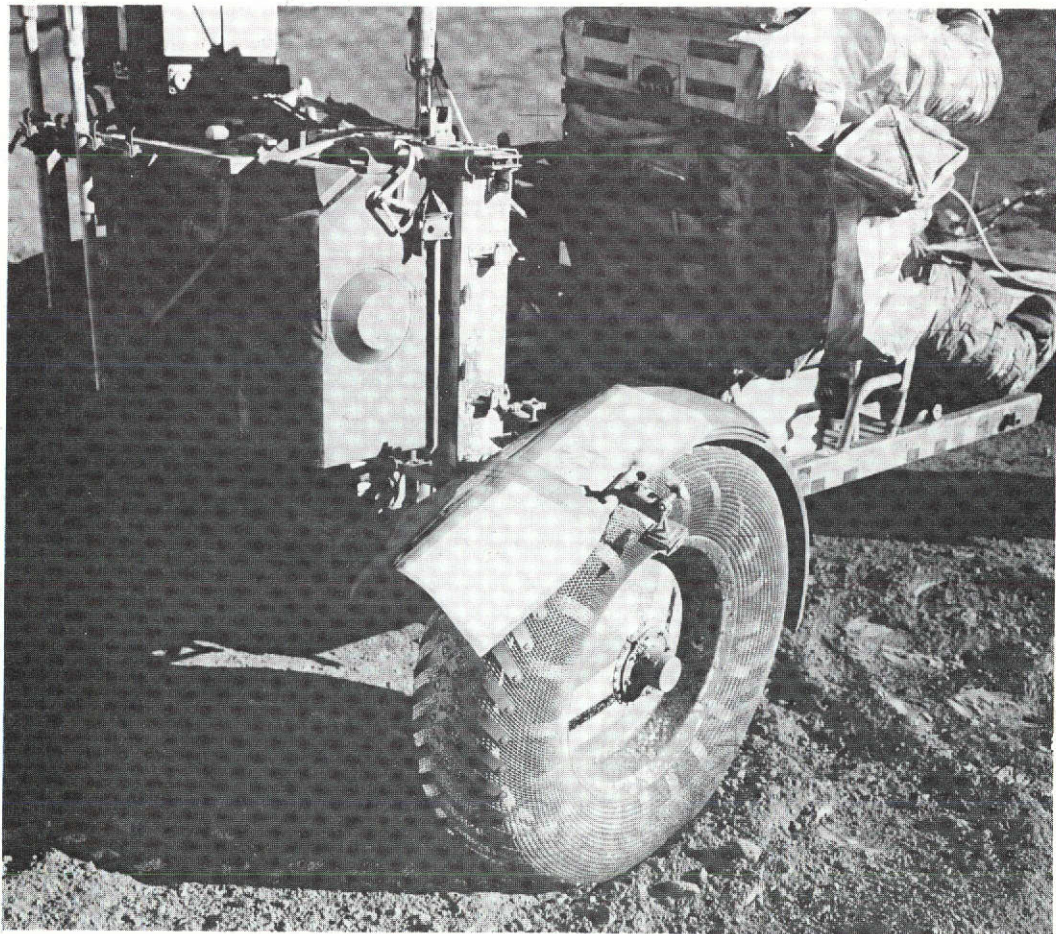
Fig. 8-2   Gravimeter ready for EVA 2.

To prevent rotation of the traverse gravimeter about the side mounts the two back feet (of the TG) are restrained by brackets mounted on the isoframe. System constraints were due to operational, thermal, and volumetric requirements (both on the Rover and in the LM).

Operationally the requirements were for one-hand operation (by the astronaut) in removing and installing the traverse gravimeter. The release forces of the handle and pins were subject to astronaut approval.

The design was influenced by thermal consideration because of the thermal isolation required on the moon. Also, a minimum number of penetrations through the thermal blanket was essential. The handle had to be mounted to the TG by means of a thin-walled NEMA G-10 cylinder, since it contacted the isoframe.

There was also a volume constraint. The volume in the LM storage area was bounded by the pallet carrying handles. Thus, the handle on mounts could not exceed those limitations. On the Rover, another restraint was the clearance required between the traverse gravimeter blanket and the Rover fender, when the pallet was rotated 90 degrees. Because of this, the TG (and the mounting system) had to be located as close to the pallet as possible.

The gravimeter was removed from the Rover six times during the flight. The flight commander commented during EVA 1 that remounting the gravimeter was a "piece of cake." During EVA 3, Captain Cernan mentioned that the accumulation of lunar soil (dirt) was making "even the gravimeter" more difficult to relatch. The gravimeter attachment proved very reliable as on previous field trips over rough terrain. When the geology pallet swung open, while the crew was driving the Rover between Station 9 and the Lunar Module, the traverse gravimeter remained secure although other tools were lost as the tail gate undoubtedly swung back and forth against its stops.

SECTION 9

INSTRUMENT ERROR ANALYSIS

The gravimeter error analysis describes the component constribution to system errors. The analysis takes into account all known major error sources.

9.1   Background Notes

The vibrating-string accelerometers produce a signal (the difference frequency of the two string outputs) that can be expressed as a series in gravity.

$$\Delta f = f_1 - f_2 = K_0 + K_1 g + K_2 g^2 + K_3 g^3 + \ldots \qquad (9\text{-}1)$$

where

Δf =   difference frequency
K_0 =   bias (Hz)
K_1 =   scale factor (Hz/g)
K_2 =   2nd order correction term (Hz/g^2)
K_3 =   3rd order correction term (Hz/g^3)

For the data reduction, K_2 and K_3 will be used (higher order terms are negligible), but for the error analysis, we can consider

$$\Delta f = K_0 + K_1 g \qquad (9\text{-}2)$$

In the instrument error budget, K_0 is called the VSA "bias" and K_1 is the "scale factor."

9.2   VSA Shock Sensitivity

We can find the VSA sensitivity to mechanical shocks as follows:

$$g = \frac{\Delta f - K_0}{K_1} \qquad (9\text{-}3)$$

$$\Delta g = -\frac{\Delta K_0}{K_1} = -\frac{1}{129.1}(\Delta K_0) \text{ for } K_1 \text{ constant} \qquad (9\text{-}4)$$

53

$$\Delta g = \frac{K_0}{K_1^2} (\Delta K_1) = \frac{7.21}{(129.1)^2} (\Delta K_1) \text{ for } K_0 \text{ constant} \qquad (9\text{-}5)$$

To keep the absolute error in a gravity measurement less than 5 mgal, therefore, the scale factor shift during launch must be less than 0.012 Hz/g. Launch vibration testing indicated that a worst-case scale-factor shift was 0.0003 Hz/g, so that this term can be reasonably ignored.

To keep the same 5-mgal error however, the bias shift would need to be less than 0.00065 Hz. Since vibration testing indicated this shift is quite possible, provision was made for measuring and updating the bias on the moon to correct for a launch shift.

(Field tests indicated that Rover vibration and gravimeter deployment were below the threshold for causing bias shifts, and normal procedures did not plan for bias updates at each traverse station. Post-flight analysis implied, however, that Rover-deployment shifts were the greatest error sources although no exact cause could be found.)

9.3 Δ Bias (VSA)

This is the random portion of the bias term which is not reflected in the linear bias drift equation. The 1σ value of this term is provided by regression analysis of bias as a function of time on actual VSA's which are temperature controlled to about $\pm 0.001^\circ$C. A typical value of the ΔBias is 0.1 mgal for a good instrument.

9.4 Δ Bias as f (T) (VSA)

This term is the change in bias due to change in temperature of the VSA. Assumption is that the actual temperature of the VSA is the indicated temperature $\pm 0.01^\circ$C and is equally likely to be anywhere in that range.

$$\frac{0.02}{\sqrt{12}} \approx 0.006^\circ\text{C} = \sigma_{Temp} {}^{*} \qquad (9\text{-}6)$$

A typical value of the temperature sensitivity of bias is 5 mgal/$^\circ$C for a good instrument. Therefore, the 1σ value for ΔBias f (T) is (0.006)(5) = 0.03 mgal.

---

*For a uniformly distributed random variable between a and -a, the standard deviation is $\frac{2a}{\sqrt{12}}$.

9.5 ΔSF

Determination of the linear scale factor by a least-squares regression to actual data taken from good, but typical, VSA's leaves a random portion unaccounted for by the regression equation. The 1σ value for SF is 0.04 ppm. The contribution to system measurement error then is a linear function of the value of g being measured. Therefore, on the moon, the 1σ error term should be:

$$(0.04)\ (10^{-6})\ (1.6)\ (10^5 \text{ mgal}) = 0.0064 \text{ mgal} \qquad (9\text{-}7)$$

9.6 ΔSF f(T)

Using the same value for the 1σ temperature deviation as in ΔBias f(T), and using the ΔSF assumptions as before, we can calculate the measurement error due to the change in scale factor which is a function of temperature. The sensitivity of scale factor to changes in temperature is typically 35 ppm/$^{\circ}$C. On the moon, the 1σ error value is:

$$(35)\ (10^{-6})\ (0.006)\ (0.16)\ (10^6) = 0.035 \text{ mgal} \qquad (9\text{-}8)$$

9.7 Leveling (cos θ)

This is the error term due to the slight offset of the VSA input axis from vertical. The pendulums level the gimbal assembly to within ± 3 arc minutes of their null. There is, in addition, a slight angular offset of the pendulum null from the VSA input axis.

Appendix F details the derivation of the following error. With the typical pendulum-VSA angle of 1 arc minute and a typical pendulum deadband of ± 3 arc minutes, the standard deviation of the gravity measured will be:

$$\sigma_g = 0.04 \text{ mgal (moon)} \qquad (9\text{-}9)$$

9.8 Quantization

There is a slight loss of accuracy in the measurement due to the digital readout. The quantization (mgal/count) can be considered a range over which each count may be. If we assume a uniform distribution, then the variance σ^2 is found by

$$\sigma^2 = \frac{Q^2}{12} \qquad (9\text{-}10)$$

where:

Q = quantization in mgal

σ = standard deviation in mgal

(See chart in Appendix C)

For typical cases

$$\sigma^2 = 0.0002 \text{ mgal}^2 \text{ (moon)} \tag{9-11}$$

9.9 VSA Amplifier Power-Supply Sensitivity

Tests indicate that good but typical VSA amplifiers can show a sensitivity of approximately 0.4 ppm to changes of 0.2% in power-supply voltages. The power-supply outer limits on VSA amplifier voltage is $\pm 1/4\%$. The short-term random noise of the power supply is about 0.04% (this would affect short-term repeatability). Again, taking the most conservative distribution (uniform) the 1σ value of power supply changes would be $\dfrac{0.4\%}{12} = 0.12\%$

so on the moon

$$(0.4 \times 10^{-6}) \left(\tfrac{1}{6} \times 10^6\right) \left(\tfrac{0.12\%}{0.2\%}\right) = 0.04 \text{ mgal} \tag{9-12}$$

9.10 VSA Amplifier Temperature Sensitivity

VSA amplified temperature sensitivity is 2 mgal/$^\circ$C so that the 1σ gravity error on the moon is

$$(2/^\circ C) (0.006^\circ C) \sigma 0.012 \text{ mgal} \tag{9-13}$$

9.11 Slow-Loop Bias Uncertainty

The slow-loop uncertainty is a shift around any constant linear bias drift in the phase-locked loop. Earth tests imply a 1σ value for the phase-locked loop of 0.5 mgal on earth, which becomes 0.1 mgal on the moon.

9.12 Environment

We conservatively pick 0.1 mgal as a 1σ error due to Rover vibration (or equivalent surface motion), although the curves in the appendix show this as a "maximum" level. (See Environmental Error Analysis, Appendix G).

9.13 Summary

In evaluating the resultant total system error, it should be kept in mind that the summation in Table 9-1 implies that all the terms are independent. Obviously, there will be significant correlations between the three terms which are functions

56

of temperature. However, these terms are all relatively small, and therefore their correlations should not add significantly to the system error.

Finally, it is reasonable to treat the resultant system error as normally distributed (by Central Limit Theorem) which therefore implies that approximately 68% of the time the system will operate within the ± 1σ errors derived in Table 9-1.

TABLE 9-1

SUMMARY OF ERRORS

Term	Source	Moon	
		σ	σ^2
1	Δ Bias	0.1	0.0100
2	Δ Bias f(T)	0.03	0.0009
3	G Δ SF	0.01	0.0001
4	G Δ SF f(T)	0.035	0.0012
5	Leveling	0.04	0.0016
6	Jitter	0.10	0.0100
7	Environment	0.10	0.0100
8	Loop Bias	0.10	0.0100
9	VSA Amp f (PS)	0.04	0.0016
10	Quantization	~	0.0002
11	VSA Amp f (T)	0.012	0.0001
	Total	(σ_T^2)	0.0457

$$\sigma_T = \sqrt{\sigma_T^2} = 0.21$$

SECTION 10

ENGINEERING TESTING

The Traverse Gravimeter was designed to be a completely self-contained instrument for measuring lunar gravity differences of one part in 10 million. It was planned that the unit would operate for 15 days, sealed in a protective blanket, using the vacuum of space to provide adequate thermal isolation for the precision oven assembly around the vibrating-string accelerometer (VSA) used as a gravity sensor. It was, therefore a very difficult instrument to test in the one-g air-filled earth environment.

After the basic design was verified by electrical breadboard and mechanical mock-up testing, an engineering model was built to preliminary flight standards. This model provided the first test of the gravimeter as a working system. The unit was continually updated, throughout the test program, to the latest flight hardware design, and proved quite useful in test evaluation and concept verification.

10.1   Performance Tests

Provision was made for general performance testing by including a vacuum fitting in the intermediate oven design, thereby allowing the double-oven temperature-control system to maintain a stable temperature for the VSA. A different countdown logic was also incorporated to scale the accelerometer output on earth for the display format of the lunar mode. Pressure-switch bypasses and an external power plug completed the test modification.

The initial performance tests with the engineering model were 6-hour stability tests made on a large granite slab isolated from the surrounding floor. These tests checked gravimeter drift and determined the standard deviation (repeatability) of the displayed output in a constant-gravity environment. Seventy-two measurements were normally made during this period to maximize the data sample. Other tests were also run to determine VSA-bias and scale-factor stability, (see Fig. 10-1). Accurate logs were kept to follow these values throughout the test program. These performance tests verified the ability of the gravimeter to consistently measure gravity to the desired accuracy over a period of time approximating a lunar traverse.
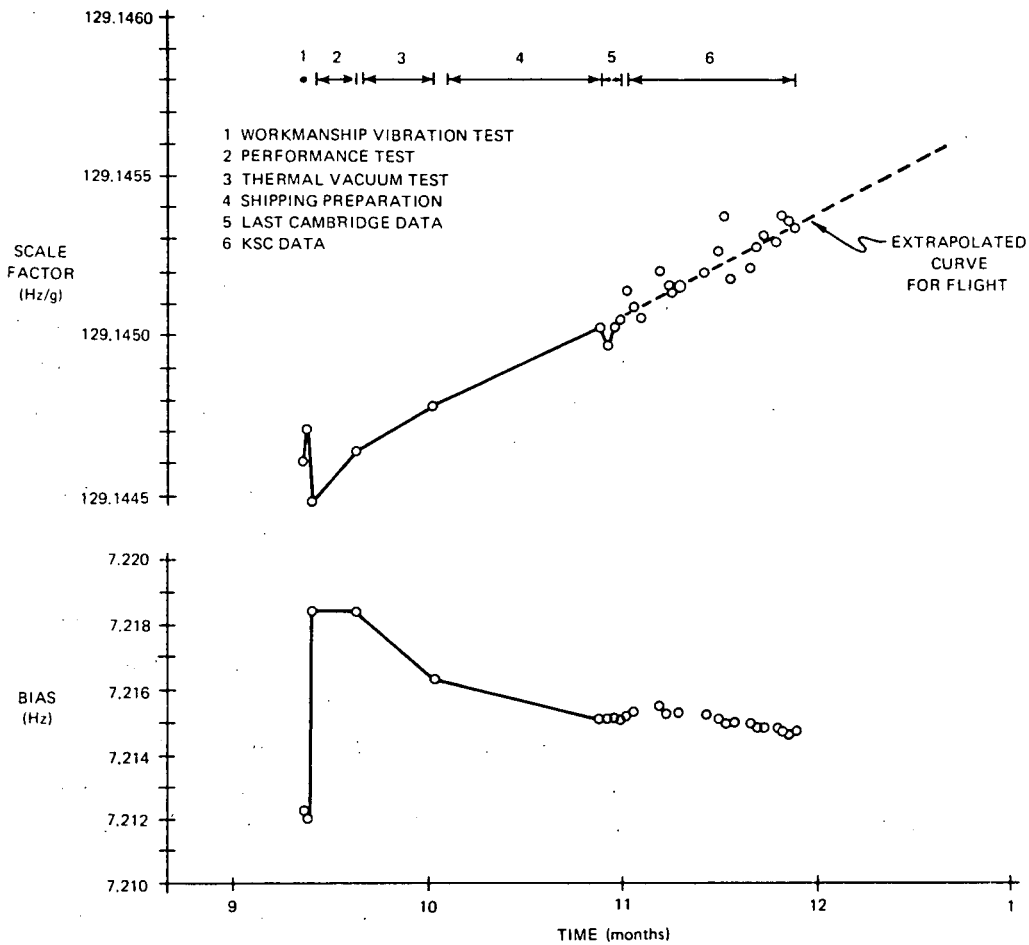
Fig. 10-1 Scale factor and bias vs. time for prime flight gravimeter.

10.2 Thermal Tests

The next step in testing was the verification of the system's ability to measure gravity in the thermal environment of the moon. The thermal-vacuum chamber, with a detailed Rover-pallet simulator, was used to produce the environmental inputs of possible lunar missions to the gravimeter. A well-instrumented but nonfunctional thermal model was used in the early design stages to define performance parameters, prepare the test apparatus, and develop a mathematical computer model of the gravimeter.

Thermal testing of individual modules verified their ability to withstand the temperature extremes expected. It remained for the engineering model, this time complete with blanket and battery, to ensure that the gravimeter would give accurate data under thermal-vacuum conditions simulating those of a real mission. These

engineering tests also were used to update the computer model of the gravimeter. The accuracy of the computer predictions of gravimeter temperature profiles proved invaluable in evaluating different mission conditions without the time and expense of the thermal-vacuum facility. (A complete description of the test apparatus and TG thermal-vacuum tests may be found in another report.)*

10.3   Mechanical Tests

Concern over the ability of the gravimeter (particularly the VSA) to withstand the Saturn V launch motivated considerable vibration testing. A mechanical model accurately simulating the dynamics of the gravimeter but containing a vibration accelerometer in place of the VSA was used to evaluate the shock and vibration environment of the VSA. Although the VSA parameters (bias and scale factor) were known to be sensitive to shocks, it was felt that the levels experienced at the inner (precision) oven were low enough to preclude VSA damage.

The engineering model underwent vibration testing in April 1972, using "workmanship" vibration levels. The test was run for 1 minute, and the gravimeter was checked afterwards to ensure that no damage was caused. The test was then continued for 3 more minutes, and the gravimeter was again checked, but this time there was no VSA output. A teardown inspection** revealed that one of the VSA string-mass-cross-tie systems had broken. Further investigation showed that the VSA mass system had secondary vibration modes at frequencies close to those of the oven-gimbal structure.

Two major design changes were then initiated. First, the wires used to hold the intermediate-oven to the electronics frame (inner gimbal) were increased in diameter to change the oven resonant frequencies, at a slight decrease in thermal efficiency. Second, a shock-abosrbing isolation frame was designed to interface between the Rover pallet and the gravimeter. Later engineering testing and the Qualification and Acceptance Testing of the flight gravimeters verified the ability of the improved design to survive the full flight vibration levels with acceptable bias and scale factor shifts.

---

*Dafnoulelis, C.V., R.T. Martorana, and W.A. Vachon, Thermal-Vacuum Test of the Apollo 17 Lunar Traverse Gravimeter Experiment, Charles Stark Draper Laboratory   Report E-2759, April 1973.

**See memos GRV-112-A, GRV-167-T, and Internal Failure Report TG 017.

10.4 Field Tests

Field testing proved to be an invaluable aid in developing procedures for using the gravimeter during the flight and in giving the flight crew experience with a working instrument in near-flight configuration. The engineering model was modified with a new front foot and a flight-like blanket. The front foot incorporated an external power-input plug and switch and a temperature-control circuit to enable use without a vacuum pump. The front cover and flight-like blanket had a trap-door installed to facilitate battery changing between field trips for a faster turn-around time. This prototype thus resembled a flight unit yet would give accurate data on earth.

The first field trip was to Kennedy Space Center (KSC) in July 1972. An electromagnetic interference test was held with all other Rover equipment on Apollo 17, and the results indicated no problems for the gravimeter. While at KSC, a test was made using the training Rover to evaluate the traverse shock environment of the Rover. The gravimeter experienced two bias shifts, but at the end of the test it was discovered that the pallet latch was loose and that the pallet had more free play than usual. (This served to invalidate the Rover test, although a loose dust-covered latch would plague the flight gravimeter at the end of the mission.)

It was decided to replace the engineering model VSA with one of better performance, which had just become available (the two best VSA's were saved for the primary and spare flight units.) The KSC test was eventually repeated in October with a better VSA and a latched Rover tailgate. This series of tests demonstrated no major reaction to Rover rides.

Two field tests were made with the astronauts. One was a trip to Black Hawk, California, a site which was hoped to be geologically similar to the Taurus Littrow landing site. The traverse gravimeter not only showed excellent agreement with a commercial survey gravimeter but also gave valuable insight into the sub-surface structure of the area. (The techniques used by the Principal Investigator in evaluating the Black Hawk data proved quite useful to him in making real-time inputs to the flight plan.)

The second trip with the flight crew was to Flagstaff, Arizona for a full dress rehearsal with training equipment, communications links, etc. (See Fig. 10-2). The gravimeter performed as expected, and valuable experience was gained for the mission support crew.

As the time line became finalized at NASA, some of the geologists became worried at the prospect of waiting 3 minutes at the beginning of each stop on the traverse before being allowed to pan the TV camera. The original constraint was

Fig. 10-2   Astronaut Cernan at Flagstaff.

imposed for fear of the gravimeter measurements being affected by Rover vibrations excited by the TV camera. Gravimeter performance (stability) tests were run at Johnson Spacecraft Center (JSC) on a Rover suspended by 90-foot "bungee cords" to off-load 5/6 of the weight and produce lunar dynamic responses. These tests were run, with the TV and other systems running, to search for possible vibration sources. No other instrument, including the TV, appeared to have any effect on gravimeter accuracy, and the TV constraint was relaxed.

10.5 Flight-Unit Testing

The flight units (primary and spare) went through extensive, quality-control-witnessed tests to qualify the design and accept both units. These tests were largely repeats of engineering tests run on the prototype, designed to get additional operating parameters peculiar to each unit. One exception was the phase-lock-loop warm-up data taken during thermal-vacuum testing on each flight unit. Switching the gravimeter from STBY to ON produced a noticeable transient in normal gravity readings (when the phase-lock-loop was used). Tests showed that, within 20 minutes, the loop stabilized, but that the first reading could be especially misleading. For this reason the flight procedures called for turning the gravimeter ON at least 5 minutes before the first gravity measurement of each EVA. As may be seen in the flight data, when turned on, only READ is pressed, to get temperature-alarm data immediately, about 10 minutes before the first GRAV measurement.

After both flight units passed acceptance tests, periodic measurements were made in Cambridge before shipment and at KSC just prior to the flight to update the scale-factor value and verify the drift rate. Figure 10-3 shows the flight unit after removal of all of the test connections. After sealing each unit in flight-ready status, it was checked in a vacuum chamber to verify all connections and pressure-switch operations. These tests maximized the confidence in the functioning and accuracy of both units.
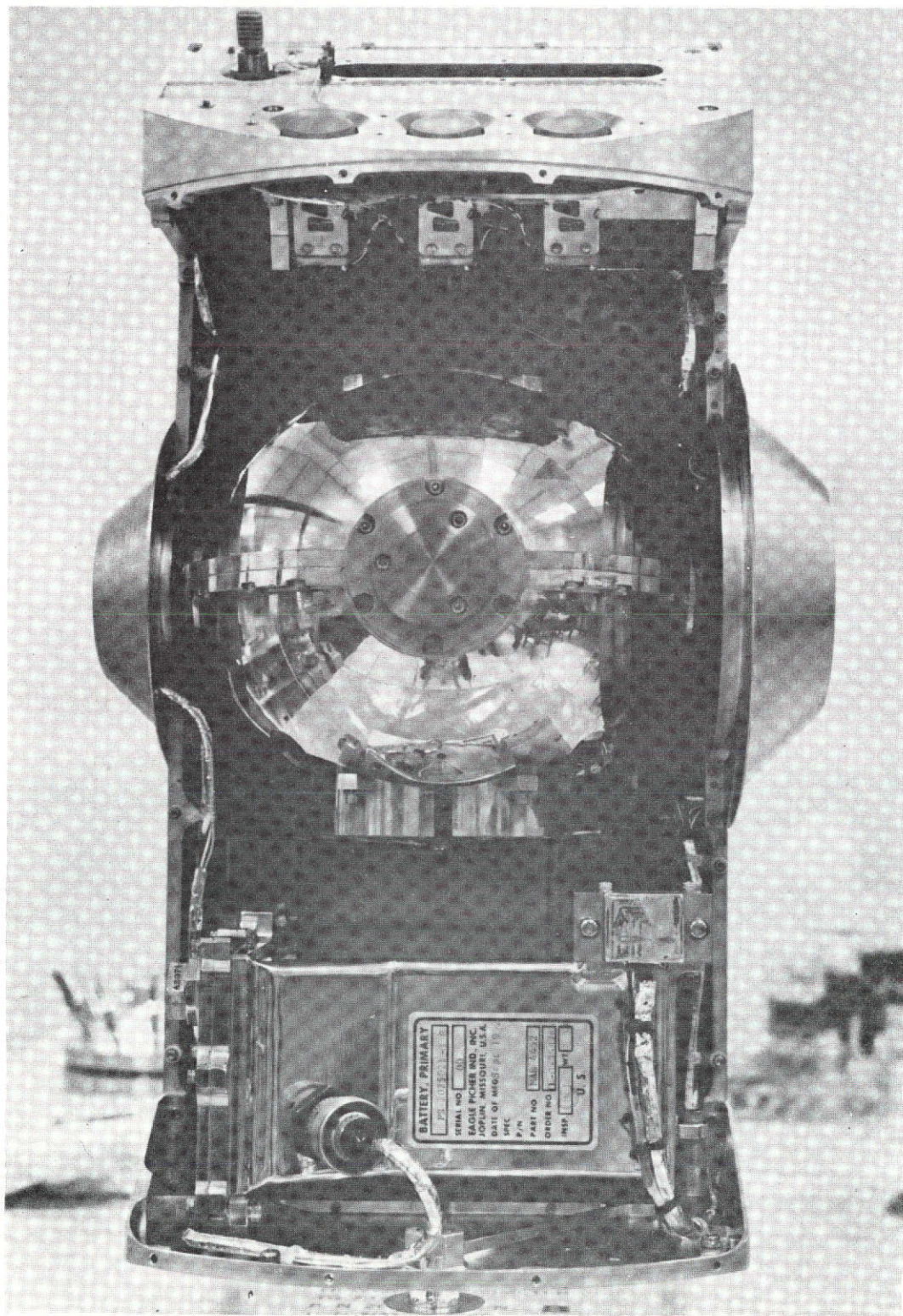
Fig. 10-3   Gravimeter interior detail.

SECTION 11

MISSION RESULTS

Final assembly of the prime flight gravimeter began during the early hours of Monday, 27 November 1972, following 4 weeks of testing at the Kennedy Spaceflight Center. Daily checks were made on FS-1's scale factor and bias in order to confirm instrument-drift trends as shown in Fig. 10-1. A functional test was performed with the flight-configured gravimeter installed in a vacuum chamber followed by a fit check with the geology pallet. The traverse gravimeter was installed in Quad III of the lunar module (LM-12) inside the protective shroud of the Saturn 5 launch vehicle on a rainy Tuesday evening (see Fig. 11-1).
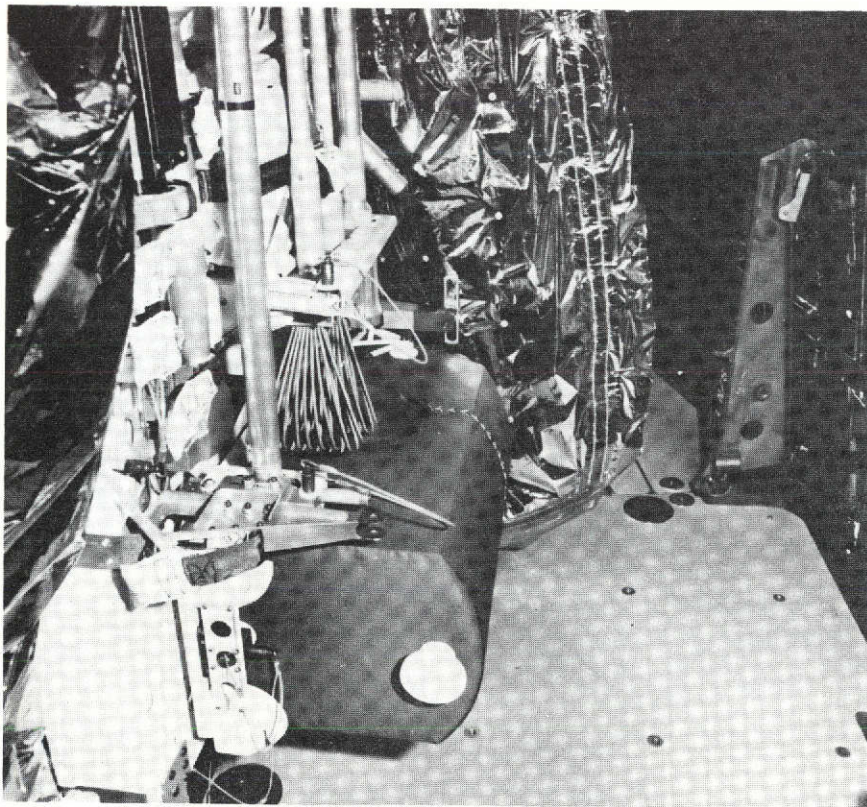
Fig. 11-1   Gravimeter installed before launch.

The flight of Apollo 17 began at 12:33 A.M., E.S.T., Thursday, 7 December 1972 following a false start earlier in the evening. As the huge rocket thundered skyward, the traverse gravimeter came to life at an altitude of 50,000 feet when a baroswitch completed the circuit to the internal battery. During the next 4 days, the precision VSA oven reached $122^\circ F$ and stabilized after the cold start.

In order to understand the flight results, it is necessary to convert the instrument display readings. The displayed number is a nine-digit number consisting of seven gravity digits followed by the temperature digits. At the beginning of each traverse, readings 1, 10, and 18 on Table 11-1, the display was read upon turning the STBY/ON switch to ON. For these readings, only the eighth digit is meaningful; the eighth digit indicates the status of various temperature alarms (see Section 7). The ninth digit is valid during any gravity or bias measurement. A displayed number less than 7 indicates the VSA temperature is in control.

The conversion of the displayed number to gravity in milligals is performed as follows:

$$\frac{1.92 \times 10^8}{D_N} = K_0 + K_1 g + K_2 g + K_3 g^3 \tag{11-1}$$

$$\frac{4.8 \times 10^7}{D_I} = -K_0 + K_1 g - K_2 g^2 + K_3 g^3 \tag{11-2}$$

(In computing $K_2 g^2$ and $K_3 g^3$, a value of 0.167 g is assumed for g.)

where

D_N = Displayed value for gravity (normal) measurement

D_I = Displayed value for bias (inverted) measurement

K_0 = Bias

K_1 = VSA scale factor

K_2 = VSA second-order term

K_3 = VSA third-order term

For the purpose of these preliminary calculations, the following values are used based on laboratory tests:

K_2 = -0.00034 Hz/g^2

K_3 = 0.00300 Hz/g^3

K_1 = 129.14550 Hz/g

TABLE 11-1

APOLLO 17 TRAVERSE GRAVITY DATA

Reading No.	EVA No.	Site	TG Display	Updated LM Baseline	Gravity Difference [*]				Type of Reading
					Display	± 2σ	mgal	± 2σ	
1		LM	xxxxxxx-0y						Temperature
2		LM	6700031-01	6700031	0	± 15	-	± 0.49	GRAV on Rover
3		LM	6700172-01	6700172	0	± 20	-	± 0.65	GRAV on Surface
4		LM	3374540-01	6700172	N/A		-		BIAS on Surface
5	1	Alsep	6700026-01	6700172	-146	± 20	4.74	± 0.65	GRAV on Rover
6		Sta. 1a	6700129-01	6700172	-43	± 20	1.40	± 0.65	GRAV on Rover
7		SEP	6700101-01	6700172	-71	± 20	2.30	± 0.65	GRAV on Rover
8		LM	0001330-01	6700172	N/A				GRAV on Surface
9		LM	6700215-01	6700200	15	± 25	-0.49	± 0.81	GRAV on Surface
10		LM	xxxxxxx-0y	6700200	N/A				Temperature
11		LM	6700177-01	6700200	-23	± 25	0.75	± 0.81	GRAV on Surface
12		Sta. 2	6701552-01	6700200	1352	± 25	-43.88	± 0.81	GRAV on Rover
13		Sta. 2a	6701235-01	6700200	1035	± 25	-33.59	± 0.81	GRAV on Rover
14	2	Sta. 3	6700497-01	6700200	297	± 25	-9.64	± 0.81	GRAV on Rover
15		Sta. 4	6700125-01	6700200	-75	± 25	2.43	± 0.81	GRAV on Rover
16		Sta. 5	6700314-01	6700200	114	± 25	-3.70	± 0.81	GRAV on Rover
17		LM	6700235-01	6700250	-15	± 30	0.49	± 0.97	GRAV on Surface
18		LM	xxxxxxx-0y	6700250	N/A				Temperature
19		LM	6700270-01	6700250	20	± 30	-0.65	± 0.97	GRAV on Surface
20		Sta. 6	6701098-01	6700250	848	± 30	-27.52	± 0.97	GRAV on Surface
21		Sta. 8	6700960-01	6700250	710	± 30	-23.04	± 0.97	GRAV on Rover
22	3	Sta. 8	6701173-01	6700425	748	± 50	-24.28	± 1.62	GRAV on Surface
23		Sta. 9	6700378-01	6700425	-47	± 50	1.53	± 1.62	GRAV on Rover
24		Sta. 9	6700571-01	6700600	-29	± 75	0.94	± 2.43	GRAV on Surface
25		LM	6700107-01	N/A	N/A				GRAV on Surface
26		LM	3374171-01	N/A	N/A				BIAS on Surface

Weighted Average for Sta. 8 = -23.20 mgal
Sta. 9 = + 1.30 mgal
[*] Absolute value for LM = 162,694.45 mgal

11.1 Discussion

The traverse gravimeter functioned throughout all three EVA's. The last two digits were 0 and 1 for every gravity and bias measurement, indicating excellent temperature control and that at no time during the EVA's did any of the temperature alarms activate.

The value of bias computed at the beginning of EVA 1 (readings 3 and 4) was 7.21592 Hz. A predicted value of bias based on laboratory test was 7.2144 Hz. Total shift during the translunar phase was 0.0015 Hz. This corresponds to about an 11-mgal bias shift, which is considered reasonable as compared to typical bias shifts experienced during acceptance and vibration testing. A 141-count (4.6-mgal) shift also occurred while taking the traverse gravimeter off the Rover at the LM site (readings 2 and 3). At this time, it was suspected that a shock due to handling caused this shift. At the end of EVA 1, the first displayed reading (reading 8) was 000xxxx, indicating loss of lock in the phase-lock loop. In order to induce this (especially on the surface), the traverse gravimeter must have been hit, rather severely, during a measurement. The measurement was repeated and a reasonable reading was obtained. This reading at the LM site was 1.4 mgal lower than reading 3.

EVA 2 went fairly smoothly. A large gravity change was found at Station 2. This caused the Principal Investigator to request an additional reading on the way to Station 3. This reading is indicated in Table 11-1, as Station 2A. The closeout reading at the end of EVA 2 (reading 17) was close to the closeout of EVA 1 (reading 9) or 0.7 mgal different. This EVA was considered most valuable by the Principal Investigator.

During EVA 3, no reading was taken at Station 7, due to time-line considerations. At Stations 8 and 9, readings were taken both on and off the Rover. The differences off the Rover were 6.9 and 6.2 mgal less than on the Rover for Stations 8 and 9 respectively. This is not much different from the 4.5-mgal difference obtained at readings 2 and 3 at the beginning of EVA 1. The fact that the changes were of the same magnitude and in the same direction, indicated that some type of Rover motion, or astronaut handling, or surface phenomena, may have induced this. On the way from Station 9 to the LM site, the pallet on which the traverse gravimeter was mounted swung open. Previous experience indicates that the shock effect that may have resulted from this could cause a bias shift. At the LM site at the end of EVA 3, both a gravity and bias measurement were obtained on the surface (readings 25 and 26) to close out the traverse. Figure 11-2 summarizes the results.

As a result of the shifts on readings 3, 22, and 24, post-mission engineering tests were run on the flight spare and engineering prototype gravimeters. (Reference

Sta 6
−27.5 mgal

Sta 8
−23.2 mgal

LM SITE
169,694.45 ± 5 mgal

ALSEP
+4.7 mgal

Sta 4
+2.4 mgal

Sta 9
+1.3 mgal

Sta 5
−3.7 mgal

Sta 3
−9.6 mgal

SEP
+2.3 mgal

Sta 1 A
+1.4 mgal

Sta 2 A
−33.6 mgal

Sta 2
−43.9 mgal
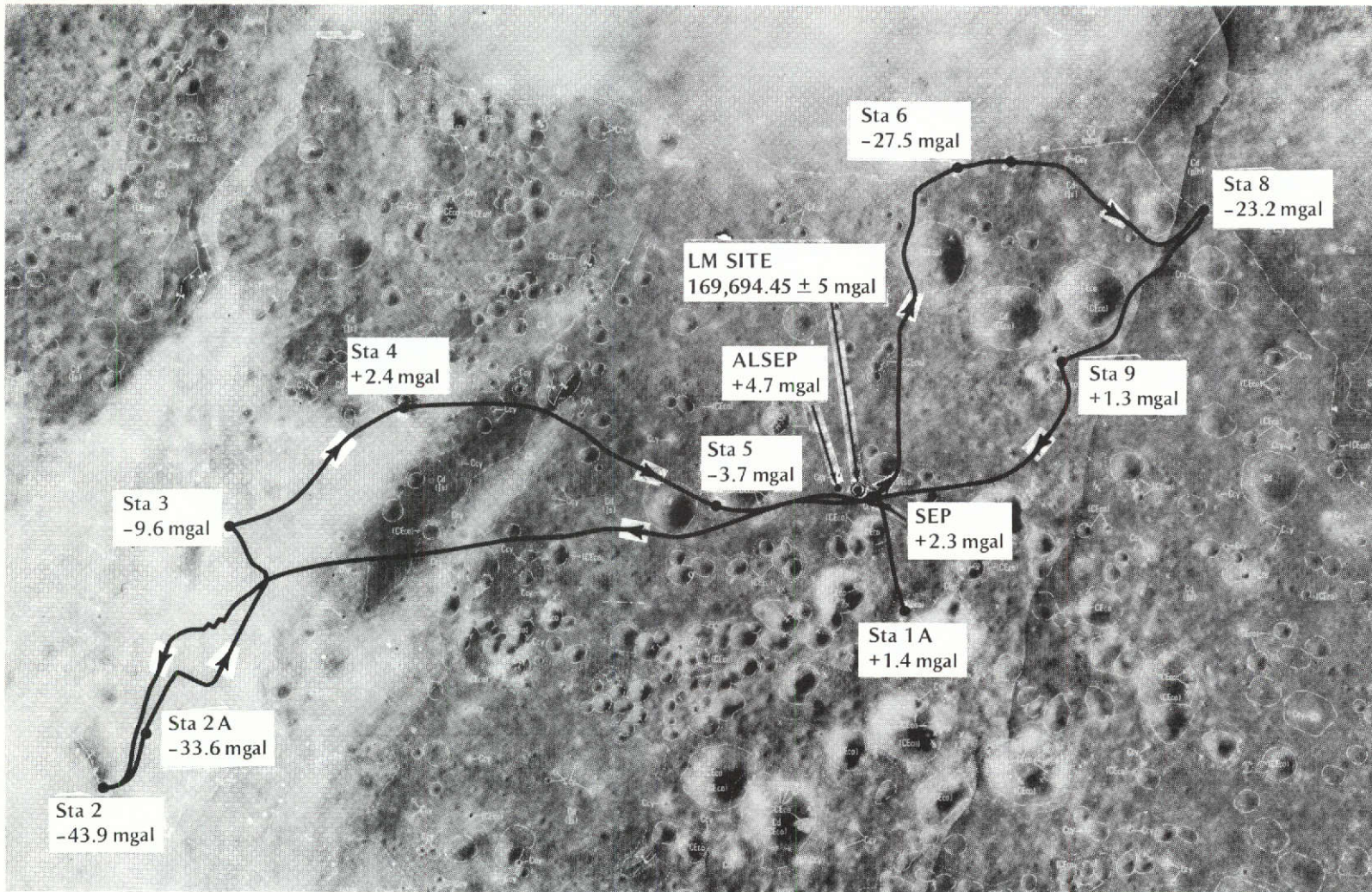
Fig. 11-2   Traverse gravity values from Apollo 17.

GRV-228-T). These tests indicated that repeatable one-way shifts could be induced by hitting the gravimeter handle supports. The spare flight gravimeter (FS-2) recovered from these shifts in about 1 hour, while the engineering model largely failed to recover, exhibiting a "staircase" shock reaction.

It appears that the flight gravimeter had a staircase reaction to being transferred from the Rover to the ground (see Fig. 11-3). If we assume that each surface deployment resulted in an upward shift, and that the gravimeter, if left alone, would stay at that new value, we get the gravity deviations listed in Table 11-1. The "updated LM Baseline" represents the equivalent reading that the unit would give if transferred to the LM at that time. It is used to compute the deviations needed for the gravity measurement. The $\pm$ 2-σ column reflects a 95% confidence level, and is shown increasing since the gravimeter performance appeared to degrade with the number of shocks. The new LM baseline is roughly the average of any readings taken before being mounted on the Rover again. In the case of readings 22 and 24, the confidence factor is inflated because no accurate closeout was made for EVA 3.

The last two readings (25 and 26) are confusing. It is known that the tailgate flew open during the drive from Station 9 back to the LM. This would normally be a severe shock-inducing environment for the gravimeter. The last two readings however, imply a bias shift of only 0.0006 Hz from the start of EVA 1, and a scale factor shift of 0.006 Hz/g. This is the opposite relative reaction of bias and scale factor. In our harshest vibration testing, the bias changed 0.007 Hz and the scale factor only 0.003 Hz/g, (a more typical example). We have never seen a scale factor shift of the magnitude implied by the last two measurements without a far worse bias shift (see Fig. 10-1). For this reason the last two readings are considered inconsistent and were not used in the data reduction. It may be noted that the BIAS reading alone corresponds to a GRAV reading of 6700541, if we assume no scale-factor change and absorb all of the shift in the bias term (a reasonable approximation based on past data). This is more consistent with the 6700600 baseline assumed for Station 9.

The absolute value of gravity may be determined from the data. It is felt that readings 3 and 4 provide the most-complete least-suspect measurements to take for the transfer, and they yield a value of 162,694.45 mgals at the LM site.

Figure 11-4 shows the gravimeter mounted on the Rover at the start of EVA 2.
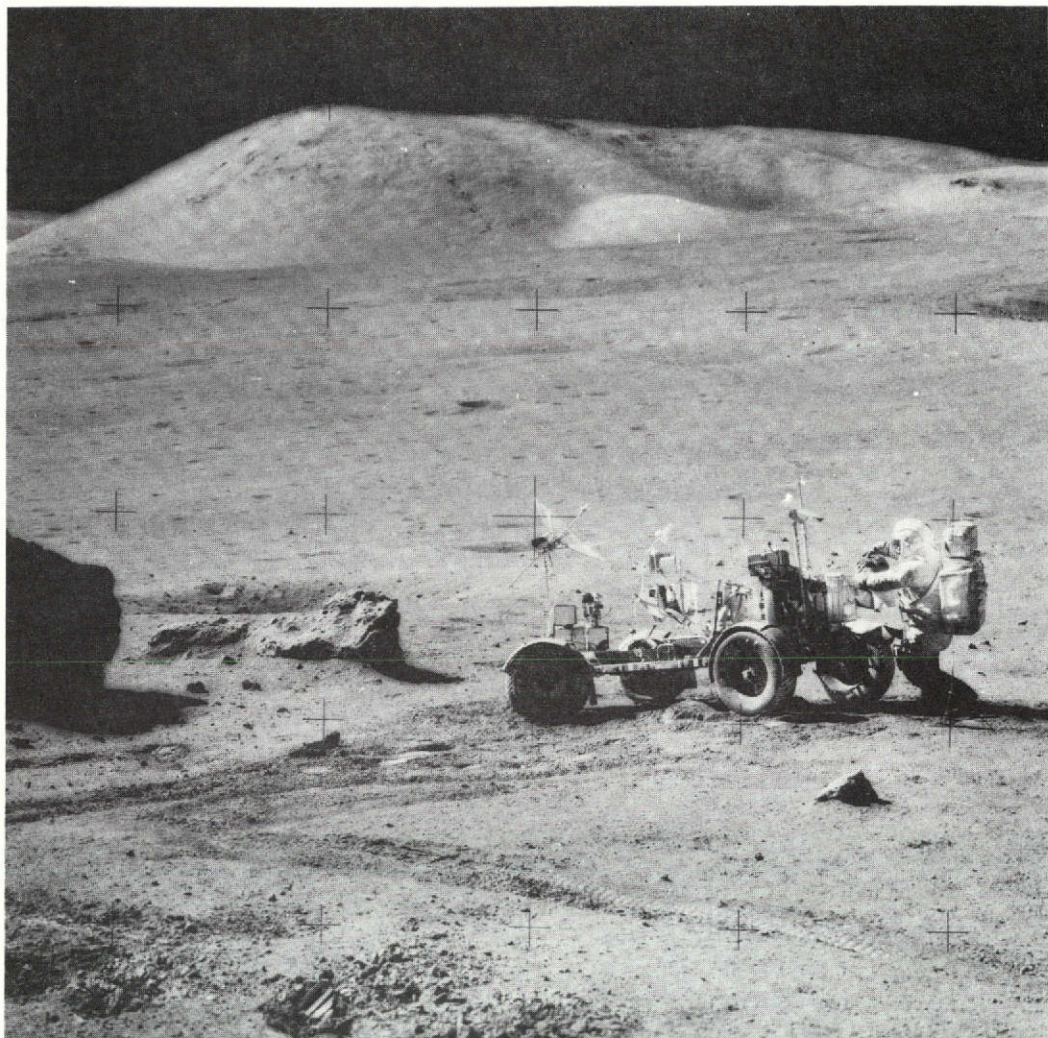
Fig. 11-3   Gravimeter being unloaded at Station 6.

11.2   Conclusion

The traverse gravimeter performed well throughout all three EVA's. Temperature control was excellent. There is no reason to believe that there were any electronic problems. Gravimeter performance appeared to be degraded by shocks, however. First, the Rover-to-surface deployment presented an unanticipated shock hazard. Second, the tailgate's opening at the end of EVA 3 appeared to stress the instrument. Despite these problems, gravimeter data, in particular during the crucial EVA 2, appeared useful and accurate.

71
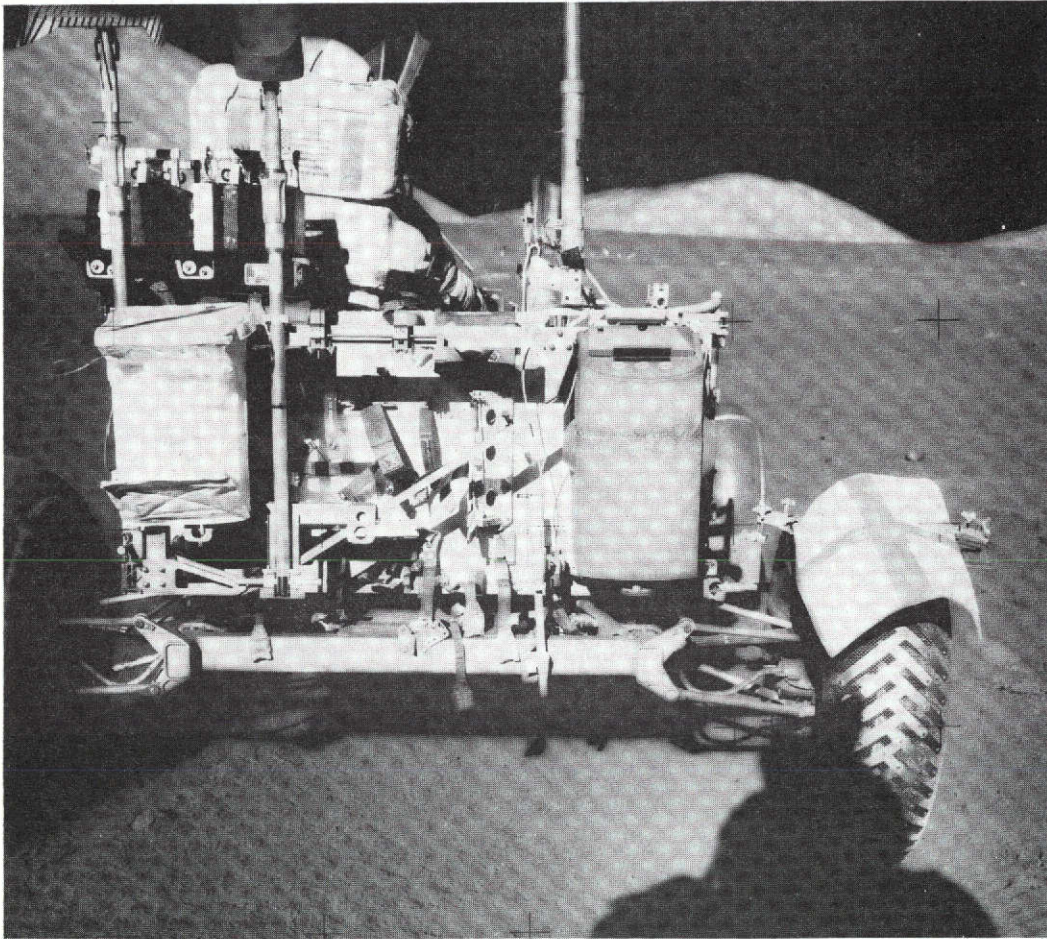
Fig. 11-4   Traverse gravimeter mounted on geology pallet.

The Principal Investigator's findings from the gravimeter readings are summarized in a paper presented at the Annual Conference of the American Geophysical Union in Washington, D.C. in April 1973[*].

---

[*]Talwani, M., G. Thompson, B. Bent, H. Kahle, S. Buck, Traverse Gravimeter Results on Apollo 17, to be published by NASA as part of the preliminary science report.

APPENDIX A

DERIVATION OF SUM FREQUENCY AND
HIGHER-ORDER TERMS OF VSA OUTPUT

A.1 Sum Frequency Derivation

A further manipulation of the power series representing the outputs of the two VSA strings reveals helpful interrelationships between the sum frequency, $f_1 + f_2$, and the instrument scale factor. From Eqs (4-5) and (4-7) an expression for $f_1 + f_2$ can be obtained as

$$f_1 + f_2 = \frac{T_0^{1/2}}{2} \left[\left(\frac{1}{\left(L_1 m_1\right)^{1/2}} + \frac{1}{\left(L_2 m_2\right)^{1/2}} \right) + \frac{MA}{2T_0} \left(\frac{1}{\left(L_1 m_1\right)^{1/2}} - \frac{1}{\left(L_1 m_1\right)^{1/2}} \right) + \cdots \right] \qquad (A-1)$$

This series converges very quickly and to a good approximation to

$$f_1 + f_2 = \frac{T_0^{1/2}}{2} \left(\frac{1}{\left(L_1 m_1\right)^{1/2}} + \frac{1}{\left(L_2 m_2\right)^{1/2}} \right) \qquad (A-2)$$

Using the expressions for f_1 and f_2 in Eqs.(4-5) and (4-7), it can be seen that

$$f_1 - f_2 = \frac{T_0^{1/2}}{2} \left[\left(\frac{1}{\left(L_1 m_1\right)^{1/2}} - \frac{1}{\left(L_2 m_2\right)^{1/2}} \right) \right.$$
$$+ \frac{1}{2} \frac{MA}{T_0} \left(\frac{1}{\left(L_1 m_1\right)^{1/2}} + \frac{1}{\left(L_2 m_2\right)^{1/2}} \right)$$
$$- \frac{1}{8} \left(\frac{MA}{T_0} \right)^2 \left(\frac{1}{\left(L_1 m_1\right)^{1/2}} - \frac{1}{L_2 m_2^{1/2}} \right)$$
$$\left. + \frac{1}{16} \left(\frac{MA}{T_0} \right)^3 \left(\frac{1}{\left(L_1 m_1\right)^{1/2}} + \frac{1}{\left(L_2 m_2\right)^{1/2}} \right) + \cdots \right] \qquad (A-3)$$

73

Comparing Eq.(A-3) to Eq.(4-11) one obtains

$$K_1 = \frac{M}{4T_0^{1/2}} \left(\frac{1}{(L_1 m_1)^{1/2}} + \frac{1}{(L_2 m_2)^{1/2}} \right) \qquad \text{(A-4)}$$

Thus

$$K_1 = \frac{R}{f_1 + f_2} \qquad \text{(A-5)}$$

where

$$R = \frac{M}{8} \left(\frac{1}{(L_1 m_1)^{1/2}} + \frac{1}{(L_2 m_2)^{1/2}} \right)^2 \quad Hz^2/g$$

The term R will vary only if the lengths of the individual strings vary. R will be largely insensitive to changes in sensed input since the lengths of the strings will change in opposite directions. R will vary with changes in temperature; since for temperature variations, changes in the lengths of both strings will be of the same polarity.

A.2 Derivation of Higher-Order Terms

Referring again to the power-series expression for the difference frequency Eq.(A-3), similarities are apparent between the K_0 and K_2 terms and between K_1 and K_3 terms.

Equating the fourth term in Eq.(A-3) to K_3, one obtains

$$K_3 = \frac{M^2 K_1}{8T_0^2} \qquad \text{(A-6)}$$

$$\frac{R}{K_1^2} = \frac{2T_0}{M} \qquad \text{(A-7)}$$

Thus

$$K_3 = \frac{1}{2} \frac{K_1^5}{R^2} = \frac{1/2 \, K_1^3}{(f_1 + f_2)^2} \qquad \text{(A-8)}$$

74

Before proceeding further it is helpful to write Eq.(4-8) for input accelerations of plus and minus one g

$$(f_1 - f_2)_{+g} = \Delta f_{(+g)} = K_0 + K_1\, g + K_2\, g^2 + K_3\, g^3 \tag{A-9}$$

$$(f_1 - f_2)_{-g} = \Delta f_{(-g)} = -K_0 + K_1\, g - K_2\, g^2 + K_3\, g^3 \tag{A-10}$$

The sum and difference of Eqs.(A-9) and (A-10) are

$$\Delta f_{(+g)} + \Delta f_{(-g)} = 2K_1\, g + 2K_3\, g^3 \tag{A-11}$$

$$\Delta f_{(+g)} - \Delta f_{(-g)} = 2K_0 + 2K_2\, g^2 \tag{A-12}$$

Equation (A-8) can now be substituted into Eq.(A-11) to give an expression for the instrument scale factor in terms of the difference frequency counts at plus and minus one g input and the sum frequency.

$$K_1 = \frac{\Delta f_{(+g)} + \Delta f_{(-g)}}{2} - \frac{\left(\Delta f_{(+g)} + \Delta f_{(-g)}\right)^3}{16\,(f_1 + f_2)^2} \tag{A-13}$$

Then by use of Eq.(A-8), the value for K_3 can be determined.

In an analogous fashion, the interrelationship between the K_0 and K_2 terms can be used to determine unique values for K_0 and K_2; i.e.,

$$K_0 = \left(\Delta f_{(+g)} - \Delta f_{(-g)}\right)\left(1 + 2\,K_3/K_1^2\right) \tag{A-14}$$

$$K_2 = \frac{-2\,K_3\,K_0}{K_1^2} \tag{A-15}$$

APPENDIX B

GRAVIMETER ELECTRONICS SCHEMATIC

Page intentionally left blank

APPENDIX C

CALCULATION OF MAXIMUM TEMPERATURE
ON VERTICAL SURFACE OF MULTILAYER BLANKET

As mentioned in Section 7, a vertical adiabatic surface on a flat moon receiving both solar and lunar radiation can reach a temperature above that of the moon. The following is a derivation of the governing relationship. A maximum blanket temperature and sun angle are calculated based on the assumption of pure black-body radiation.

First, parameters are defined:

S	=	Solar radiation flux constant = 442 Btu/h-ft^2
α_s	=	Solar absorbtivity
θ	=	Sun elevation angle
ϵ_H	=	Infrared emittance
$F_{s,m}$	=	View factor from vertical surface to moon = 0.5
$F_{s,o}$	=	View factor from vertical surface to outer space = 0.5
T_m	=	Moon temperature
T_s	=	Surface temperature

A steady-state heat balance can be written for a unit area of an adiabatic vertical surface perpendicular to the solar plane as follows:

$$Q_{in} - Q_{out} = 0 \tag{C-1}$$

$$S \alpha_s \cos \theta + \epsilon_H F_{s,m} \sigma (T_m^4 - T_s^4) - \epsilon_H F_{s,o} \sigma T_s^4 = 0 \tag{C-2}$$

The blanket surface can be assumed to be adiabatic in that on the order of one percent of the net thermal flux on the blanket is conducted inward to the TGE case.

If the lunar surface is assumed to be a pure black-body absorber and radiator the following expression for moon temperature may be substituted:

$$T_m^{\,4} = \frac{S}{\sigma} \sin \theta \qquad\qquad\qquad (C\text{-}3)$$

which, after including the view factors, leaves the following equation for the temperature of a vertical adiabatic surface as a function of sun angle:

$$T_s = \left(\frac{S\,\alpha_s}{\sigma\,\epsilon_H} \cos \theta + 0.5\frac{S}{\sigma} \sin \theta \right)^{1/4} \qquad\qquad (C\text{-}4)$$

If the blanket surface is a pure black-body radiator $\alpha_s = \epsilon_H = 1.0$, the equation simplifies. By taking the derivative with respect to θ and setting it equal to zero, it is found that the sun angle for maximum thermal radiation is 26.6 degrees, producing surface temperatures of approximately 274^OF.

APPENDIX D

THERMAL MODELING AND MISSION PREDICTIONS

The thermal design of the TGE relied heavily on computerized predictions of thermal performance in many different conditions. Initially the computer model of the thermal analog was created purely from mathematical calculations of thermal transport coefficients and thermal masses. The model was then put through a mathematically simulated environment equivalent to a worst-case lunar mission (cold and hot) and the performance observed. As design deficiencies or needs were observed, the design and the math model were altered. When it became clear that there was a thermal design that worked mathematically, a thermal mock-up was built, instrumented, and tested. Specific tests were conducted in a vacuum chamber (see Section 10) and the results correlated with mathematical simulations of the tests. The math model was altered where its response did not match that of the mock-up. Subsequently, the math model was put through a full worst-case lunar simulation and design margins observed. The resulting mathematical computer model is described in Appendix E.

In order to mathematically model the instrument, definite mission assumptions were required. Some involved a definition of the environment (see Section 7.1) and others were somewhat contrived to lend to mathematical analysis. Table D-1 is a summary of the base line assumptions required to model the nominal, hot, and cold missions. The hot and cold missions represent worst-case assumptions.

Table D-1 requires a brief explanation. The blanket for the TGE is of a deep, almost cobalt-blue color, selected to be a good optical background for reading the display. In lab measurements, both the dacron fabric and the painted plastic exhibited a solar absorptance and infrared emittance of approximately 0.6 and 0.9 respectively. In a cold mission, these real values were retained in the assumptions because they represent the worst case. In the hot and nominal missions, however, it was assumed that the blanket was covered with lunar dust, approximated by $\alpha_s = \epsilon_H = 1.0$.

TABLE D-1

TGE THERMAL MISSION ASSUMPTIONS

	HOT MISSION	NORMAL MISSION	COLD MISSION
(1) Quad III Pallet Temperature	Hottest as supplied by Grumman (160-hour duration)	$50^{\circ}F$ during translunar and soakback (160-hour translunar)	Coldest as supplied by Grumman (160-hour duration)
(2) Post-Touchdown Quad III Soakback	20 hours	6 hours	6 hours
(3) Landing Sun Elevation	20.3°	13.3°	6.8°
(4) Blanket Surface Characteristics	$\alpha_s = \epsilon_H = 1.0$	$\alpha_s = \epsilon_H = 1.0$	$\alpha_s = 0.6,\ \epsilon_H = 0.9$
(5) Pallet-to-Case Conductance in Stowage	0.032 Btu/h-$^{\circ}F$	0.032 Btu/h-$^{\circ}F$	0.128 Btu/h-$^{\circ}F$
(6) Rest Periods	Edge of LM Shadow	In full LM Shadow	In full LM Shadow
(7) No. of Gravity Measurements per Traverse	10	10	10

It was found in modeling the instrument and later in tests that during the Quad III stowage period, during which time the three hard-mount pins were present, the pallet-to-case conductance through the pins was an important parameter in specifying the initial conditions for the lunar mission. If the conductance was very low, as in the hot and nominal missions, the case is well isolated and its own internal heat dissipation during the long translunar coast warms the unit well above the pallet temperature. Therefore, a low conductance is again a worst-case hot assumption. In the cold mission, though, the opposite is true. The worst-case cold assumption is when the unit is well coupled to the cold pallet. The numbers used were measured during thermal-vacuum tests of the thermal mockup and engineering model.

As described earlier, during lunar rest periods the TG is placed in the shade of the LM for cooling. While in the shade, though, the instrument can still receive radiative heat inputs from the LM and nearby warm lunar terrain that has a clear view to the TG. This could be especially true in a mountainous region such as the Apollo 17 Taurus-Littrow site. Rather than spend time constantly accounting for such effects, it was assumed for modeling purposes that the TGE sits on the shaded edge of the LM shadow in hot missions and receives no radiative flux from the LM and hot moon in the nominal and cold missions.

The period of time during which the TG must remain in Quad III following lunar landing is an important parameter in the hot mission only. If the LM Quad III is pointing directly at the sun following landing, the TG should be removed within 20 hours of landing or it runs the risk of overheat later in the mission.

The computer predictions for thermal performance of the TG during hot, nominal, and cold missions are shown in Figs. D-1 to D-3. The time line begins at the time of lunar landing and extends through three EVA's. Key points to observe in these three figures are the following:

(1)   The P oven and VSA temperatures are controlled at $122^{\circ}F$.

(2)   In order to maintain P-oven control, the maximum permissible I-oven temperature is $117^{\circ}F$.

(3)   The hottest temperatures for the I oven and battery occur approximately 2 to 3 hours following the first EVA.

(4)   The portions of the TG which are most physically removed from the case respond progressively less severely to the case thermal response.
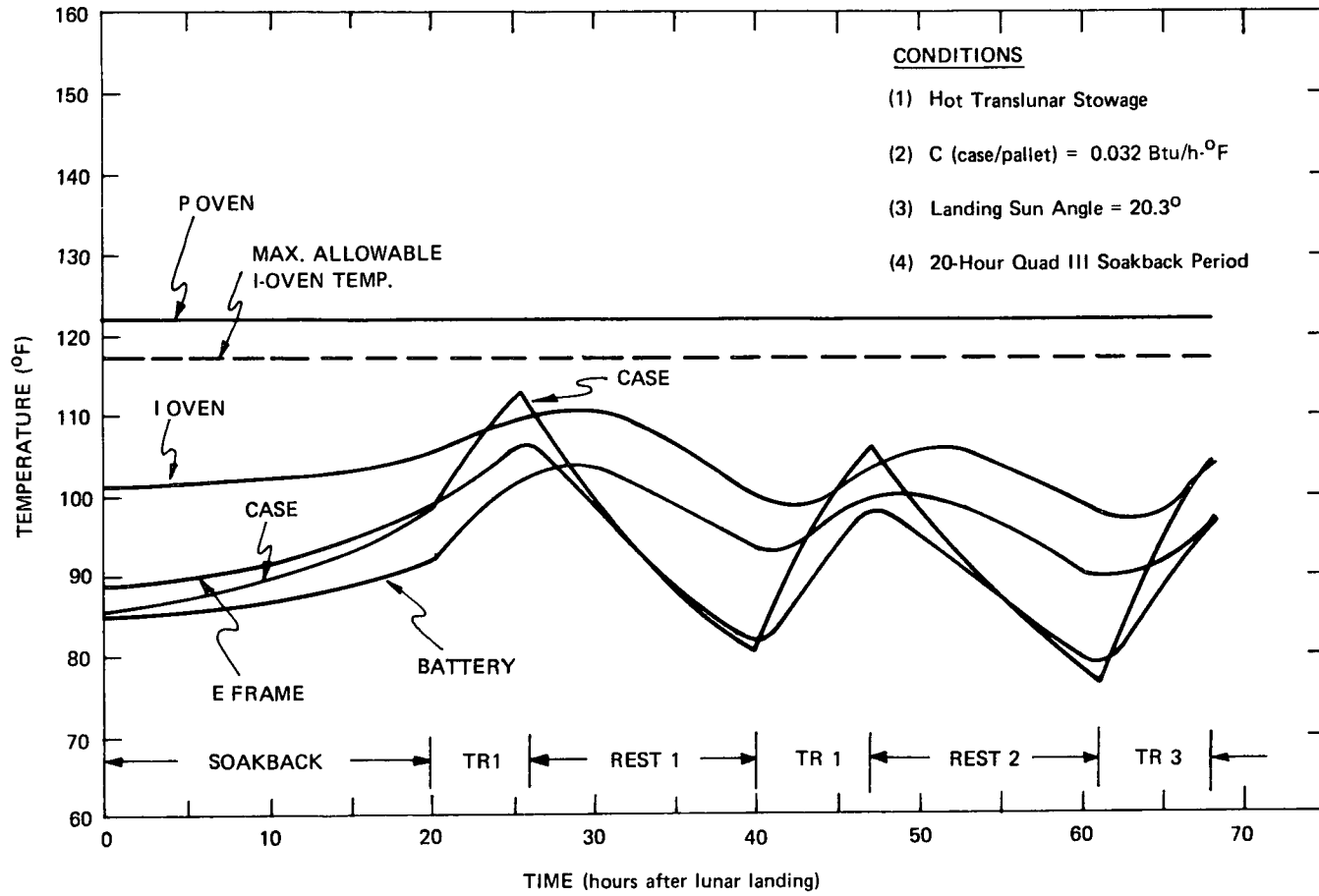
Fig. D-1   Hot-mission thermal response.
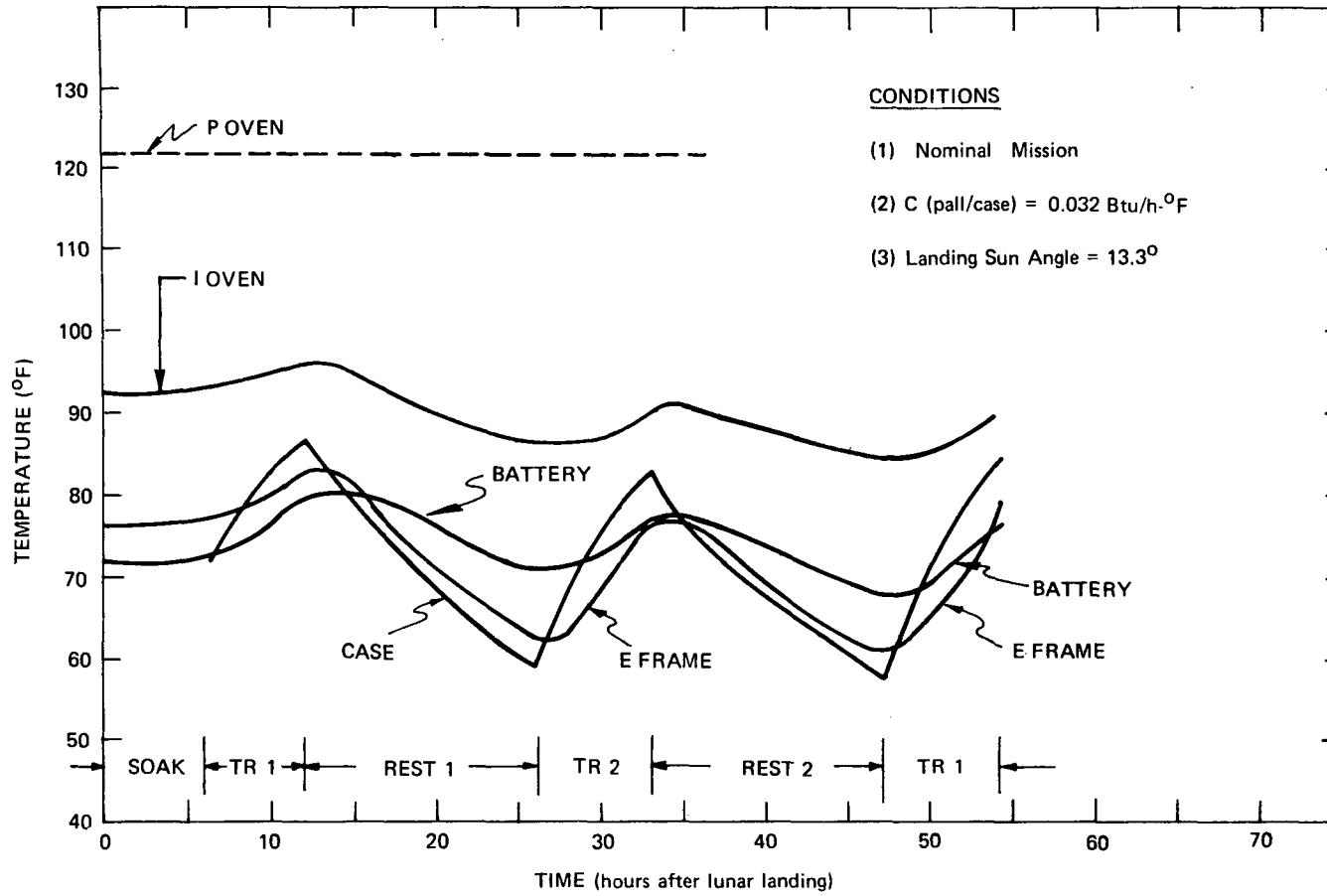
Fig. D-2 Normal-mission thermal response.
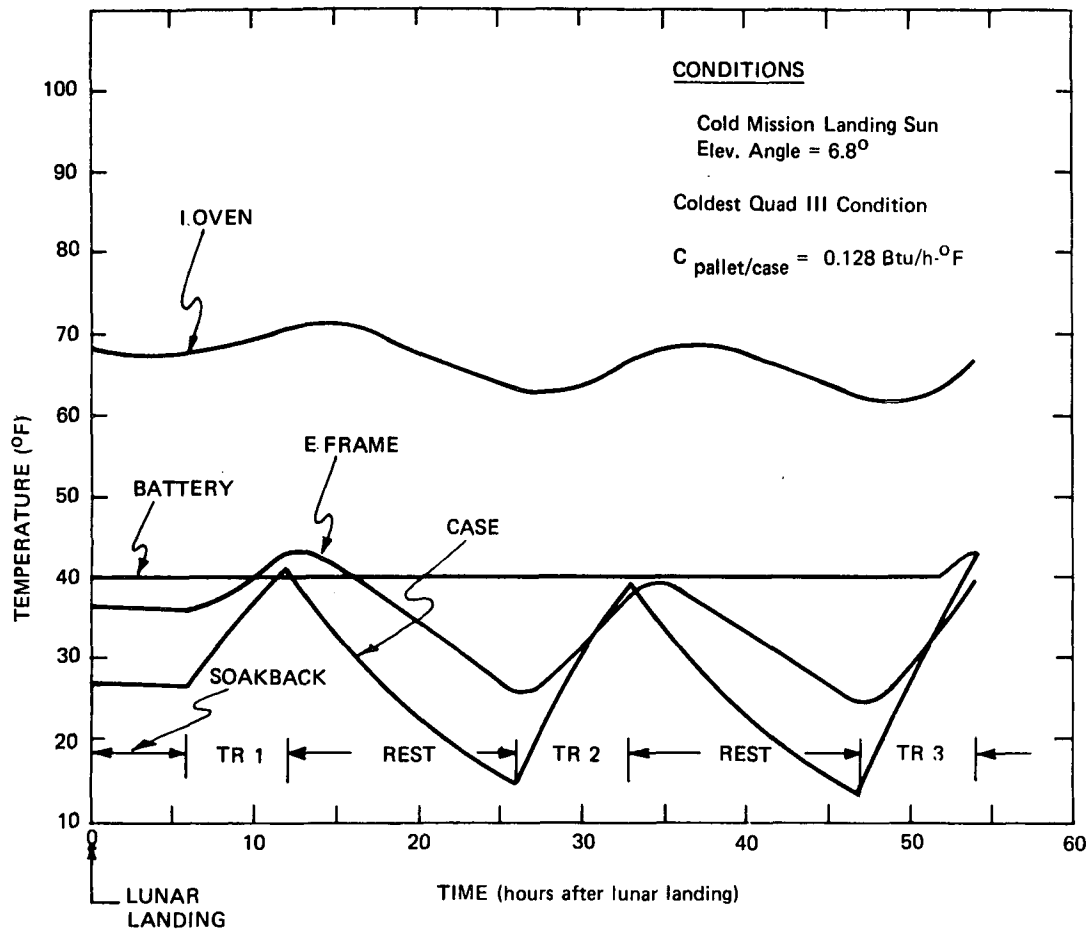
Fig. D-3   Cold-mission thermal response.

It should be noted that in a hot mission the temperature change of the I oven between the beginning of EVA 1 and the hottest temperature is approximately $5^\circ F$. This fact graphically explains the $110^\circ F$ very warm alarm on the I oven. This alarm led to the mission rule that if the alarm was seen at the beginning of EVA 1 the TG would be placed in the LM shade for cooling until EVA 2. If only a warm alarm were seen, the hottest the I oven could be is $110^\circ F$, resulting in a peak I-oven temperature of approximately $115^\circ F$ during the subsequent rest period. With a $117^\circ F$ red-line limit on the I oven, P-oven control is assured.

The computerized thermal prediction for the cold mission (Fig. D-3) also enables the computation of the worst-case electrical power consumption. Power is potentially dissipated for four functions: electronics power for gravity measurement and display, P-oven control power, I-oven control power, and battery control power. The I-oven control power is found to be always zero, even in the coldest mission, because its minimum temperature is only approximately $62^\circ F$. Table D-2 is a breakdown of the electrical power consumed by each source during each mission

88

TABLE D-2

COLD-MISSION POWER-BUDGET BREAKDOWN

ASSUMED CONDITIONS:
(1) Prelaunch Temperature = 60°F Throughout
(2) 160-Hour Translunar Stowage Period
(3) Landing Sun Elevation Angle = 6.8 degrees
(4) 6-Hour Quad III Soakback Period

Heat Source Mission Phase	Electronics (Watt-hours)	P Oven (Watt-hours)	Battery Heater (Watt-hours)	Totals (Watt-hours)
0 - 3 Hours	0.46	3.9	0	4.36
3 - 166 Hours (Included 6-hour Quad III Soak)	28.5	91.5	28.8	148.8
Lunar Operations (48 Hours)	51.8	29.9	8.0	89.7
Totals	80.76	125.3	36.8	242.86

phase. The first 3 hours of translunar stowage is a separate category in that during that time the P oven is assumed to be warming up from a 60^OF ground ambient temperature to 122^OF. The total energy dissipation of 242.86 watt-hours should be compared with the manufacturer's battery rating of 340 watt-hours. Only 71% of the battery energy would be consumed in the worst case cold mission while maintaining complete thermal control.

APPENDIX E

THERMAL-MATHEMATICAL COMPUTER MODEL DESCRIPTION

As described in Appendix D, a strong tool for designing and evaluating the thermal performance of the TG was a mathematical analog of the thermal design of the complete instrument. The analog model employed most often for analysis is shown in Fig. E-1. The model consists of 14 separate structures or surfaces which are represented as nodes. The nodes are represented as junction points in an equivalent resistive and capacitive electronic circuit. The thermal mass, mc_p, (mass times specific heat) of each structure is the direct equivalent to electrical capacitance, nodal temperature the equivalent of voltage, and thermal transfer, whether by conduction, convection, or radiation is represented by a resistance. Our modeling was confined to vacuum only, eliminating convection transfer. The resistances in Fig. E-1 are only directly equivalent to linear electrical resistors when thermal conduction is the sole mode of heat transfer between the two nodes concerned. In this case, the equivalent resistance is L/KA, where L is the length between nodes, A the average area through which the heat must flow, and K the thermal conductivity of the material.

In addition to conduction resistances there is in general a parallel, non-linear resistance (not shown in Fig. E-1) which accounts for the radiation heat transfer. The radiation thermal transfer between nodes is generally of the form $\sigma A \, \epsilon_{EQ} \, F \, (T_{Hot}^4 - T_{Cold}^4)$, where ϵ_{EQ} is an equivalent emittance factor and F the geometrical view factor between the surfaces. In the tabulation of resistances which will follow, the radiative terms include the product $A \, \epsilon_{EQ} F$ and have the units of area.

Electrical power is put directly into each node as heat. Solar heating when present is put directly into the TG case node with an attenuation factor of 0.01, equal to the measured average effective emittance of the multilayer blanket. Cyclic or varying powers, such as the display-mode power which is present for only 15 seconds after the display button is pushed, are input as an average heat over a full EVA, depending on the number of expected display readings.

Table E-1 is a list and description of the nodes of the thermal analog model. The thermal mass of each node, mc_p, is also given. Table E-2 is a list of nodal

91
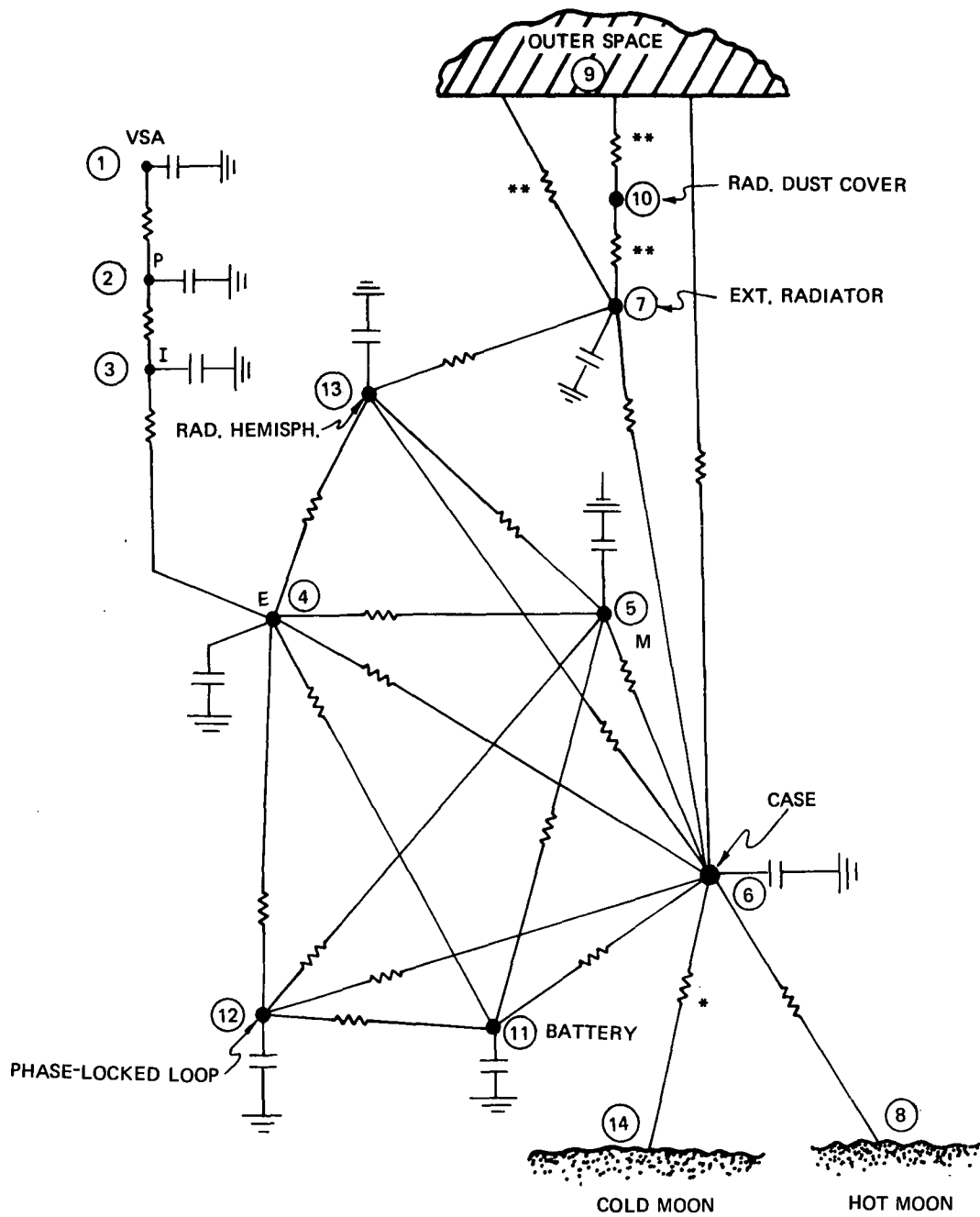
*PATH 6-14 PRESENT ONLY WHEN IN LM SHADE

**PATHS 7-10 & 9-10 PRESENT ONLY WHEN RADIATOR DUST COVER CLOSED.
PATH 7-9 PRESENT ONLY WHEN RADATOR DUST COVER OPEN.

Fig. E-1   Thermal-mathematical analog model.

TABLE E-1

TGE - 14-NODE MODEL

Node No.	Location	Thermal Mass (Btu/°F)
1.	VSA	0.091
2.	Precision Oven (Isothermal Node at temperature of 122°F at all times that the Intermediate-oven temperature is less than 117°F	Constant Temp.
3.	Intermediate Oven	0.259
4.	Electronics Frame	0.629
5.	Middle Gimbal	0.577
6.	Case, Electronics Power Supply, Logic, Display, and Crystal Oscillator	3.328
7.	External Surface Radiator	0.042
8.	Lunar Surface and Lunar Roving Vehicle (temperature-controlled nodes at same temperatures)	Variable-Temp. Sink
9.	Space	Constant Temp. (0°R)
10.	Dust Cover for External Surface Radiator	0
11.	Battery	1.49
12.	Phase-Locked Loop	0.219
13.	Internal Radiator Hemisphere	0.042
14.	Cold Lunar Shade	Constant Temp. (-100°F)

TABLE E-2

THERMAL ANALOG MODEL — NODAL COUPLING

Connecting Nodes		Coupling Coefficients	
		Radiation (ft^2)	Conduction $(Btu/h-^{o}F)$
1	2	0.00674	1.7
2	3		0.0401
3	4	0.0138	0.056
4	5	0.03443	0.278
4	6	0.0026	0.050
4	11	0.0053	
4	12	0.00055	
4	13	0.087	
5	6	0.025	0.308
5	11	0.0031	
5	12	0.00055	
5	13	0.003	
6	7		0.007
6	8	0.0318	0.01
6	9	0.01762	
6	11	0.0535	0.092
6	12	0.0052	0.007
6	13		0.08
6	14	0.01582*	0.01*
7	10	0.00072**	
7	9	0.06086**	
7	13		0.139
9, space	10	0.072**	
11	12		1.0

* Path 6-14 present only when in LM shade.

** Paths 7-10 and 9-10 present only when radiator dust cover closed.
Path 7-9 present only when radiator dust cover open.

conduction and radiation transfer coefficients for each node during an EVA on the Rover. It should be noted that for some nodes only one mode of transfer is given because it was found to dominate. Secondly, the Rover pallet is not given as a separate node because it is assumed to be at the local hot lunar temperature which is assumed to be a function only of the sun elevation angle.

The multinode model was solved in its most general nonlinear transient form on a digital computer. The solution technique, developed by the Arthur D. Little Company of Cambridge, Massachusetts, employs backward differencing techniques which enable relatively large solution time steps to be taken and a stable solution obtained. The linear portion of the solution is handled by a Gauss-Seidel iterative technique while the nonlinear portion (radiation terms) is handled by a Newton-Raphson technique. The transfer coefficients were stored in the computer as elements of a vector eliminating the need for an n x n matrix of coefficients, most of which are zero, when one solves n simultaneous first-order differential equations.

APPENDIX F

DERIVATION OF LEVELING ERROR

$$G = \left[1 - \cos \theta_T\right] g$$

$$G/g = 1 - \cos \theta_T \approx 1 - \left[1 - \frac{\theta_T^2}{2}\right]$$

$$G/g \approx \frac{\theta_T^2}{2}$$

Define $\quad Z = \frac{\theta_T^2}{2}, \qquad x = \theta_x^2, \qquad y = \theta_y^2, \qquad$ with

$$\underline{\sigma_Z^2 = E\left\{(Z-\bar{Z})^2\right\} = \underline{E\left\{Z^2\right\} - (E\left\{Z\right\})^2}} \qquad (A)$$

Then $\quad E\left\{Z^2\right\} = E\left\{\left(\frac{x+y}{2}\right)^2\right\}$

$$= \frac{1}{4}\left[E\left\{x^2\right\} + E\left\{y^2\right\} + 2 E\left\{xy\right\}\right]$$

$\hspace{11cm}$ (F-1)

and $\quad E\left\{Z\right\} = E\left\{\frac{x+y}{2}\right\}$

$\hspace{11cm}$ (F-2)

$$= \frac{1}{2}\left[E\left\{x\right\} + E\left\{y\right\}\right]$$

If we assume that x and y are uncorrelated yet have the same distribution function,*

$$E\left\{x\right\} = E\left\{y\right\}$$

$$E\left\{x^2\right\} = E\left\{y^2\right\}$$

$$E\left\{(x - \bar{x})(\bar{y} - \bar{y})\right\} = E\left\{xy\right\} - E\left\{x\right\} E\left\{y\right\} = 0$$

$$\implies E\left\{xy\right\} = E\left\{x\right\} E\left\{y\right\}$$

---

*Reasonable, since knowing x gives no information about y, yet both axes should have the same type of distribution.

97

Now, Eq.(F-1) becomes

$$E\{Z^2\} = \frac{1}{4}\left[E\{x^2\} + E\{x^2\} + 2(E\{x\})^2\right]$$

$$= \frac{1}{2}\left[E\{x^2\} + (E\{x\})^2\right] \qquad \text{(F-3)}$$

and Eq.(F-2) becomes

$$E\{Z\} = \frac{1}{2}\left[E\{x\} + E\{x\}\right] = E\{x\} \qquad \text{(F-4)}$$

Thus, Eq.(A) becomes:

$$\sigma_Z^2 = \frac{1}{2}(E\{x^2\} + (E\{x\})^2) - (E\{x\})^2$$

$$\sigma_Z^2 = \frac{1}{2}\left[E\{x^2\} - (E\{x\})^2\right] \qquad \text{(B)}$$

but x can now be represented as θ^2 (dropping the axis-subscript), so that

$$\sigma_Z^2 = \frac{1}{2}\left[E\{\theta^4\} - (E\{\theta^2\})^2\right] \qquad \text{(C)}$$

For a uniform distribution of θ between a and b,

$$p(\theta) = \begin{cases} \dfrac{1}{b-a} & a \le \theta \le b \\[2ex] 0 & \text{otherwise} \end{cases}$$

i.e.

98
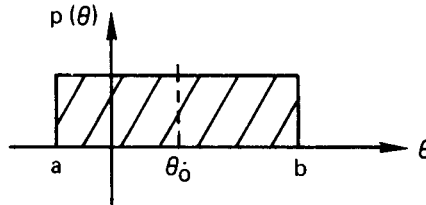
then
$$E\{\theta^2\} = \int_a^b \theta^2 \frac{d\theta}{b-a} = \frac{\theta^3}{3(b-a)} \Bigg]_a^b = \frac{b^3 - a^3}{3(b-a)}$$

and
$$E\{\theta^4\} = \int_a^b \theta^4 \frac{d\theta}{b-a} = \frac{b^5 - a^5}{5(b-a)}$$

Therefore, Eq.(C) becomes

$$\sigma_Z^2 = \frac{1}{2}\left[\frac{b^5 - a^5}{5(b-a)} - \left(\frac{b^3 - a^3}{3(b-a)}\right)^2\right]$$

(where a and b are in <u>radians</u>)

From this we get

Initial Offset	a (+3 m$\widehat{\text{in}}$)	b (-3 m$\widehat{\text{in}}$)	σ_Z
θ_0 m$\widehat{\text{in}}$	m$\widehat{\text{in}}$ (rad)	m$\widehat{\text{in}}$ (rad)	(g's)
0	-3 (-8.73×10^{-4})	3 (8.73×10^{-4})	0.161×10^{-6}
1	-2 (-5.8×10^{-4})	4 (1.16×10^{-3})	0.262×10^{-6}
3	0 (0)	6 (1.75×10^{-3})	0.642×10^{-6}
5	2 (5.8×10^{-4})	8 (2.33×10^{-3})	1.05×10^{-6}
10	7 (2.04×10^{-3})	13 (3.78×10^{-3})	2.08×10^{-6}
With Wider Deadband			
θ_0	a (+ 3.75)	b (- 3.75)	
1	-2.75 (-8×10^{-4})	4.75 (13.8×10^{-4})	0.26×10^{-6}

$$\sigma_{g_{earth}} = (\sigma_Z) \times 10^6 \text{ mgal}$$

$$\sigma_{g_{moon}} = (\sigma_Z) \times \frac{10^6}{6} \text{ mgal}$$

Figure F-1 is a plot of error due to leveling system bias.
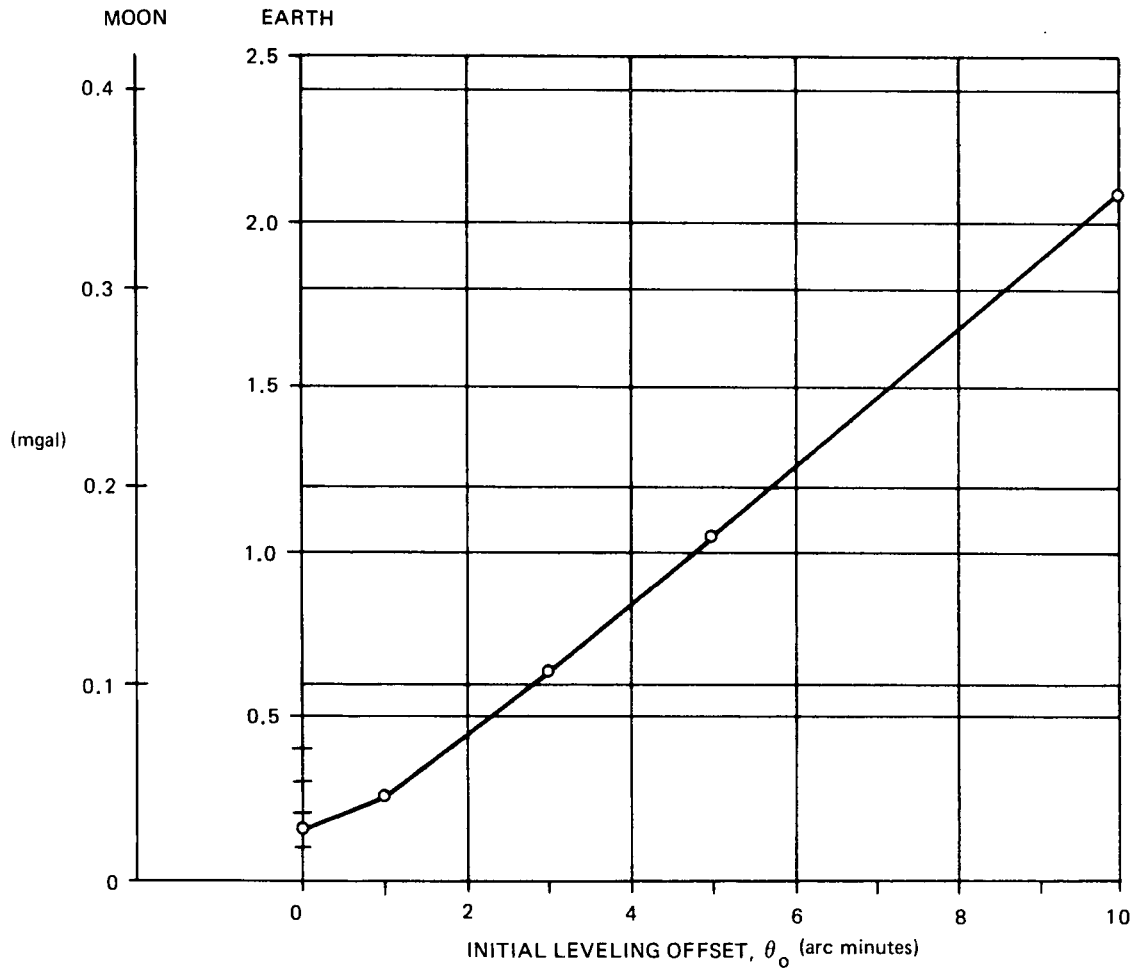
Fig. F-1 Error due to leveling system bias (assuming ± 3 arc minute pendulum deadband).

APPENDIX G

ANALYSIS OF ENVIRONMENTAL ERRORS FOR THE TG

The important information in the VSA signal lies in the difference frequency of the two string outputs. This difference frequency is, basically, proportional to the measured gravity (125 Hz/g being a typical scale factor). If the input axis of the VSA is subjected to vibration (primarily from the Rover), the signal will be frequency-modulated. If we measure this frequency at a point such that the signal proportional to the gravity at that point is F, then we will measure Z where

$$Z = F + A \sin \omega t \tag{G-1}$$

where A represents the amplitude (in Hz), and ω the frequency (in rad/s) of the vibration disturbance.

If we time average Z for T seconds we get

$$\bar{Z} = \frac{1}{T} \int_0^T Z \, dt \tag{G-2}$$

or

$$\bar{Z} - F = \frac{A}{\omega T} \left[1 - \cos \omega T \right] \tag{G-3}$$

Let $\bar{Z} - F$ be called E since it is, in fact, an error in our measurement. Then

$$E_{max} = \frac{2A}{\omega T} \tag{G-4}$$

This error in frequency measurement can be converted to a gravity error by the scale factor (125 Hz/g). Amplitude A can also be converted from a frequency amplitude to an acceleration amplitude, whence

$$C = \frac{A}{125} \quad , \quad E_g = \frac{E_{max}}{125} \tag{G-5}$$
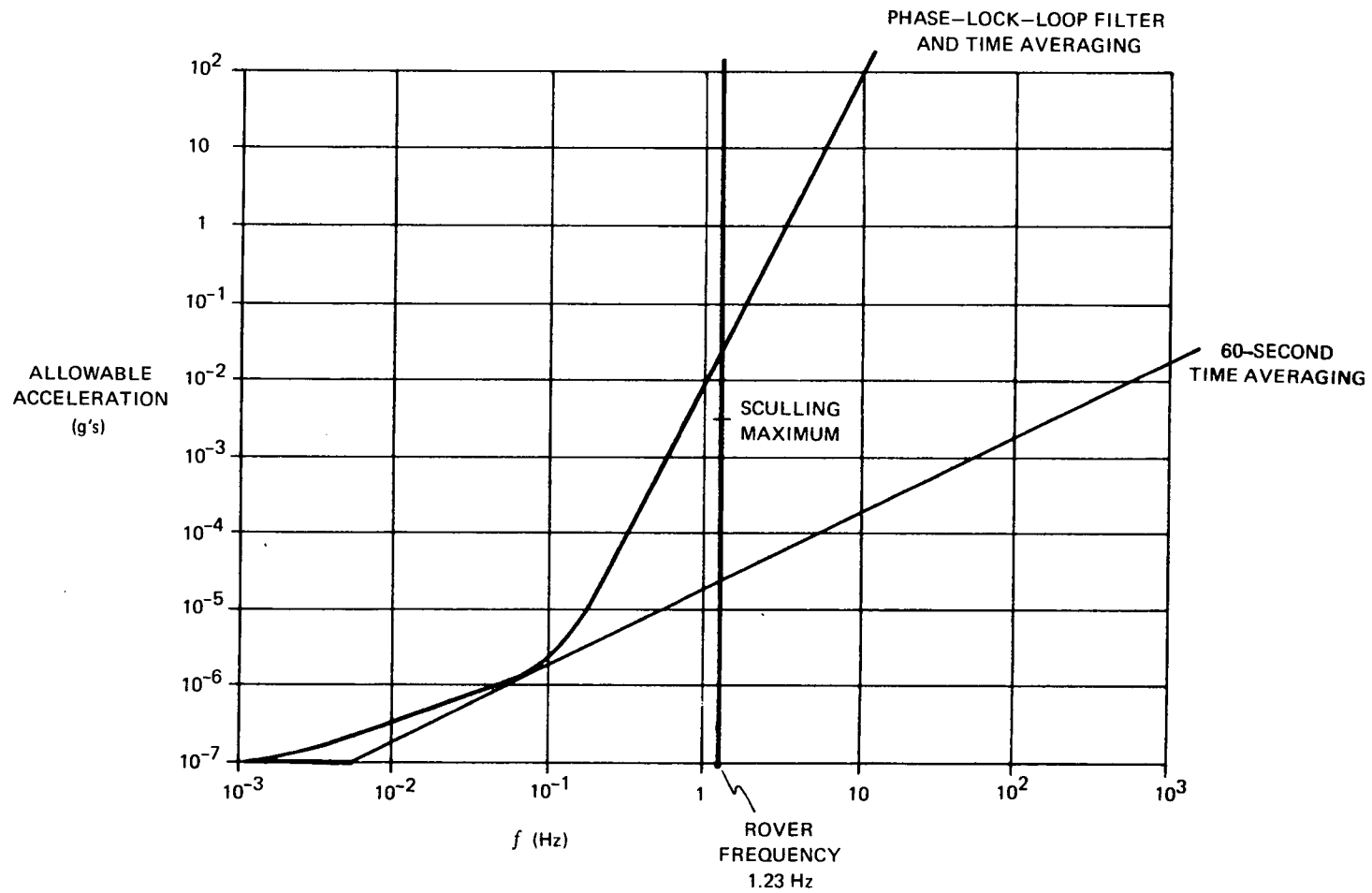
Fig. G-1   Vibration sensitivity.

If we want E_g to be a maximum of 10^{-7} g, then

$$\frac{2C_m}{\omega T} = 10^{-7} \tag{G-6}$$

$$\frac{C_m}{f} = 1.9 \times 10^{-5}$$

where $$\omega = 2\pi f \tag{G-7}$$

This defines a high-frequency error for our measurement. If, instead, there is a very-low-frequency disturbance, clearly $C_m = 10^{-7}$ is the maximum that we can tolerate for a measured error of 10^{-7} g.

With these two assymptotes the "60-second TIME AVERAGING" curve in Fig. G-1 can be generated.

The phase-lock loop acts like a frequency filter on a frequency-modulated signal, so that its filtering characteristics (a third-order roll-off with break frequency equal to 0.14 Hz) (see Fig. G-2) can be interpreted as an increase in allowable vibration error. With this knowledge, the phase-lock-loop curve in Fig. G-1 can be generated.
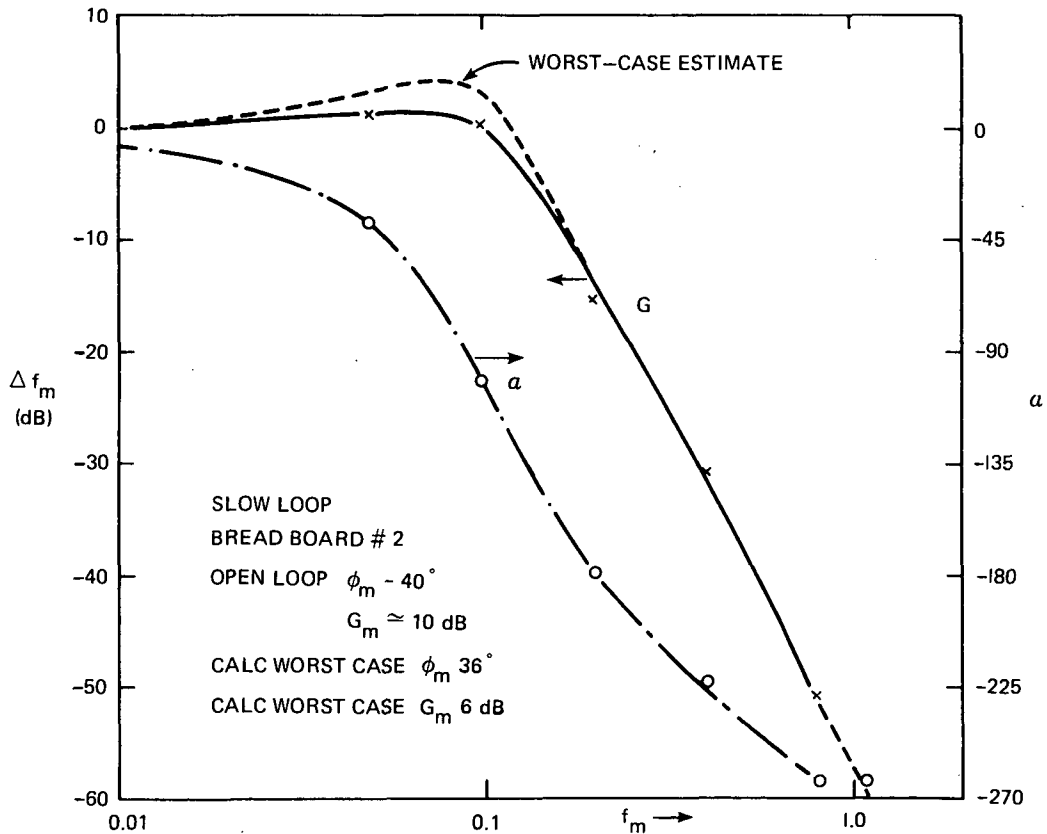
Fig. G-2 Phase-locked loop - Bode plot.

Let us denote these curves as $\ddot{x}$ (f) in g's.

Then

$$x\,(f) = \left| \frac{\ddot{x}\,(f)}{\omega^2} \right| \tag{G-8}$$

since we want x (f) in inches where $\ddot{x}$ (f) is in g's,

$$x\,(f) = \frac{390 \text{ in. } / \sec^2}{g} \times \frac{\ddot{x}\,(f)}{4\,\pi^2\,f^2} = \frac{10}{f^2}\,\ddot{x}\,(f) \tag{G-9}$$

Thus, Fig. G-3 can be generated by adding log $(\frac{10}{f^2})$ to Fig. G-1.

G.1   Sculling Error

Due to coupling between the vertical- and horizontal-vibration modes of the Rover, there is a rectified error in the gravity measurement. This error can be expressed as

$$E_s = \ddot{u}\,(t)\,\theta\,(t) = u\,\theta\,\sin^2\,\omega t \tag{G-10}$$

$$(\overline{E}_s)_{max} = \frac{\ddot{u}\,\theta}{2} \tag{G-11}$$

where

> $\ddot{u}$ = horizontal acceleration
> θ = angle of displacement

From the Rover, we know

$$\ddot{u} = \frac{1}{3}\,\ddot{\omega} \tag{G-12}$$

and
$$\theta = 0.18\,\ddot{u}$$

where

> $\dot{\omega}$ = vertical acceleration

Thus,

$$(\overline{E}_s)_{max} = 0.09\,(\ddot{u})^2 = 0.01\,(\ddot{\omega})^2 \tag{G-13}$$
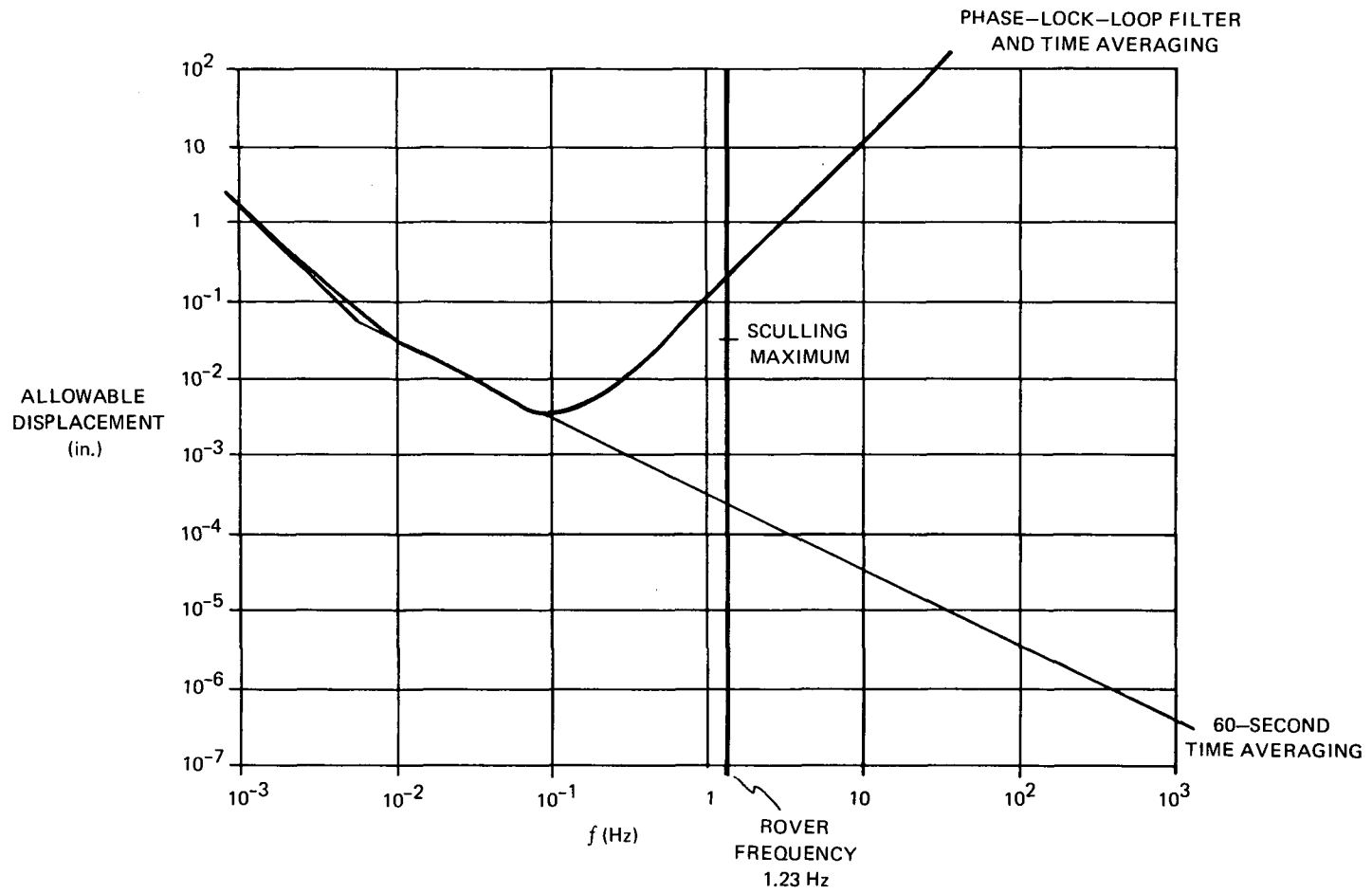
Fig. G-3 Displacement sensitivity.

To keep this error less than 10^{-7} then,

$$\ddot{\omega}_{max}{}^2 = 10^{-5} \qquad \text{(G-14)}$$

$$\ddot{\omega}_{max} = \sqrt{10} \times 10^{-3} \, g \qquad \text{(G-15)}$$

This is shown as "SCULLING MAXIMUM" in Fig. G-1 (and its corresponding displacement of 3×10^{-2} inches at 1.23 Hz).

PART II

FINAL ADMINISTRATIVE REPORT

by

Ralph Bailey
Robert P. Malieswski

SECTION 1

PURPOSE

The purpose of this part of the report is to provide a record of the tasks accomplished to design, develop, fabricate, test, and deliver a flight qualified Traverse Gravimeter Experiment, including associated hardware and documentation.

This report has been prepared in a logical sequence considering all program tasks as they appear in the contract and Statement of Work (S. O. W.). Time sequence and organizational sequence are not considered relevant.

SECTION 2

DELIVERABLE HARDWARE

The items to be delivered were as follows:

Unit	Description	Reference	Delivery Schedule
		TGE INSTRUMENT	
1	Breadboard Unit	Preliminary Design and Concept Evaluation	Residual
2	Engineering Unit	Section 1.4.4 of Exhibit B	Residual
3	Structural/Thermal Mock-up	Section 1.4.6 of Exhibit B	Residual
4	Interface Mock-up	Section 1.4.7 of Exhibit B - one each for LM and Rover	7-1-71
5	Training Mock-up	Section 1.4.7 of Exhibit B	8-1-71
6	Prototype Unit	Section 1.4.3 of Exhibit B	12-1-71 To be returned to Contractor for refurbishment as Flight Unit #2
7	Qualification Unit	Section 1.4.2 of Exhibit B	1-15-72
8	Flight Unit #1	Section 1.4.1 of Exhibit B	4-11-72
9	Flight Unit #2 Refurbished Prototype	Section 1.4.1 of Exhibit B	5-15-72
10	GSE Prototype		12-1-71 1 set
11	GSE #1	Section 1.4.8 of Exhibit B	2-1-72 1 set
12	GSE #2		4-11-72 1 set

2.1 Breadboard Unit

Development of the Breadboard Unit began in January 1971 and was completed in August 1971. The Breadboard Unit is considered residual hardware.

The Breadboard Unit verified the gravimeter conceptual design and was used to demonstrate the functional and operational modes at the Critical Design Review in September 1971 thereby establishing design baseline. Thermal testing of the Oven Assemblies for design evaluation was also accomplished using the Breadboard Unit.

2.2 Engineering Unit

The development of the Engineering Unit began in January 1971 and the assembly was completed in September 1971. The Engineering Unit is considered residual hardware.

The unit was used to verify environmental design goals and instrument performance. Environmental testing was performed using dummy-mass modules to verify design and environmental and functional tests; actual modules were completed to verify performance. Failure of the VSA during vibration testing initiated the design of a vibration shock mount (ISOFRAME) which was fabricated and successfully tested.

Upon completion of all engineering tests, the Engineering Unit was retrofitted with a flight spare E Frame/Oven Assembly and was used for all field tests relative to astronaut/pallet/Rover interface verification.

2.3 Structural Mock-up Unit

The structural mock-up was developed to test the mechanical integrity of the gravimeter design. Effort began April 1971 and testing was conducted through March 1972. The structural mock-up is considered residual hardware.

Vibration tests with the shock mount attached to the structural mock-up verified the design of the Isoframe.

The thermal blanket was installed on the structural mock-up and was vibrated successfully in the X, Y and Z flight axes.

2.4 Thermal Mock-up

The development of a thermal mock-up unit required for simulated-mission environmental testing verified the calculations obtained from the computer thermal model.

The thermal resistances of the gimbal bearings, temperature-controlled-heater sizes, hot-mission thermal margin, and the cold-mission power budget were determined by environmental testing.

This effort was started June 15, 1971 and completed November 15, 1971. The thermal mock-up unit is considered residual hardware.

2.5 Astronaut Interface Unit

An astronaut interface model was presented at the Delta Preliminary Design Review in Houston April 15, 1971 for JSC evaluation. This unit was requested by JSC, but was not considered contractual hardware.

2.6 Interface Mock-up Units

The development of two interface mock-up units required for astronaut, lunar rover vehicle, and lunar module stowage pallet interface verification was started April 1971 and completed March 1972.

The Interface mock-up S/N 001 was sold off and hand carried to JSC March 29, 1972.

The Interface mock-up S/N 002 has not been sold off pending JSC action.

2.7 Training Mock-up Unit

The development of a Training mock-up unit for Interface verification and astronaut training was started in April 1971 and delivered to JSC October 29, 1971; reference GRV-54-L, TGE Monthly Progress Report for October 1971.

A retrofit kit for the training unit was sold off and shipped February 24, 1972.

2.8 Prototype Unit

The requirement for the production prototype was deleted from the contract by MSC acceptance of Engineering Change Proposal number 11. The ECP was submitted November 5, 1971 and approved by JSC March 2, 1972 (reference CCA Number 4). |Where applicable, Class A parts of the prototype unit were utilized for the flight units.

2.9 Qualification Unit

The requirement for a Qualification unit was deleted from the contract by Contract Change Amendment number 4, March 2, 1972.

2.10 Flight Unit S/N 1

Flight unit S/N 1 effort started September 1971 and was certified for acceptance testing at QTRR, July 20, 1972. The flight unit was tested successfully, sold off, and shipped to Kennedy Spacecraft Center November 1, 1972.

2.11 Flight Unit S/N 2

Flight Unit S/N 2 was used for formal acceptance and qualification testing. The flight unit was certified at QTRR, July 20, 1972. The flight unit was then reworked and functionally retested for flight spare status.

This effort started December 1971 and was sold off and shipped to Kennedy Spacecraft Center November 6, 1972.

2.12 Ground Support Equipment

Development of ground support equipment started in February 1971 and was completed in October 1972. In July 1972 additional ground support end items were developed to support the instrument during transportation, handling, and testing at Kennedy Spacecraft Center.

2.12.1 GSE Prototype

Prototype ground support equipment was used to support functional and environmental qualification and acceptance testing performed at the Charles Stark Draper Laboratory. GSE prototype hardware is considered residual.

2.12.2 GSE #1, GSE #2

Ground support equipment for flight systems S/N 1 and S/N 2 was sold off and delivered to Kennedy Spacecraft Center, October 26, 1972.

SECTION 3

DELIVERABLE DOCUMENTATION

Documentation items were to be delivered as follows:

Item	Exhibit A Section Reference No.	Document	Document Type
1	5.2.1	Monthly Progress and Financial Management Reports	II
2	5.2.23	Interface Information Documentation	II
3	5.2.2	End Item Specifications Prelim - 3 wks prior to CDR Final - 2 wks after CDR	I
4	5.2.3	Engineering Drawings	I
5	5.2.4	Quality Assurance Plan	I
6	5.2.5	Quality Test Specification	I
7	5.2.6	Qualification Test Procedures	II
8	5.2.7	Qualification Test Report	II
9	5.2.8	Acceptance Test Specification	I
10	5.2.9	Acceptance Test Procedure	II
11	5.2.10	Acceptance Review Reports	I
12	5.2.11	Reliability Program Plan	I
13	5.2.12	Safety Plan	I
14	5.2.13	Management Plan	I
15	5.2.14	Spares Requirements	I
16	5.2.15	Review Minutes	I
17	5.2.16	Pre-Launch Test Requirements Package	II
18	5.2.17	Hardware Support Requirements	II

Item	Exhibit A Section Reference No.	Document	Document Type
19	5.2.18	Operation and Instruction Manuals	II
20	5.2.19	Acceptance Data Packages	II
21	5.2.20a	Certification Test Specification	I
22	5.2.2b	Other Test Specifications	I
23	5.2.20c	Test Procedures	II
24	5.2.20d	Test Reports	II
25	5.2.20e	GSE Calibration Data Reports	II
26	5.2.21	Final Report	I
27	5.2.22	Technical Reports	II

3.1 Monthly Progress and Financial Management Reports

Monthly progress and financial management reports were submitted to JSC in accordance with the contract schedule. Reports were submitted as follows:

Month	Year	Date Submitted	Reference
January	1971	17 February 1971	GRV-14-L
February		25 March 1971	GRV-19-L
March		7 May 1971	GRV-20-L
April		2 June 1971	GRV-25-L
May		7 July 1971	GRV-30-L
June		5 November 1971	GRV-48-L
July		5 November 1971	GRV-48-L
August		5 November 1971	GRV-48-L
September		8 November 1971	GRV-49-L
October		24 November 1971	GRV-54-L
November		22 December 1971	GRV-57-L
December		9 March 1972	GRV-63-L
January	1972	9 March 1972	GRV-63-L
February		9 March 1972	GRV-63-L
March		21 April 1972	GRV-66-L
April		25 May 1972	GRV-71-L
May		28 June 1972	GRV-75-L

Month	Year	Date Submitted	Reference
June	1972	14 August 1972	GRV-79-L
July		29 August 1972	GRV-86-L
August		2 October 1972	GRV-93-L
September		9 November 1972	GRV-95-L
October		9 November 1972	GRV-95-L
November		December 1972	GRV-98-L

3.2 Interface Information Documentation

MIT/CSDL attended interface meetings and supplied technical interface requirements that were approved by GAEC and JSC. No deliverable Type I - Interface Information Documentation was generated by MIT/CSDL. The Traverse Gravimeter Experiment complies to the Interface requirements as defined in the CE IDS 2025000.

3.3 End Item Specifications

Contract End Item Specifications for the TGE 2025000 and TGE/GSE 2025900 were prepared in accordance with the requirements of paragraph 5.2.2 Exhibit A, S. O. W. Traverse Gravimeter. After initial release the specifications were controlled and maintained by MIT/CSDL Design Review Board and Configuration Control Board in accordance with the requirements of E-2509 NASA Experiments Configuration Plan, approved by JSC May 4, 1971; reference EG14-71-87-EH.

Revision B to Contract End Item Detail Specification, Part I - Performance/Design and Qualification Requirements for the Traverse Gravimeter experiment, 2025000 was approved by JSC on May 31, 1972 (ECR 20510). Revision B reflects the final performance and design requirements of the TGE.

Revision D to Contract End Item Detailed Specification, Part II - Product Configuration and Acceptance Test Requirements for the Traverse Gravimeter Experiment, 2025000 was approved by JSC on 14 October 1972 (ECR 20578). Revision D reflects the final configuration of the TGE.

Revision C to Contract End Item Detail Specification, Performance/Design and Qualification Requirements for the Traverse Gravimeter Ground Support Equipment, 2025900 was approved by JSC on 25 October 1972 (ECR 20610). Revision C reflects the final configuration of the Ground Support Equipment.

3.4 Engineering Drawings

Engineering drawings were prepared to the normal drafting standards of MIT/CSDL and met the content and format requirements of paragraph 5.2.3, Exhibit A, S. O. W. Traverse Gravimeter Experiment. The following deliverable drawings were prepared:

275 Flight Hardware Mechanical Drawings

  75 Electrical Assemblies

100 Source Control Documents (SCD's)

  17 Schematics

130 Ground Support Equipment drawings

All deliverable drawings were maintained and controlled by Engineering Change or Release order and approved by MIT/CSDL Design Review Board and Configuration Control Board in accordance with the requirements of E-2509 NASA Experiments Configuration Plan approved by JSC May 4, 1971; reference EG14-71-87-EH.

3.5 Quality Assurance Plan

The Quality Assurance Plan was prepared in accordance with paragraph 5.2.4, and Appendix I, Exhibit A, S. O. W. Traverse Gravimeter Experiment. The plan was approved by JSC, reference NASA memo EG 14-71-87-EH, and subsequently implemented.

3.5.1 Quality Operating Plan

Quality Operating Procedures (QOP) were submitted to JSC to fulfill requirements for a Quality Operating Plan.

3.5.2 Process Specifications

Process Specifications for welding and soldering were prepared and implemented in accordance with the contractual welding and soldering requirements; reference TGE Process Specifications 5000, 5006 and GRV-57-T, Review of PS5000 - Weld Specification.

3.5.3 Corrosion, Contamination, and JSC Criteria and Standards

The requirements for corrosion prevention, contamination control and MSC Criteria and Standards, MSC8080, were met and incorporated in the hardware build documentation; reference GRV-69-L, GRV-72-L, GRV-110-A and GRV-74-L, MSC Criteria and Standards for TGE and Ground Support Equipment.

3.6 Quality Test Specification

The Qualification Test Specification 2025808 was prepared in accordance with the requirements of the TGE Contract End Item Detail Specification 2025000, Part I. The document was initially released May 10, 1972 ECR No. 20379 and approved by JSC May 31, 1972; reference EG9-72-88.

The following revisions to the document were incorporated through the approval of Engineering Change Releases.

Revision	ECR No.	MSC Approval Date
A	20509	July 7, 1972
B	20536	August 11, 1972
C	20556	September 20, 1972
D	20576	October 4, 1972

3.7 Qualification Test Procedures

The Qualification Test Procedures, 2025810, were prepared and met the content of paragraph 5.2.6 Exhibit A, S. O. W. Traverse Gravimeter Experiment. The document was initially released and approved June 1, 1972; reference ECR No. 20475.

The following revisions were formally submitted and approved by MIT/ CSDL Design Review Board and Configuration Control Board and submitted to JSC.

Revision	ECR No.	MIT/CSDL Approval Date
A	20508	July 7, 1972
B	20557	August 30, 1972
C	20575	October 4, 1972

The Qualification Support Battery test procedure was prepared and approved August 28, 1972; reference GRV 209T, ERR No. P-10187.

3.8 Qualification Test Report

Results of qualification tests were documented in Qualification Test Report 2025815 and submitted to JSC, November 23, 1972; reference GRV-97-L.

3.9 Acceptance Test Specification

The acceptance test requirements for the Traverse Gravimeter Experiment were incorporated in the Contract End Item Detail Specification 2025000, Part II.

3.10 Acceptance Test Procedures

The Acceptance Test Procedure, 2025811, was prepared and met the content of paragraph 5.2.9, Exhibit A, S. O. W. Traverse Gravimeter Experiment.

The document was initially released and approved July 14, 1972; reference ECR No. 20513. Revision A was formally submitted and approved September 9, 1972; reference, ECR No. 20558.

3.11 Acceptance Review Reports

An Acceptance Review Report was prepared for the Customer Acceptance Readiness Review; October 19, 1972, and met the requirements of paragraph 5.2.10, Exhibit A. S. O. W. Traverse Gravimeter; reference GRV94L, Minutes of QAR and CARR, Traverse Gravimeter.

The Review Item Dispositions and the Open Item List were closed out prior to sell off of the equipment; reference Acceptance Data Packages.

3.12 Reliability Documentation

The reliability program documentation was prepared and the reliability plan was implemented in accordance with paragraph 5.2.11, and Appendix II, Exhibit A, S. O. W. Traverse Gravimeter Experiment.

3.12.1 Reliability Program Plan

The Reliability Program Plan 2025805 was prepared and submitted for JSC approval March 29, 1971; reference GRV-18-L, Submittal of Reliability Program Plan. The Reliability Program Plan was approved May 4, 1971; reference NASA Memo EG14-71-87EH.

3.12.2 Nonmetallic Materials

The nonmetallic materials used in the Traverse Gravimeter Experiment were identified and a list submitted to JSC September 21, 1972; reference GRV-90-L.

3.12.3 Failure Modes and Effects Analysis

Failure Modes and Effects Analysis were completed in accordance with Quality Operating Procedure Number 18. The Failure Modes and Effects Analysis report was presented at the Critical Design Review. Copies of the report were submitted to JSC September 27, 1972; reference GRV-92-L, NASA memo EG 9-72-20, GRV-52-L.

3.12.4 Problem Failure Reporting and Corrections

Problem Failure Reporting and Corrections were prepared and incorporated in the end item data packages.

3.12.5 Electrical, Electronic and Electromechanical Parts List

The Electrical, Electronic and Electromechanical Parts List was prepared and submitted to JSC January, 1972. The Parts List was updated as requested by JSC and resubmitted April 6, 1972 and September 6, 1972; reference GRV-62-L, GRV-107-A, GRV-89-L, NASA memo EG9-72-19.

3.12.6 Deviation and Waiver Reports

Deviation and Waiver Reports were formally submitted to JSC and were shipped as part of the end item acceptance data packages.

3.13 Safety Plan

The Safety Plan 2025804 was prepared in accordance with the requirements of Paragraph 5.2.12 and Appendix IV, Exhibit A, S. O. W. Traverse Gravimeter Experiment.

The Safety Plan was initially released and submitted July 21, 1971; reference GRV32L. JSC approved the document September 27, 1971; reference, EG9-71-161-EH.

3.14 Management Plan

The Management Plan, E2509 "NASA Experiments Configuration Plan" was prepared and met the content of paragraph 5.2.13, and Appendix III Exhibit A, S. O. W. Traverse Gravimeter Experiment.

The Management Plan was submitted December, 1970 and approved by JSC May 4, 1971; reference EG14-71-87-EH.

3.15 Spares Requirements

The Spares Requirement document was prepared and met the content of paragraph 5.2.14, Exhibit A, S. O. W. Traverse Gravimeter Experiment. The document was submitted February 23, 1971; reference GRV16L.

Additional spares requirements are identified in the Acceptance Data Packages.

3.16 Review Minutes

The Review Minutes for the Preliminary Design Review and the Critical Design Review were prepared and met the requirements of paragraph 5.2.15 Exhibit A, S. O. W. Traverse Gravimeter Experiment.

The Preliminary Design Review minutes were approved by JSC, March 8, 1971, reference, GRV-17-L, Minutes of Preliminary Design Review, Traverse Gravimeter Experiment.

The Critical Design Review minutes were approved by JSC, September 29, 1971, reference GRV/DOC 71-25, Minutes of Critical Design Review, Traverse Gravimeter Experiment.

The final disposition of action items (RID's) defined at CDR were submitted to JSC November 9, 1971, reference GRV-50-L, Disposition of RID's originated at CDR.

3.17 Integration and Pre-Launch Test Requirements Package

Pre-Launch Test Requirements 2025806 was initially released and approved (ECR 20614) by JSC October 27, 1972. The test requirements package was prepared to describe the TGE test requirements and Pre-Launch Test Specifications and Procedures. Included in the package were special handling instructions for the TGE, detailed test procedures to be performed at KSC and operation instructions for the Ground Support Equipment to be used at KSC.

3.18 Hardware Support Requirements

A document containing the Hardware Support Requirements for the Traverse Gravimeter Experiment was not formally prepared. Internal MIT/CSDL memos and verbal agreements between JSC, KSC, GAEL, and MIT/CSDL defined the extent of support required.

3.19 Operation and Instruction Manuals

The Traverse Gravimeter Operation and Instruction manual 2025899 was prepared and met the requirements of paragraph 5.2.18, Exhibit A, S. O. W. Traverse Gravimeter Experiment. The manual was submitted to JSC, September 18, 1972; reference GRV-91-L Transmittal of Type II Documentation.

Special handling for the TGE and operations and instructions for the Ground Support Equipment are contained in the Pre-Launch Test Requirements document 2025806; reference: Customer Acceptance Readiness Review (CARR) Review Item Disposition (RID), number four.

3.20 Acceptance Data Packages

Acceptance Data Packages for each deliverable end item of flight and GSE hardware were prepared in accordance with the requirements of paragraph 5.2.19 Exhibit A, S. O. W. Traverse Gravimeter Experiment and Section 7, Appendix I, Traverse Gravimeter Experiment-Quality Program Requirements. Data packages were shipped with each deliverable end item.

3.21 Test Documentation

3.21.1 Certification Test Specification

The Certification Test Specification 2025807 was prepared in accordance with the technical requirements of the TGE Contract End Item Detail Specification, 2025000. The document was released at Revision A and approved by JSC June 6, 1972; reference EG9-72-83.

The following revisions to the documents were incorporated through the approval of Engineering Change Releases.

Revision	ECR Number	JSC Approval Data
B	20511	5/31/72
C	20608	10/20/72

The Ground Support Equipment for the TGE is classified as MSE Class II and thereby eliminated the need for a GSE Certification Test Specification.

3.21.2 Other Test Specifications

The Certification Test Specification 2025807, Qualification Test Specification 2025808, and the TGE Contract End Item Detail Specification, 2025000, Part II defined the performance criteria and test requirements for the Traverse Gravimeter Experiment.

3.21.3 Test Procedures

Test procedures were prepared for each type of test and met the requirements of paragraph 5.2.20c, Exhibit A, S. O. W. Traverse Gravimeter Experiment. The following test procedures were prepared and approved by MIT/CSDL Design Review Board and Configuration Control Board and submitted to JSC as Type II documents:

QUALIFICATION TEST PROCEDURES

TITLE	NUMBER	REV.	ECR No.	APPROVAL DATE
(Traverse Gravimeter)				
Launch Depressurization	25085	IR	20475	5/24/72
TG Visual Inspection	25055	IR	20475	5/24/72
TG Workmanship Vibration	25030	IR	20475	5/24/72
		A	20550	9/14/72
TG Performance Test	20545	IR	20492	6/8/72
		A	20535	8/17/72
		B	20553	9/14/72
		C	20597	10/17/72
TG Current Monitor	25015	IR	20475	5/24/72
		A	20519	7/1472
		B	20547	9/14/72
TG Temperature Test	25025	IR	20475	5/24/72
		A	20549	9/14/72
Baseline Verification Test	25075	IR	20475	5/24/72
		A	20520	7/14/72
		B	20554	9/14/72
TG Level Test	25020	IR	20517	7/14/72
		A	20548	7/14/72
		B	20567	10/4/72
TG Thermal Vacuum	25035	IR	20521	7/21/72
		A		8/2/72
Qualification Vibration	25080	IR	20542	8/17/72
Operational Test During TV	25036	IR	20528	7/26/72
		A	20551	9/14/72
Vibration Verification	25076	IR	20531	7/28/72
(Isoframe)				
Isoframe/Mechanical Unit Vib.	25081	IR	20532	7/28/72
TG Isoframe Inspection	25056	IR	20540	8/17/72

ACCEPTANCE TEST PROCEDURES

TITLE	NUMBER	REV.	ECR No.	APPROVAL DATE
(Traverse Gravimeter)				
Launch Depressurization	25086	IR	20541	8/17/72
		A	20555	9/14/72
TG Weight & CG Inspection	25057	IR	20561	9/14/72
TG Blanket Inspection	25058	IR	20562	9/14/72
TG Workmanship Vibration	25030	IR	20475	5/24/72
		A	20550	9/14/72

ACCEPTANCE TEST PROCEDURES (Continued)

TITLE	NUMBER	REV.	ECR No.	APPROVAL DATE
(Traverse Gravimeter)				
TG Performance Test	25045	IR	20492	6/8/72
		A	20535	8/17/72
		B	20553	9/14/72
		C	20597	10/17/72
TG Current Monitor	25015	IR	20475	5/24/72
		A	20519	7/14/72
		B	20547	9/14/72
TG Temperature Test	25025	IR	20475	5/24/72
		A	20549	9/14/72
Baseline Verification Test	25075	IR	20475	5/24/72
		A	20520	7/14/72
		B	20554	9/14/72
TG Level Test	25020	IR	20517	7/14/72
		A	20548	9/14/72
		B	20567	10/4/72
TG Thermal Vacuum Test	25037	IR	20521	7/21/72
		A	20552	9/14/72
Operational Test During TV	25036	IR	20528	7/26/72
		A	20551	9/14/72
Vibration Verification	25076	IR	20531	7/28/72
Assembly of Thermal Blanket	25200	IR	20568	10/4/72
TGE Assembly and Disassembly Procedures	25201	IR	20581	9/15/72
(Isoframe)				
TG Isoframe Inspection	25056	IR	20540	8/17/72
(Ground Support Equipment)				
Breakout Box	25905	IR	20559	9/14/72
I Oven Vacuum Fixture	25900	IR	20559	9/14/72
Pushbutton Actuator	25901	IR	20559	9/14/72
		A	20570	9/26/72
Level/Measure Light	25903	IR	20559	9/14/72
		A	20599	10/12/72
Power Panel Assembly	25902	IR	20607	10/2/72
Earth Moon Adapter	25906	IR	20574	10/2/72
		A	20583	10/25/72
		B	20613	10/26/72
Tee Connector Assembly	25904	IR	20587	10/2/72
		A	20612	10/25/72

3.21.4 Test Reports

The following Test Reports have been prepared for the tests conducted in accordance with the requirement of the Contract End Item Detail Specification, 2025000, and meet the content of paragraph 5.2.20d.

1. Traverse Gravimeter FS-2 Qualification Unit Test Report - 2025814, submitted to JSC November, 1972.

2. Traverse Gravimeter Pre-Installation Test Report — 2025806, submitted to JSC November 1972.

3. Calculated Effective Emittance of Radiator Cover Based on Engineering Tests - GRV-199-T. Submitted to JSC, June 26, 1972.

4. Wire Test Requirements of MSCM 8080 Standard 95A; reference GRV-127-T. Submitted to JSC, December, 1971.

3.21.5 Calibration Data Reports.

Ground support equipment that required calibration was calibrated and tagged by MIT/CSDL Calibration Department prior to sell off of the equipment. Calibration Data Reports for each deliverable set of GSE were not prepared in accordance with paragraph 5.2.20e, Exhibit A, S. O. W. Traverse Gravimeter Experiment.

3.22 Final Report

This two-part document comprises the final report on the Traverse Gravimeter Experiment.

3.23 Technical Reports

The following technical reports were prepared and contain the results of studies and analyses performed during the development phase of the program:

1. Testing of a Vibrating String Accelerometer for use in a Lunar Gravimeter - E-2721. Submitted to JSC December, 1972.

2. Traverse Gravimeter for the Lunar Surface E-2603. Submitted to JSC July, 1972.

3. Traverse Gravimeter Final Engineering Report. Part I of this document.

4. Five-Day Mission Evaluation Report — GRV-227-T. Submitted to JSC December, 1972.

5. Traverse Gravimeter Users Guide. Submitted to JSC April, 1971.

6. Traverse Gravimeter Training Unit Manual. Submitted to JSC March 29, 1972.

7. Interim Test Plan of the Traverse Gravimeter Experiment- ITP 202500. Submitted to JSC, May, 1972.

8. Lunar Gravimeter Interim Study Report E2535. Submitted to JSC, December 15, 1970.

SECTION 4

ENGINEERING CHANGE PROPOSALS

Engineering Change Proposals were prepared and submitted to JSC in accordance with Appendix III, Exhibit A, S. O. W. Traverse Gravimeter Experiment.

Engineering Change Proposals were submitted to JSC resulting in contract modifications or disapproval.

The following list identifies the ECP's submitted and the resulting CCA's.

No.	Title	Date Submitted	Ref. Document	CCA# & Date Approved	Date Dis-approved
1	Fabrication of Human Factors Model of the TGE	8/10/71	CSDL Proposal No. 71-241	CCA #1 11/29/71	
2	Logic/Display Design Change	4/15/71	GRV-68-A		11/29/71
3	Update & Modify Mock-up for Solar Simulator Evaluation	5/27/71	GRV-68-A		11/29/71
4	Additional Analysis for Performance Margin in Circuits	5/27/71	GRV-68-A		11/29/71
5	Eagle Picher Consultation of Battery	4/15/71	GRV-68-A		11/29/71
6	Power Up Launch	10/19/71 10/15/71	GRV-43-L GRV-42-L		12/6/71
7	Contract Specification Revision	11/10/71	DSR No. 60-451	Incorporated by amendment 5S	2/11/72
8	Rework of Production Prototype	11/22/71	GRV-86-A		(withdrawn 1/5/72)
9	Screening Tests on D4E Accelerometers	12/13/71	CSDL Proposal No. 71-451 DSR No. 60-451	CCA #3 3/2/72	

No.	Title	Date Submitted	Ref. Document	CCA# & Date Approved	Date Disapproved
10	Screening of 54L Series Integrated Circuits	1/17/72	GRV-94-L	CCA #2 1/5/72	
11	Alternate Contract Approach	3/2/72	GRV-101-A	CCA #4 3/30/72	
12	Capability Retention: Post Acceptance Testing and Operational Support	3/3/72	GRV-102-A	CCA #6 6/29/72	
13	Vibration Isolation	5/24/72	GRV-112-A	CCA #5 5/2/72	
14	Astronaut Field Training	5/9/72	GRV-118-A GRV-122-A	CCA #7 7/12/72	
15	Spare E-Frame Assembly	7/24/72	GRV-131-A	CCA #8 8/14/72	

SECTION 5

PROGRAM MEETINGS

5.1 Preliminary Design Review (PDR)

The preliminary Design Review (PDR) was held at the Charles Stark
Draper Laboratory, Cambridge, Mass., on February 23 and 24, 1971.

Copies of all presentation material was distributed to all attendees
at the time of presentation. Each distrubution included:

    87 View Graphs
     1 TGE Functional Description
     1 Preliminary Copy of Part I of Contract End Item Specification
     1 Agenda

Additionally, the Spares Requirements list was submitted for approval as
required by the contract.

Meeting minutes were submitted to JSC and all attendees on February 26,
1972; reference GRV-17-L.

Elaboration and detailed design information relative to thermal design
was requested by NASA personnel in attendence and was made the sub-
ject of a subsequent meeting.

5.2 Delta Preliminary Design Review (ΔPDR)

The Delta Preliminary Design Review was held at Johnson Spacecraft
Center, Houston, Texas on April 15, 1971.

Detailed design information relating specifically to the TGE thermal design,
pallet interface, and astronaut controls and displays was presented. Ana-
lytical results from a thermal model of the instrument indicated the feasi-
bility of operating on thermal inertia during a traverse with the radiator
closed.

The basic thermal design was approved as were the controls, display and
TGE/pallet interface designs.

The final disposition of action items (RID's) defined at ΔPDR were submit-
ted to JSC June 14, 1971; reference GRV-65-T, "RID's from Delta PDR
on April 15, 1971."

128

5.3 Critical Design Review (CDR)

The Critical Design Review (CDR) was held at the Charles Stark Draper Laboratory on September 1 and 2, 1971. A power-down configuration at launch was presented as the baseline.

The following presentation material was distributed to all attendees:

Agenda (recommended by NASA/JSC)

Copies of Viewgraphs

Technical Description

    Appendix A - TGE CEI, Part I
    Appendix B - TGE CEI, Part II
    Appendix C - TGE CEI, Part I
    Appendix D - PIT Procedure

Certification Test Specification (preliminary)

Interim Test Plan (Type III)

TGE Thermal Design for CRR

TGE Thermal Design Trade-Offs

GSE Shipping Container Drawing

GSE Test Fixture Drawing

Preliminary Lunar Time Line Operations

The following hardware and documentation was on display during the CDR:

TGE Thermal Blanket Assembly (Thermal Unit)

Base Housing Assembly (Engineering Unit)

Radiator Subassembly (Engineering Unit)

Precision Oven (Engineering Unit)

Middle Gimbal (Thermal Unit)

Electronic Frame (Engineering Unit)

Gear Box Assembly (Thermal Unit)

Electronic Frame and Harness (Engineering Unit)

Battery Pack Assembly (Thermal Unit)

Battery Pack Cover (Engineering Unit)

Battery Pack Case (Engineering Unit)

Battery Cell - Typical

TGE Training Mock-Up Unit

Geology Pallet Mock-Up Unit

TGE Interface Mock-Up Units (actual earth weight)

Complete Set of TGE Drawings

Copy of each document released through the Design Review Board (DRB)

Copy of the TGE Reliability Plan

Copy of the TGE Documentation Plan

The meeting opened with a presentation of the program goals, accomplishments and schedule. Subsequent presentations defined design objectives and parameters including construction and packaging techniques of the instrument. Development testing was identified and the Interface, Training and Breadboard Units were demonstrated. Proposed ground support equipment, KSC preflight operations and a Lunar Operations Time Line were identified.

Engineering drawings, SCD's and the reliability program were reviewed in a separate meeting.

Meeting minutes were submitted to JSC; reference GRV/DOC 71-25, Minutes of Critical Design Review, Traverse Gravimeter Experiment.

The final disposition of action items (RID's) defined at CDR were submitted to JSC November 9, 1971; reference GRV-50-L, Disposition of RID's Originated at CDR.

5.4 Qualification Test Readiness Review (QTRR)

The Qualification Test Readiness Review was held at the Charles Stark Draper Laboratory on July 18, 19 and 20, 1972. The Traverse Gravimeter Serial Number (FS-2) was certified for qualification testing after MIT/CSDL closed out the action items (RID's) generated at QTRR; reference GRV-133A - Minutes of Traverse Gravimeter QTRR and FTRR, 18 - 20, July 1972.

The Traverse Gravimeter, serial number (FS-1) was certified for flight acceptance testing upon completion of the build cycle.

Program documentation was presented and examined to verify that the documentation reflected the design presented at CDR in September, 1971.

The final disposition of action items (RID's) defined at QTRR, and the meeting minutes were submitted July 25, 1972 and approved by JSC July 29, 1972; reference GRV-133A. Additional close out of pending action items was completed via telephone conversations with JSC.

5.5 Customer Acceptance Readiness Review (CARR)

A Customer Acceptance Readiness Review was held at Charles Stark Draper Laboratory, October 18, 1972. A Flight Worthiness Certification document for the Traverse Gravimeter, serial number, FS-1 and FS-2, was issued by JSC.

A Qualification Assessment Review was held to review the qualification test data for the Traverse Gravimeter, serial number, FS-2. The test data was approved by JSC resulting in the issuance of a JSC Certification Test Review document.

The Pre-Installation Test Procedure was reviewed. JSC's request that special handling procedures for the TGE, and instructions for the operation of Ground Support Equipment be incorporated in the PIT document, eliminated the need for a separate Operations and Instruction manual for the GSE.

The Ground Support Equipment for the Traverse Gravimeter and related documentation was reviewed and open items were identified by JSC.

The MIT/CSDL Office of Naval Research was directed by the JSC program. Technical Manager to verify the close out of all open items prior to delivery of any hardware.

The QAR and CARR meeting minutes were prepared and approved by JSC October 19, 1972; reference GRV-94-L, Minutes of QAR and CARR, Traverse Gravimeter.

BIBLIOGRAPHY

Reference	Subject	From	To	Date
P.S. 5000	Weld Specification	MIT/DL	NASA	3/1/70
P.S. 5006	Solder Specification	MIT/DL	NASA	3/1/70
E-2535	Lunar Gravimeter Interim Study Report	MIT/DL	NASA	12/15/70
NAS 9-11555	Contract for Traverse Gravimeter Experiment	NASA	MIT/DL	1/17/71
E-2509	NASA Experiments Configuration Plan	MIT/DL	NASA	1/28/71
GRV-14-L	Monthly Progress Report, January	MIT/DL	NASA	2/17/71
GRV-16-L	Submittal of TGE Spares Requirements	MIT/DL	NASA	2/22/71
GRV-17-L	Minutes of Preliminary Design Review - Traverse Gravimeter Experiment	MIT/DL	NASA	2/26/71
2025805	Reliability Program Plan	MIT/DL	NASA	3/1/71
C.C.A. No. 4	Alternate Contract Approach	NASA	MIT/DL	3/2/71
GRV-19-L	Monthly Progress Report, February	MIT/DL	NASA	3/25/71
GRV-18-L	Submittal of Reliability Program Plan	MIT/DL	NASA	3/29/71
GRV-110-A	MSC Criteria and Standards for TGE and GSE	MIT/DL	NASA	4/11/71
	Traverse Gravimeter Users Guide	MIT/DL	NASA	4/14/71
GRV-65-T	RID's from Delta Preliminary Design Review	MIT/DL	NASA	4/15/71
GRV-69-L	MSC Criteria and Standards for TGE and GSE	MIT/DL	NASA	5/3/71
CEI 2025000	TGE Contract End Item Specification	MIT/DL	NASA	5/4/71
GRV-20-L	Monthly Progress Report, March	MIT/DL	NASA	5/7/71
GRV-72-L	MSC Criteria and Standards for TGE and GSE	MIT/DL	NASA	5/25/71
	Interim Test Plan for the Traverse Gravimeter Experiment	MIT/DL	NASA	5/26/71
GRV-25-L	Monthly Progress Report, April	MIT/DL	NASA	6/2/71
GRV-57-T	Review of P.S. 5000 Weld Specification	MIT/DL	NASA	6/2/71
GRV-74-L	MSC Criteria and Standards for TGE and GSE	MIT/DL	NASA	6/12/71

BIBLIOGRAPHY (Continued)

Reference	Subject	From	To	Date
GRV-32-L	Submittal of TGE Safety Plan	MIT/DL	NASA	7/2/71
GRV-30-L	Monthly Progress Report, May	MIT/DL	NASA	7/7/71
GRV-50-L	Disposition of RID's originated at CDR	MIT/DL	NASA	9/9/71
EG9-71-161-EH	Approval of TGE Safety Plan	NASA	MIT/DL	9/27/71
GRV/DOC 71-25	Minutes of Critical Design Review - Traverse Gravimeter Experiment	MIT/DL	NASA	9/29/71
CEI-2025900	GSE Contract Item Specification	MIT/DL	NASA	10/25/71
C-207-01	Stress Analysis of Traverse Gravimeter	Littleton Research and Engineering Corp	MIT/DL	10/29/71
E.C.P. No. 11	Alternate Contract Approach	MIT/DL	NASA	11/5/71
GRV-48-L	Monthly Progress Report, June	MIT/DL	NASA	11/5/71
GRV-48-L	Monthly Progress Report, July	MIT/DL	NASA	11/5/71
GRV-48-L	Monthly Progress Report, August	MIT/DL	NASA	11/5/71
GRV-49-L	Monthly Progress Report, September	MIT/DL	NASA	11/8/71
GRV-57-L	Monthly Progress Report, November	MIT/DL	NASA	11/22/71
GRV-54-L	Monthly Progress Report, October	MIT/DL	NASA	11/24/71
GRV-127-T	Wire Test Requirements of MSCM 8080 Standard 95A	MIT/DL	NASA	12/13/71
EG 9-72-20	Critical Failures	NASA	MIT/DL	2/10/72
GRV-63-L	Monthly Progress Report, December	MIT/DL	NASA	3/9/72
GRV-63-L	Monthly Progress Report, January	MIT/DL	NASA	3/9/72
GRV-63-L	Monthly Progress Report, February	MIT/DL	NASA	3/9/72
GRV-62-L	Response to NASA Memos EG 9-72-19, 14, 20	MIT/DL	NASA	3/9/72

Reference	Subject	From	To	Date
C-207-2	Calculated Natural Frequencies of Vibration of the Traverse Gravimeter	Littleton Research and Engineering Corp	MIT/DL	3/14/72
C-207-3	Estimated Acoustic Response of the Traverse Gravimeter	Littleton Research and Engineering Corp	MIT/DL	3/14/72
TG-017	Internal Failure Report	MIT/DL	NASA	3/24/72
GRV-167-T	Test Procedure - 24 March 1972	MIT/DL	NASA	3/24/72
	Traverse Gravimeter Training Unit Manual	MIT/DL	NASA	3/29/72
GRV-107-A	Submittal of Electrical, Electronic and Electromechanical Parts List	MIT/DL	NASA	4/6/72
GRV-66-L	Monthly Progress Report, March	MIT/DL	NASA	4/21/72
GRV-167-T	Test Procedure - 24 March 1972	MIT/DL	NASA	4/24/72
EG 14-71-87-EH	Approval of TGE Plans	NASA	MIT/DL	5/4/72
ECR 20379	Quality Test Specification Initial Release	MIT/DL	NASA	5/10/72
EG 9-72-19	Electrical, Electronic and Electromechanical Parts List	NASA	MIT/DL	5/15/72
C-207-4	Finite Element Stress Analysis of TGE - Sub-Base	Littleton Research and Engineering Corp	MIT/DL	5/15/72
GRV-71-L	Monthly Progress Report, April	MIT/DL	NASA	5/25/72
ECR 20511	Certification Test Specification, Rev. B	MIT/DL	NASA	5/31/72
ECR 20510	CEI 202500 Part I Revision for TGE Performance & Design	MIT/DL	NASA	5/31/72
EG 9-72-88	MSC Approval of Quality Test Specification	NASA	MIT/DL	5/31/72

BIBLIOGRAPHY (continued)

Reference	Subject	From	To	Date
ECR 20475	Qualification Test Procedures 2025810, Initial Release	MIT/DL	NASA	6/1/72
EG 9-72-83	Approval of TGE Certification Test Specification 2025807	MIT/DL	NASA	6/6/72
C-207-5	Finite Element Stress Analysis of Redesigned TGE Sub-Base	Littleton Research and Engineering Corp	MIT/DL	6/8/71
GRV-196-T	Traverse Gravimeter Experiment - Isolator Natural Frequencies and Maximum Acceleration (Predicted and Actual)	MIT/DL	NASA	6/13/72
GRV-199-T	Calculated Effective Emittance of Radiator Cover Based on Engineering Tests	MIT/DL	NASA	6/26/72
GRV-79-L	Monthly Progress Report, May	MIT/DL	NASA	6/28/72
ECR-20509	Quality Test Specification, Rev. A	MIT/DL	NASA	7/7/72
ECR-20508	Quality Test Procedures, Rev. A	MIT/DL	NASA	7/7/72
E-2603	Traverse Gravimeter for the Lunar Surface	MIT/DL	NASA	7/7/72
ECR-20513	Acceptance Test Procedures Initial Release	MIT/DL	NASA	7/14/72
GRV-133-A	Minutes of QTRR and FTRR	MIT/DL	NASA	7/20/72
ECR-20536	Quality Test Specification, Rev. B	MIT/DL	NASA	8/11/72
GRV-79-L	Monthly Progress Report, June	MIT/DL	NASA	8/14/72
ERR P-10187	Qualification Support Battery Test Procedure	MIT/DL	NASA	8/28/72
GRV-209T	Transmittal of Qualification Support Battery Test Procedure	MIT/DL	NASA	8/29/72
GRV-86-L	Monthly Progress Report, July	MIT/DL	NASA	8/29/72
ECCR 20557	Qualification Test Procedures, Rev. B	MIT/DL	NASA	8/30/72
R-729 (ND 2025899)	Traverse Gravimeter Operation and Instruction Manual	MIT/DL	NASA	9/72
GRV 89-L	Electrical, Electronic and Electromechanical Parts List	MIT/DL	NASA	9/6/72
ECR 20558	Acceptance Test Procedures, Revision A	MIT/DL	NASA	9/9/72

Reference	Subject	From	To	Date
GRV-91-L	Transmittal of Type II Documentation - TGE Operation and Instruction Manual	MIT/DL	NASA	9/18/72
GRV-90-L	TGE Non-metallic Materials List	MIT/DL	NASA	9/19/72
ECR 20556	Quality Test Specification, Rev. C	MIT/DL	NASA	9/20/72
GRV-216-T	Traverse Gravimeter/LRV Vibration/Environmental Test	MIT/DL	NASA	9/21/72
GRV-92-L	TGE Failure Modes and Effects Analysis Report	MIT/DL	NASA	9/27/72
GRV-93-L	Monthly Progress Report, August	MIT/DL	NASA	10/2/72
ECR 20576	Quality Test Specification, Rev. D	MIT/DL	NASA	10/4/72
ECR 20575	Qualification Test Procedures, Rev. C	MIT/DL	NASA	10/4/72
GRV-217-T	Results of KSC Rover Ride Test	MIT/DL	NASA	10/11/72
ECR 20578	CEI 20250000 Part II TGE Produce Configuration Revisions	MIT/DL	NASA	10/14/72
R-735 (ND 2025814)	Traverse Gravimeter - CEI 2025000 SS-2 Qualification Unit Test Report	MIT/DL	NASA	10/17/72
GRV-94-L	Minutes of QAR and CARR	MIT/DL	NASA	10/19/72
ECR 20608	Certification Test Specification, Rev. C	MIT/DL	NASA	10/20/72
ECR 20610	CEI 2025900 - Product Configuration Revision	MIT/DL	NASA	10/25/72
ECR 20614	Pre-Launch Test Requirements 2025806 - Initial Release	MIT/DL	NASA	10/27/72
GRV-95-L	Monthly Progress Report, September	MIT/DL	NASA	11/9/72
GRV-95-L	Monthly Progress Report, October	MIT/DL	NASA	11/9/72
GRV-52-L	Transmittal of Report, Traverse Gravimeter Failure Mode Effect and Criticality Analysis	MIT/DL	NASA	11/10/72
GRV-97-L	Transmittal of Type II Documentation	MIT/DL	NASA	11/23/72
GRV-98-L	Monthly Progress Report, November	MIT/DL	NASA	12/72
GRV-96-L	Transmittal of Type I Documentation - Final Report	MIT/DL	NASA	12/8/72

BIBLIOGRAPHY (Continued)

Reference	Subject	From	To	Date
GRV-227-T	Five Day Mission Evaluation Report	MIT/DL	NASA	12/14/72
E-2721	Testing of a Vibrating String Accelerometer for use in a Lunar Gravimeter	MIT/DL	NASA	12/15/72
GRV-228-T	Summary of Post-Mission Test Results	MIT/DL	NASA	2/21/73
R-739	Traverse Gravimeter Experiment Final Report	MIT/DL	NASA	4/73
E-2759	Thermal-Vacuum Test of the Apollo 17 Lunar Traverse Gravimeter Experiment			